Technical Report

DSWA-TR-98-47

Batteryless Sensor for Intrusion Detection and Assessment of Threats

Approved for public release; distribution is unlimited.

August 2003

DNA 001-95-C-0175

Gerald F. Ross
Lee R. Cain
Steven M. Ciccarelli

Prepared by:

ANRO Engineering, Inc.
63 Great Road
Maynard, MA 01754

DESTRUCTION NOTICE

Destroy this report when it is no longer needed.
Do not return to sender.

PLEASE NOTIFY THE DEFENSE THREAT REDUCTION AGENCY, ATTN: IMMI, 8725 JOHN J. KINGMAN ROAD, MS-6201, FT BELVOIR, VA 22060-6201, IF YOUR ADDRESS IS INCORRECT, IF YOU WISH IT DELETED FROM THE DISTRIBUTION LIST, OR IF THE ADDRESSEE IS NO LONGER EMPLOYED BY YOUR ORGANIZATION.

DISTRIBUTION LIST UPDATE

This mailer is provided to enable DTRA to maintain current distribution lists for reports. (We would appreciate you providing the requested information.)

- ❑ Add the individual listed to your distribution list.
- ❑ Delete the cited organization/individual.
- ❑ Change of address.

Note:
Please return the mailing label from the document so that any additions, changes, corrections or deletions can be made easily. For distribution cancellation or more information call DTRA/IMMI (703 767-4726.

NAME: _____

ORGANIZATION: _____

OLD ADDRESS	NEW ADDRESS
_____	_____
_____	_____
_____	_____

TELEPHONE NUMBER: ( ) _____

DTRA PUBLICATION NUMBER/TITLE	CHANGES/DELETIONS/ADDITONS, etc. *(Attach Sheet if more Space is Required)*
_____	_____
_____	_____
_____	_____

DTRA or other GOVERNMENT CONTRACT NUMBER: _____

CERTIFICATION of NEED-TO-KNOW BY GOVERNMENT SPONSOR (if other than DTRA):

SPONSORING ORGANIZATION: _____

CONTRACTING OFFICER or REPRESENTATIVE: _____

SIGNATURE: _____

DEFENSE THREAT REDUCTION AGENCY
ATTN: IMMI
8725 John J. Kingman Road, MS-6201
Ft Belvoir, VA 22060-6201

DEFENSE THREAT REDUCTION AGENCY
ATTN: IMMI
8725 John J. Kingman Road, MS-6201
Ft Belvoir, VA 22060-6201

REPORT DOCUMENTATION PAGE

Form Approved
OMB No. 0704-0188

1. AGENCY USE ONLY (*Leave blank*)	2. REPORT DATE	3. REPORT TYPE AND DATES COVERED
	August 2003	Technical 950927 - 980527

4. TITLE AND SUBTITLE

Batteryless Sensor for Intrusion Detection and Assessment of Threats

5. FUNDING NUMBERS

C - DNA 001-95-C-0175
PE - DNAOSD PSEAG
PR - AE
TA - RP
WU - DH62373

6. AUTHOR(S)

Gerald F. Ross, Lee R. Cain and Steven M. Ciccarelli

7. PERFORMING ORGANIZATION NAME(S) AND ADDRESS(ES)

ANRO ENGINEERING, INC.
63 Great Road
Maynard, MA 01754

8. PERFORMING ORGANIZATION REPORT NUMBER

9. SPONSORING/MONITORING AGENCY NAME(S) AND ADDRESS(ES)

Defense Threat Reduction Agency
8725 John J. Kingman Road, MS-6201
Fort Belvoir, VA 22060-6201

CSOS/Witter

10. SPONSORING/MONITORING AGENCY REPORT NUMBER

DSWA-TR-98-47

11. SUPPLEMENTARY NOTES

This work was sponsored by the Defense Threat Reduction Agency under RDT&ERMC code B 2638 D AE DA 62373 2352 A RP 25904D.

12a. DISTRIBUTION/AVAILABILITY STATEMENT

Approved for Public release; distribution is unlimited

12b. DISTRIBUTION CODE

13. ABSTRACT (*Maximum 200 words*)

A new series of security sensors has been sucessfully developed by ANRO Engineering, Inc. (ANRO) to detect intruders, and signal a remote alarm without batteries, external power or wiring. These wireless and self-powered (WASP) sensors are inherently covert both in the installation and presence of the sensor, and the low probability of intercept/detection (LPI/D) wireless link. Demonstration models have been constructed for hidden placement in existing doorknobs, doorjambs and windows. The operation of the sensors is not discernible to an intruder, and does not depend upon the speed of activation. A wireless link was developed that operates within the FCC Part 15 for unlicensed oepration, as well as within the guidelines for frequency allocation for many government facilities. The wireless link uses a coded signal to discriminate between more than 1024 sensors within an area. ANRO was particularly successful in keeping the cost of the sensors as low as possible. The cost of the components that are added to the lockset in a doorknob, for example, is estimated to be under $5. This new WASP sensor technology can be applied to keyless lock systems used in secure facilities and storage containers, and for commercial applications such as keyless hotel doors.

14. SUBJECT TERMS

Sensors, Door, Wireless, Intrusion, LPI/LPD, Self-Powered, Security, Alarms, Detection, Window

15. NUMBER OF PAGES

204

16. PRICE CODE

17. SECURITY CLASSIFICATION OF REPORT	18. SECURITY CLASSIFICATION OF THIS PAGE	19. SECURITY CLASSIFICATION OF ABSTRACT	20. LIMITATION OF ABSTRACT
UNCLASSIFIED	UNCLASSIFIED	UNCLASSIFIED	SAR

SUMMARY

ANRO Engineering, Inc. (ANRO) has been a pioneer in the development of Wireless and Self-Powered (WASP) sensors for the detection of vehicles, intruders, low tire pressure, etc., since the early 1970's. The significance of this class of sensors is the reduction in maintenance requirements, reduction in the amount of wire, the potential reduction of overall costs of installation, and potentially increasing reliability. The energy necessary to power pulse coded transmitters that denote an event is derived from the motion of an intruder.

The contract was structured as Phase I and Phase II SBIR program with a time gap between the phases due to funding availability. The prime thrust of the program was directed at covertly embedding these sensors in doorknobs, doorjambs, and windows. The objective of the program was to develop sensors to detect intrusions that could easily be integrated into commercial off-the-shelf (COTS) hardware systems. It is important that the presence of these sensors is difficult to detect and that they can be produced inexpensively. The activation of a sensor is detected remotely by a separately powered receiver. Ranges of greater than 100 feet indoors were required; in free space, ranges in excess of 1500 feet were realized.

The installation of these sensors is quick and easy, and is especially useful where the installation of new wiring is impractical and undesirable. The receivers can monitor up to 1024 different doors and windows and could be readily modified to time-tag alarms. The signals transmitted are low probability of intercept/detection since their duration is only a few hundred milliseconds. The transmission complies with FCC Part 15 regulations for incidental radiation (i.e., no licensing necessary), and sends a pulse width modulation signal at about 315 MHz.

The sensors provide a radiated signal no matter how slowly, for example, the doorknob is turned. The mechanism builds up potential energy in a spring, and then when a certain detent is passed, the energy is released and used to spin a generator. The voltage produced by the generator powers the transmitter (see Figures 3-5 and 3-6). We believe the hardware costs necessary to add to an existing key lockset have been reduced, under the program, to less than $5. This accomplishment was difficult to achieve, but the project was successfully completed within the contract cost and the resulting products are now ready for manufacture. In addition to meeting significant needs of the U.S. Government, it is believed that the WASP sensors have significant commercial promise for both industrial and home applications.

ANRO recommends that the sensors developed on the program be manufactured and installed by different government agencies for evaluation. ANRO is in the process of investigating several commercial opportunities for this technology. It is also recommended that an off-shoot of WASP be funded to study and develop energy producing mechanisms to operate batteryless keyless lock systems now used in security facilities and storage containers as well as hotel and motels. Once again, there should be a large market for such locks commercially.

CONVERSION TABLE

Conversion Factors for U.S. Customary to metric (SI) units of measurement.

MULTIPLY →	BY	→ TO GET
TO GET ←	BY	← DIVIDE

angstrom	1.000 000 x E -10	meters (m)
atmosphere (normal)	1.013 25 x E +2	kilo pascal (kPa)
bar	1.000 000 x E +2	kilo pascal (kPa)
barn	1.000 000 x E -28	meter^2 (m^2)
British thermal unit (thermochemical)	1.054 350 x E +3	joule (J)
calorie (thermochemical)	4.184 000	joule (J)
cal (thermochemical/cm^2)	4.184 000 x E -2	mega joule/m^2 (MJ/m^2)
curie	3.700 000 x E +1	*giga bacquerel (GBq)
degree (angle)	1.745 329 x E -2	radian (rad)
degree Fahrenheit	t_k = (t°f + 459.67)/1.8	degree kelvin (K)
electron volt	1.602 19 x E -19	joule (J)
erg	1.000 000 x E -7	joule (J)
erg/second	1.000 000 x E -7	watt (W)
foot	3.048 000 x E -1	meter (m)
foot-pound-force	1.355 818	joule (J)
gallon (U.S. liquid)	3.785 412 x E -3	meter^3 (m^3)
inch	2.540 000 x E -2	meter (m)
jerk	1.000 000 x E +9	joule (J)
joule/kilogram (J/kg) radiation dose absorbed	1.000 000	Gray (Gy)
kilotons	4.183	terajoules
kip (1000 lbf)	4.448 222 x E +3	newton (N)
kip/inch^2 (ksi)	6.894 757 x E +3	kilo pascal (kPa)
ktap	1.000 000 x E +2	newton-second/m^2 (N-s/m^2)
micron	1.000 000 x E -6	meter (m)
mil	2.540 000 x E -5	meter (m)
mile (international)	1.609 344 x E +3	meter (m)
ounce	2.834 952 x E -2	kilogram (kg)
pound-force (lbs avoirdupois)	4.448 222	newton (N)
pound-force inch	1.129 848 x E -1	newton-meter (N-m)
pound-force/inch	1.751 268 x E +2	newton/meter (N/m)
pound-force/foot^2	4.788 026 x E -2	kilo pascal (kPa)
pound-force/inch^2 (psi)	6.894 757	kilo pascal (kPa)
pound-mass (lbm avoirdupois)	4.535 924 x E -1	kilogram (kg)
pound-mass-foot^2 (moment of inertia)	4.214 011 x E -2	kilogram-meter^2 (kg-m^2)
pound-mass/foot^3	1.601 846 x E +1	kilogram-meter^3 (kg/m^3)
rad (radiation dose absorbed)	1.000 000 x E -2	**Gray (Gy)
roentgen	2.579 760 x E -4	coulomb/kilogram (C/kg)
shake	1.000 000 x E -8	second (s)
slug	1.459 390 x E +1	kilogram (kg)
torr (mm Hg, 0^0 C)	1.333 22 x E -1	kilo pascal (kPa)

*The bacquerel (Bq) is the SI unit of radioactivity; 1 Bq = 1 event/s.
**The Gray (GY) is the SI unit of absorbed radiation.

TABLE OF CONTENTS

Section		Page
	SUMMARY	ii
	CONVERSION TABLE	iii
	FIGURES	vi
	TABLES	vii
1	INTRODUCTION	1
	1.1 GENERAL	1
2	BACKGROUND	4
	2.1 PREVIOUS DEVELOPMENTS	4
	2.1.1 The Magnetic Sensor	4
	2.1.2 Tire Pressure Monitor	5
	2.1.3 Intruder Detection Using Piezoelectric Ignitors	5
	2.2 SUMMARY OF THE PHASE I WASP PROGRAM	6
	2.3 OBJECTIVES OF PHASE II	8
	2.4 FINAL PHASE II VERSIONS OF THE THREE SENSORS	9
3	MECHANICAL/ELECTRICAL ENERGY CONVERSION	10
	3.1 INTRODUCTION	10
	3.2 GENERATOR DEVELOPMENT	10
	3.3 DOORKNOB DRIVE MECHANISMS	12
	3.4 DOORJAMB DRIVE MECHANISMS	15
	3.5 WINDOW SENSOR DRIVE MECHANISMS	16
4	WIRELESS LINK TRANSMITTER AND RECEIVER	18
	4.1 INTRODUCTION	18
	4.2 FREQUENCY BAND OF OPERATION	18
	4.3 MODULATION AND SENSOR ENCODING	19
	4.4 300 MHZ BAND TRANSMITTERS AND RECEIVERS	21
	4.5 900 MHZ BAND TRANSMITTER AND RECEIVER	22
	4.5.1 Candidate Wireless 900 MHz Systems	24
	4.5.2 FCC Part 15 Requirements	25
	4.6 2.4 GHZ SPREAD SPECTRUM	27

TABLE OF CONTENTS (Continued)

Section			Page
5	ANTENNA DEVELOPMENT		30
	5.1	INTRODUCTION	30
	5.2	DIPOLE ANTENNAS	30
	5.3	COVERT MICROSTRIP ANTENNA	32
	5.4	THE MONOPOLE ANTENNA	32
6	MARKET ANALYSIS		34
	6.1	INTRODUCTION	34
	6.2	MARKET RESEARCH	34
	6.2.1	Government Markets	34
	6.2.2	Commercial and Residential Markets	35
	6.2.3	Special Opportunities for Hotel Application	35
	6.3	SUPERVISION	35
	6.4	RADIO FREQUENCY ALLOCATION	36
7	CONCLUSIONS AND RECOMMENDATIONS		37
	7.1	CONCLUSIONS	37
	7.2	RECOMMENDATIONS	38
8	DESCRIPTION OF THE APPENDICES		39

Appendix		
A	DEVELOPMENT OF A DIGITAL WIRELESS COMMUNICATION SYSTEM FOR SECURITY SENSOR APPLICATIONS	A-1
B	DESIGN AND GENERATION OF ORTHOGONAL PSEUDO-NOISE SEQUENCES FOR APPLICATION TO CODE DIVISION MULTIPLE ACCESS	B-1
C	INVESTIGATION OF AN INDOOR DIGITAL WIRELESS SYSTEM AT 900 MHZ	C-1
	DISTRIBUTION LIST	DL-1

FIGURES

Figure		Page
2-1	The batteryless magnetic sensor	4
2-2	Batteryless piezoelectric sensor	6
2-3	Rack and pinion version of batteryless sensor in doorjamb	7
2-4	Doorknob intrusion detection sensor	8
3-1	Gear-driven drive mechanism preliminary design	13
3-2	Gear-driven drive mechanism and flexible driveshaft	13
3-3	Cam and spring mechanism	14
3-4	Doorknob generator drive cam assembly	14
3-5	Rack and pinion drive components for doorknob sensor	15
3-6	WASP doorjamb sensor installed behind a door hinge	16
3-7	Window frame sensor	17
4-1	Surface mount 315 MHz transmitter and generator assembly	21
4-2	2.4 GHz spread spectrum link parameters	28
5-1	Totally flush patch antenna for metal door installation	32

TABLES

Table		Page
4-1	System requirements.....	23
4-2	Comparison between 200 and 900 MHz systems.....	26
4-3	System requirements and measured results.....	26
5-1	Measurement of radiated signal.....	31

SECTION 1
INTRODUCTION

1.1 GENERAL.

ANRO Engineering (ANRO) has pioneered the development of a number of innovative Wireless and Self-Powered (WASP) sensors for different applications. Applications for these sensors include traffic intersection control, tire pressure monitoring for vehicles, and intrusion detection and location identification for certain military and government installations. [1][2][3] The batteryless sensors derive their energy from the passing of a vehicle or person in close proximity to the sensor. Two advantages of WASP devices are (1) there are no battery replacements or external wiring necessary nor maintenance required and, (2) they are easy to install. These features represent significant cost savings and convenience in large-scale installations, and the sensors, themselves, are inexpensive. The sensors can easily be made physically covert, which is important both for cosmetic appearances and for sensitive installations. Indications of the presence, location, velocity, etc. of an intruder are transmitted via a radio link using self-generated energy. The signal transmitted is only a brief transient, typically lasting only a few hundreds of milliseconds, thereby lowering the probability of intercept for covert installations. A receiver is used to translate these coded signals to a "stretched" signal message for input to a monitoring system.

These batteryless sensors are ideal for monitoring entries over a wide-area, and may be monitored by a mobile unit. Experience, to date, indicates that the sensors require no maintenance. The sensors require no external power or cabling, have extended shelf and deployment lifetimes, and can be installed to be both cosmetically unobtrusive and physically covert. This class of sensor operates only upon detection of an event, otherwise, they remain silent. Information derived from these sensors could be used to assist in the detection and assessment of security threats against storage facilities and similar sensitive installations.

Some of the earlier WASP sensor concepts were invented over two decades ago by the Principal Investigator (PI) on the program described herein. A new member of the class of WASP Sensors was developed in this program for use with doors or windows to detect openings and closings. A receiver located in either a fixed or mobile installation detects a coded signal from the sensor, which identifies the particular door/window that has been opened/closed, and can time tag the response. The fact that no primary power is required for sensor operation is of significant importance to existing facilities where the cost of wiring in existing buildings is prohibitive. The benefit of not having to replace batteries is also important; batteries are costly to replace and maintain. Also, the periodic replacement of batteries reveals the location of the sensor, which

---

[1] G.F. Ross, et al., "Traffic Sensor", U.S. Patent #3,839,700 issued October 1, 1974.
[2] G.F. Ross, et al., "Vehicle Tire Condition Monitor", U.S. Patent #3,786,413, issued January 15, 1974.
[3] G.F. Ross, et al., "Development of a Batteryless Unattended Ground Sensor (UGS)", Contract #COW-3-90340, U.S. Department of Justice, Immigration and Naturalization, ANRO Report 83-3-T2, January, 1985.

then can be disabled by an intelligent intruder. The reliability of a WASP sensor is very high. The preferred energy source for this program is a microminiature generator manufactured by a Japanese firm. The actual movement of the door or window through a novel mechanical coupling mechanism spins the armature of the generator. The power supply filtering, coding and transmitter components are solid state chips which have, virtually, unlimited lifetime. The initial ANRO door/window sensor entitled, "Batteryless Sensor Used in Security Applications" was patented on May 31, 1994; Patent #5,317,303. An improvement patent, having the same title, based on work successfully completed under Phase I of this program, was issued on November 5, 1996, Patent #5,572,190. Under Phase II of this program, the new energy source is only 10 percent, in volume, of the original supply. Also, a new doorjamb and windowsill sensor version was developed, as well as a totally covert new doorknob model. In the totally covert doorknob model, the energy source is located within the doorknob and the antenna consists of a short length of wire; i.e., a monopole. What is significant here is that the installation consists of simply drilling a hole and replacing the doorknob key-set assembly. The turn of the door handle generates enough voltage to fully power the transmitter. Even if the intruder tries to turn the knob as slowly as possible, it doesn't make a difference because the new version is spring-loaded to spin the generator once a certain limit point is passed.

Covertness is also an important issue for this class of sensor. The sensors can be made covert, as described above, in the sense that one cannot tell the presence of the device. It can also be made cosmetically covert where wires are not observable or, at worst, a small 3/8 inch rod (i.e., for the doorjamb and windowsill application) is all that is discernible. The several hundred-millisecond duration signal radiated, which is a transient, is extremely difficult to detect by any type of coherent processing receiver.

The use of WASP sensors also has significant attraction in the commercial and do-it-yourself home security markets. ANRO teamed with the Advantor Corporation, a security systems company, which has made a market survey of the business opportunities for the WASP sensors and has helped ANRO develop a surface mount model of the transmitter used in each version of the device. ANRO, for example, has reduced the potential cost of the doorknob sensor from $860/device for the original version to what we believe now should cost under $5 in large quantities. We are currently exploring commercial business opportunities for the class of WASP Sensors developed on the program. Also, the results of our study have suggested the development of batteryless locks for use in hotels and motels. This is presently under investigation.

It is important to note that these sensors do not include a complete "supervision" function. Supervision involves checking periodically that the sensor is in place and operating. Without an energy source that is operated by an actual "opening" or "closing", we can only check the operation of the electronics by using an energy storage device (e.g., a capacitor). We believe that a capacitor can check the electronics "hourly" providing there are, at least, several "openings" or "closings" a day using the sensor.

We believe that this has been a very successful program and it remains for ANRO to explore both commercial and governmental Phase III programs for the production and installation of new WASP devices.

This report is divided into six other sections. In Section 2, some of the earlier sensors are described together with the objectives for this program. The details of the mechanical/energy generation scheme used in the current selection of WASP sensors is described in Section 3. The transmitter and the development of the UHF (AA Hz through BB Hz), L (CC-Hz through DD Hz), and S-band (EE Hz through FF Hz) receivers is discussed in Section 4. The development of antennas used for wooden as well as metal doors and windows is outlined in Section 5.

A major output of the Phase II program was the development of reproduction assemblies. Another key parameter here was cost. The trials and tribulations of this design are detailed in Section 6 for the doorknob, doorjamb, and window modes.

Finally, conclusions and recommendations are presented in Section 7. Appendix A describes the work done under the program on digital communications, Appendix B discusses an investigation on the design and generation of pseudo-noise sequences for application of Code Division Multiple Access (CDMA), and Appendix C discusses an investigation of an indoor digital wireless system operating at 900 MHz.

SECTION 2
BACKGROUND

2.1 PREVIOUS DEVELOPMENTS.

ANRO began its investigation of WASP energy sources in the early 1970s with the development of automobile monitoring devices, tire pressure monitors and intrusion detection as described briefly in the sections that follow.

2.1.1 The Magnetic Sensor.

The concept of a batteryless sensor using WASP techniques was initially developed and patented by Dr. Gerald F. Ross, founder of ANRO, for use as a vehicle traffic sensor. The basic idea of the initial batteryless sensor was simple. It consisted of using two opposing magnets mounted on iron pads and separated by a soft iron connecting rod as shown in Figure 2-1. The rod served as the core for a 20,000 turn, No. 28 wire, solenoid. When a ferromagnetic body such as the under-carriage of a vehicle (for example, a car, truck or train) passes over the buried sensor, a voltage, V, is produced by the solenoid in accordance with Faraday's Law, where $V=N\frac{Nd\varphi}{dt}$, where N is the number of turns and $d\varphi$ the differential flux lines cut by the vehicle in a given time increment dt. The output voltage, an oscillatory transient, is of sufficient amplitude to power a VHF transmitter with an effective range of about 200 feet. The duration and amplitude of the oscillatory burst depended upon the speed and height of the vehicle above the coil. To be effective, the vehicle must be in motion over the sensor. As previously indicated, a U.S. Patent was issued on this invention. The DoT of the State of California experimented with the use of the sensor. Today, with the availability of new, rare earth magnetics having a Gauss-Oersted product 50 times greater than was available in 1974, these sensors can be made much lighter and less costly.

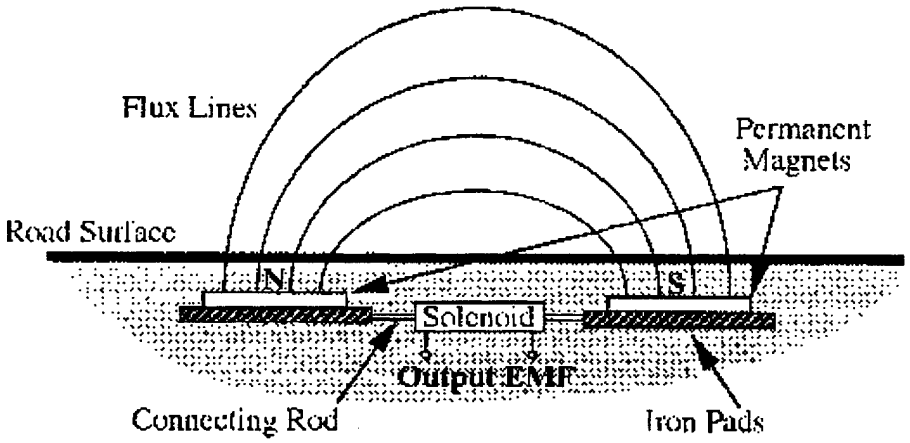

Figure 2-1. The batteryless magnetic sensor.

2.1.2 Tire Pressure Monitor.

Following the development of the magnetic traffic sensor described above, a second type of batteryless sensor was developed to monitor tire pressure on large trucks based on the energy available from a rotating wheel. Large trucks may require as many as 16 expensive tires. Tires wear quickly when tire pressure is too low; hence, the motivation for early detection of low tire pressure. Here, the energy necessary to power an oscillator source was generated by a resonant mechanical system excited by the nonharmonic acceleration at the wheel rim. A switch attached to the tire fill valve closed when the tire pressure fell below a preset threshold connecting the energy source to a frequency coded oscillator. A VHF signal was radiated to a display in the cab where the switch closure indicated a particular tire pressure was too low and identified the tire. This is also an important safety feature that may some day be extended to passenger vehicles. This patent was licensed to the Ryder Corporation circa 1980.

2.1.3 Intruder Detection Using Piezoelectric Ignitors.

Later, a third type of batteryless sensor using piezoelectric techniques was developed in the mid-1980s for use by the Immigration and Naturalization Service (INS), Department of Justice. The task was to detect the presence of illegal immigrants crossing certain sectors of our border. The advantage of a batteryless sensor, as shown before, is that there are no maintenance or battery replacement costs and the possibility of detection and theft of the sensor itself is minimized.

For the INS application, a piezoelectric energy source was chosen. It was found that simple push-button ignitor similar to those used in a commercial gas barbecue could be mounted in a special set of hydraulic cylinders (as shown in Figure 2-2) and could generate sufficient energy to radiate a VHF signal to a remotely located repeater. A Pascal cylinder arrangement was used to trade force for displacement; the equivalent of a mechanical transformer. Four pounds of force, and a 2-3/8 inch displacement were required to trip the spring-loaded ignitor. A human stepping on the sensor buried in sand four inches below the surface resulted in about 40 pounds force applied to the ignitor. The mechanical advantage provided by the Pascal cylinders was used to reduce the displacement in about the same proportion. It was estimated that the sensors shown in Figure 2-2 cost about $50 each, in quantity, and could be used to seed a preferred corridor of entry much like a minefield. The signal produced by an intruder stepping on (or very close to) the sensor is, once again, radiated by a coded oscillator source to a remote receiver used to determine entry. The sensor was used experimentally to detect illegal border crossings by the INS.

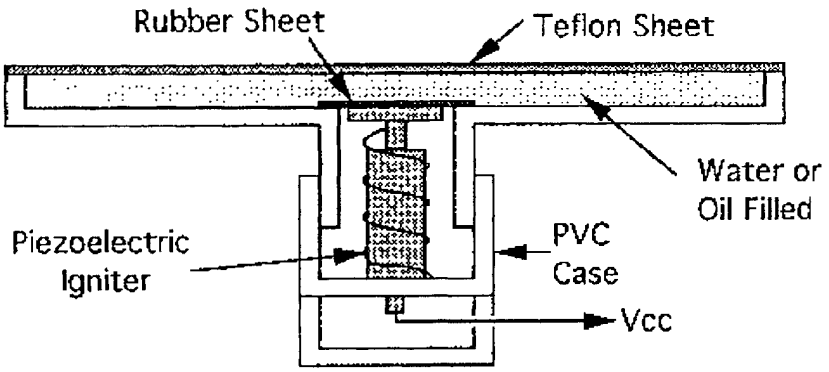

Figure 2-2. Batteryless piezoelectric sensor.

2.2 SUMMARY OF THE PHASE I WASP PROGRAM.

In 1990, ANRO developed a fourth type of WASP sensor to detect window and door openings/closings for drug interdiction application. This sensor served as the basis for the feasibility model for both the Phase I and Phase II programs described in this report.

ANRO first proposed to use a "squeeze type" piezoelectric sensor for this application. This device was preferred over the push button ignitor described earlier because of the geometry of the application. One problem associated with the push button ignitor is that it gives a large audio report each time it is activated. The audio report is difficult to muffle and, consequently, may reveal the sensor location. Also, a squeeze-type device contains twice as much PZT (Lead Titanate Zirconate) piezoelectric material as found in the ignitor and is capable of generating 20 times more energy because of the method in which the force was applied. Unfortunately, the manufacturers have stopped making squeeze devices; only the push button ignitor, today, is made in mass production. The result is that the cost of the squeeze ignitors is prohibitive.

For this reason, ANRO elected to choose a different approach. The result was the basis door/window sensor patented by ANRO in May 1994.[4] The patent covered a linear translation of a rod, located in the jamb of a door or window, which is depressed, for example, when the door is closed, to a rotary motion used to turn a miniature permanent magnetic (PM) generator through the action of a belt and pulley. Although a miniature generator and associated gear train were employed, the size of the unit was still judged too large (e.g., 2.3 cu. inches) for general installation.

A new off-the-shelf subminiature PM generator/gear train assembly was chosen on Phase I of the WASP program which made the installation much more practical. The gear and pulley

[4] G.F. Ross, et al., "A Batteryless Sensor Used in Security Applications", U.S. Patent #5,317,303, issued May 31, 1994.

arrangement used earlier was replaced by a more efficient rack and pinion, or spur gear, eliminating the belt and possible malfunction. The rack and pinion arrangement is shown in Figure 2-3.

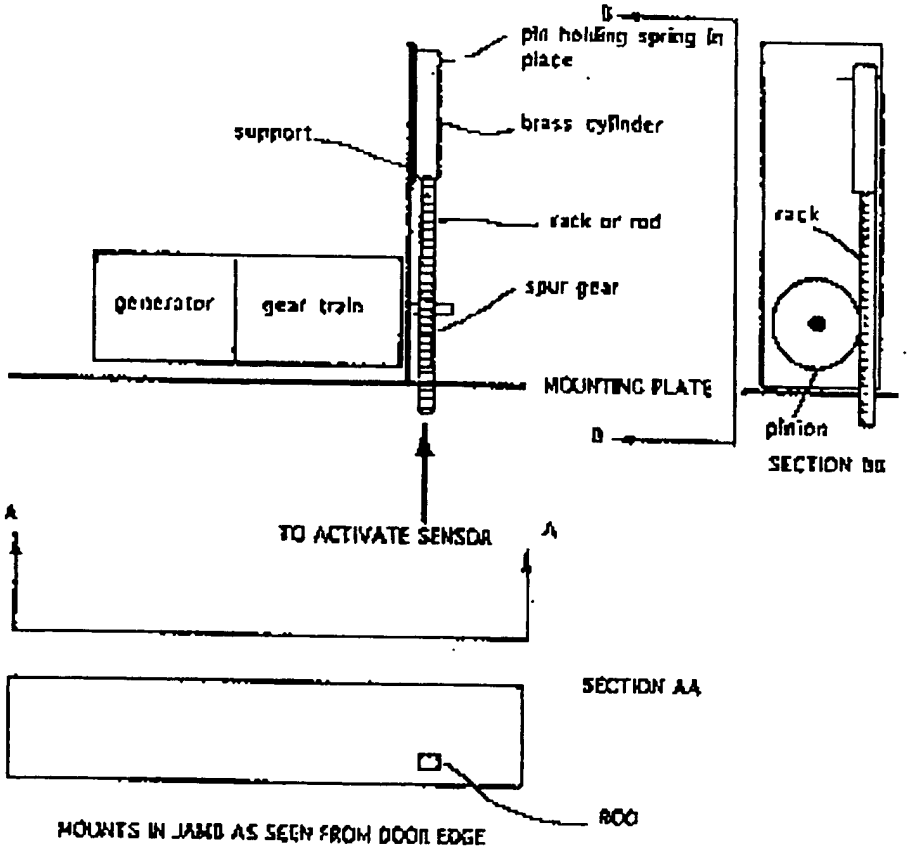

Figure 2-3. Rack and pinion version of batteryless sensor in doorjamb.

A second technique was developed under Phase I to actually place the new subminiature PM generator/gear train and transmitter into a doorknob, converting the rotation of the knob directly into a turning of the generator. The UHF oscillator (~50 MHz) contained in the electronics is attached in such a manner that an intruder, holding the knob, actually serves as the antenna. This scheme was successfully reduced to practice and a second patent was issued by the U.S. patent office based on this design.[5] The doorknob installation is shown in Figure 2-4.

[5] G.F. Ross, et al., "Batteryless Sensor Used in Security Applications", U.S. Patent #5, 572,190, issued November 5, 1996.

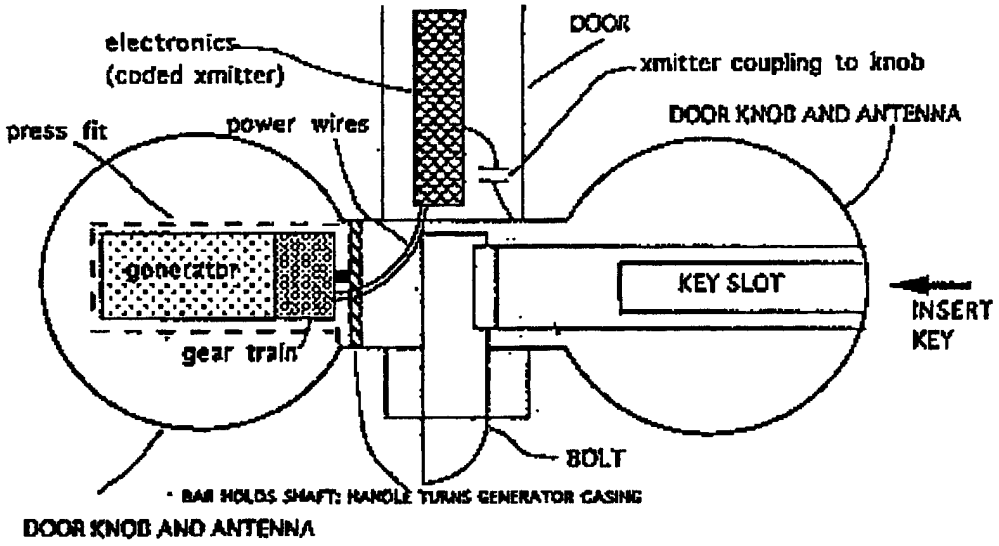

Figure 2-4. Doorknob intrusion detection sensor.

2.3 OBJECTIVES OF PHASE II.

The objectives of Phase II were to take the sensors, developed under Phase I to prove feasibility, and reduce them to devices that could be manufactured for a cost that was competitive with other approaches.

While working on Phase I, one manufacturer offered for sale a wireless sensor using a long life lithium battery for sensing door opening/closing. The initial cost was $70, which is now being offered for $50/door. This unit has the advantage of providing supervision; that is, it can power the oscillator each hour to indicate that the battery and circuitry are still functioning. It was clear from products currently being offered to the public that for a WASP sensor to be marketable, the cost must be less than $10. This was the prime cost objective of the Phase II program. We believe that we accomplished this task with the final version of the doorknob sensor shown in Figure 3-5 where the cost of $5 per device is reasonable. This version of the doorknob sensor proves the concept and is a primary result of the Phase II program.

A major technical objective of the Phase II program was to develop a mechanical mechanism that would store potential energy no matter how slowly the doorknob was turned. Then, when a prescribed limit point was reached, all the energy would be released and used to spin the generator. Since voltage is a direct function of turning speed, it was feared that an intruder who suspected the presence of a sensor would just turn the knob so slowly as to escape detection. Although the window sensor could be spoofed in this manner, experiments showed that it was difficult to avoid detection because of the large mechanical advantages here as well as the need to overcome friction.

Finally, size and space constraints were a major objective. The doorknob device had to be adaptable to other locks and a means for easy installation had to be established. ANRO believes that we have satisfied all the objectives of the program.

2.4 FINAL PHASE II VERSIONS OF THE THREE SENSORS.

In addition to the doorknob sensor shown in Figure 3-5, under Phase II we developed a doorjamb and a window opening/closing sensor. Final versions of these sensors are shown in Figures 3-6 and 3-7 respectively.

SECTION 3
MECHANICAL/ELECTRICAL ENERGY CONVERSION

3.1 INTRODUCTION.

In Phase I, a generator was developed to power the wireless transmitter. A small motor was turned at high speed by a set of gears. The motor was turned either by a linear motion, or a rotary motion, such as in a doorknob. The motor/gear train assembly used in the Phase I concept demonstration, however, was expensive, costing about $60; the motor was manufactured in Switzerland, and the gear train was manufactured in Germany, which could lead to further price increases.

The motor/gear assembly that produced enough power to meet the design specifications was actually designed to operate as a motor, not a generator. This meant that the gear train was driven in reverse from the motor drive to create a voltage. The wear and torque experiences in the generator application could cause premature failure in the unit. A new solution was sought in Phase II.

Testing in Phase I also revealed that if the doorknob was turned very slowly, the sensor could be defeated because an insufficient voltage level was generated. By turning the knob slowly, the motor was not turned rapidly enough to create the minimum level of voltage to operate the wireless transmitter. Therefore, the second major design objective in Phase II was to develop a mechanism that would ensure that the motor would spin rapidly enough to fire the transmitter, regardless of the rate of motion. An escapement type mechanism was developed so that no matter how slowly the motion that powered the generator moved, a spring was released that spun the generator at a sufficient rate. In the case of the doorknob, when turned past a point before the latch was released, normally 60 degrees of rotation, the escapement is released to power the transmitter. The important design considerations were reliability, silent non-tactile motion, and low cost.

The program plan included development of three types of drive mechanisms for integration with the generator and wireless transmitter. These are a doorknob, a window and a doorjamb installation. The motion associated with each of these drive mechanisms encompasses rotary, sliding, and linear motion. From these basic types of motion, the WASP sensor can be adapted to a very wide variety of applications.

3.2 GENERATOR DEVELOPMENT.

The required power specification was established at 5 volts, for a 5 millamphere (mA) transmitter load over a period of 250 milliseconds (ms) for a reasonable transmission range. The first approach attempted to locate a cheaper voltage source was to build our own low-cost generator mechanism. Our mechanical engineer designed and constructed a prototype stator/coil/rotor mechanism. These components were assembled and tested in the Florida

laboratory to evaluate feasibility. A solenoid was wound around the base and a coin-shaped magnet was spun around the A-axis. This first attempt was unsuccessful due to the low voltage output.

The investigation then moved to research suitable new rare earth magnets to be used in the construction of the generator. Various sample types and sizes were procured, producing over 500 Gauss. The first breadboard generator produced about 30 millivolts (mV) at 180 revolutions per minute (rpm) with a 100-turn coil.

The next generator mechanism consisted of a three-piece magnetic circuit including two pole pieces and a stator bar. The pole pieces and stator bar were machined out of iron stock. The frame of the device was machined out of brass so as not to interfere with the magnetic circuit. A coil, consisting of 100 turns of #36 magnet wire was wrapped around the stator bar, and the shaft, a brass rod with a neodymium-iron-boron type 27 permanent magnet imbedded in the area between the pole pieces, was spun at 1000 rpm. The output of the coil was connected to a step-up transformer (8:220), and a peak voltage of 1 V measured into a 1 megohm input impedance was observed. These tests indicated that a still higher output was required.

A third power generator mechanism was devised consisting of three magnets, and a larger coil. The three magnets were situated in the shaft at 120-degree intervals to provide more voltage peaks in a single rotation. Tests of this unit also showed unsatisfactory results. Dr. Walter Kahn reviewed the design and enhancements were identified which improved the output of this device significantly.

An adjustable test bed was constructed for different armatures and stators to be tested at different speeds. Coils of 100, 200, 500 and 1000 turns of #28 magnet wire were wound on similar hand-made stators of soft iron with a nominal cross section of ¼" by 1/8". The poles of the stator were positioned 1", center to center.

Rotors were fabricated using the same rare earth magnets utilized before, but positioned on the edge of a ferrous rotor to allow minimal distance from the magnet face to the stator for maximal magnetic coupling. Two rotors were fashioned; one using two magnets, and one using six magnets. The electrical characteristics of the 1000 turn stator were measured, and the DC resistance was found to be 9Ω, while the AC impedance was found to be 30Ω (DC resistance required to reduce the unloaded output by ½).

Both a transformer and a capacitive voltage multiplier circuit were tested to boost the output voltage level to the required amount. For both cost and efficiency reasons, a voltage quadrupler was investigated. This circuit produced an output of 5.3 volts into a 1000Ω load at 3000 RPM. The cost of the generator was then estimated to be less than $10. While this was a significant improvement, it was desirable to further reduce the cost, and to possibly avoid manufacturing our own generator mechanism.

A renewed effort was undertaken to obtain a commercially available motor that could be used as a generator. This meant that the gear train, if used, could not be an integral part of the motor assembly. Several gearing approaches were investigated to be used with a commercial motor. After some searching, a suitable DC motor was found. The motor manufacturer, Mabuchi, supplied a number of candidate motors that would cost under $2.50 in quantity. This was much more attractive than a special motor assembly that had to be developed internally. The motor selected, model 1302-RED, develops 4.5 volts under open circuit conditions, and 4.26 volts under a 1-kohm load. The motor measures just under 1 inch in diameter, and is 1.5 inches long, which is quite satisfactory for integration into the drive mechanisms and with the sensor wireless transmitter.

3.3 DOORKNOB DRIVE MECHANISMS.

A deficiency that was found in the Phase I prototype sensor was that if the knob was turned very slowly, and then returned to the neutral position very slowly, that activation of the transmitter was avoided. This situation was not likely to be encountered if the person opening the door was not aware of the presence of the sensor. However, as indicated in the previous section, an escapement mechanism was required to circumvent this problem. This mechanism was developed as a part of the doorknob drive mechanism, and is not discernable to the person opening the door. Based upon what was learned in the Phase I program, the following were identified as design goals for the doorknob sensor:

- The drive mechanism must not require a force that is readily detectable by a person activating the sensor (door, window, etc.)
- The drive mechanism must work in either direction when activated (e.g., a doorknob).
- The drive mechanism must work even if the activation motion is very slow. For example, cannot be defeated by turning the doorknob very slowly.
- Must be mechanically strong enough to be used in either direction.
- Must be hidden from the intruder.
- Must be very low cost.

As no off-the-shelf devices could be located, the assistance of two mechanical engineers was sought. The two engineers worked independently, on separate approaches because of the critical nature of the component. These are described below.

The first approach utilized a series of plastic gears mounted internal to the lockset mechanism. The motion of the doorknob places a load on a spring, which releases before the door latch disengages. The released spring energy drives the motor generator shaft to provide voltage to power the transmitter. Figure 3-1 shows a drawing of the mechanism.

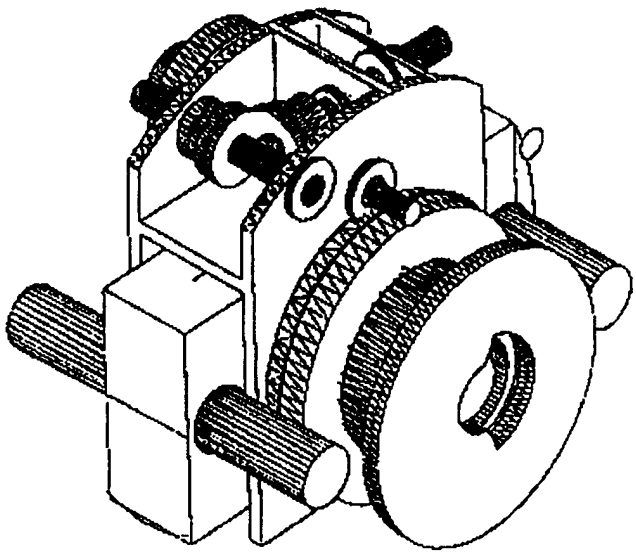

Figure 3-1. Gear-driven drive mechanism preliminary design.

A refinement of this design involves a compression spring with 10 to 12 pounds of force through a linear movement of 0.4 inches. The spring is installed in radial groves in a circular gear. One groove in the main gear and the other groove in a cam. Also installed in the grooves are two ball bearings at the ends of the springs. When the cam turns in either direction, it forces one of the ball bearings to move and compress the spring. Then the cam releases the main gear by depressing the escapement, the main gear rotates due to the build-up force in the spring. The force is transferred to the other ball bearing and forces the gear to turn. Figure 3-2 shows the gear-driven drive mechanism installed with the generator at the end of the flexible drive shaft.

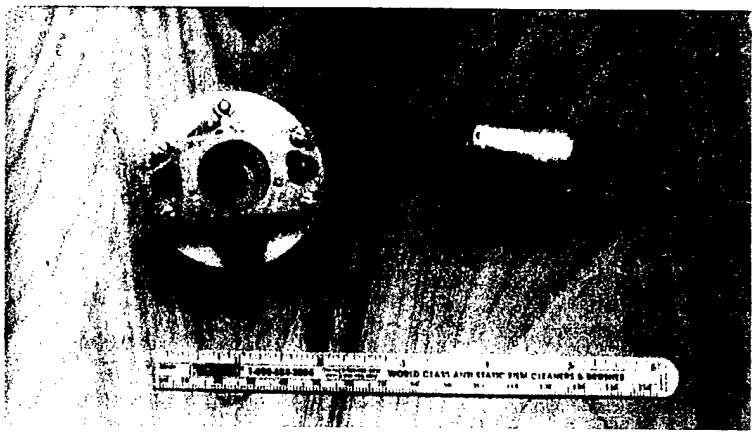

Figure 3-2. Gear-driven drive mechanism and flexible drive shaft.

The second design pursued involves a cam mounted on the shaft of the doorknob. Under rest conditions, the cam holds a spring under tension such that an off-center gear is held at a neutral position. When the doorknob is turned in either direction, the off-center gear turns other gears to generate sufficient rotational speed and duration to power the transmitter. Figure 3-3 shows a sketch of the mechanism. While functional, this design required a large force to be exerted to turn the doorknob, which did not meet the requirement for an undetectable installation.

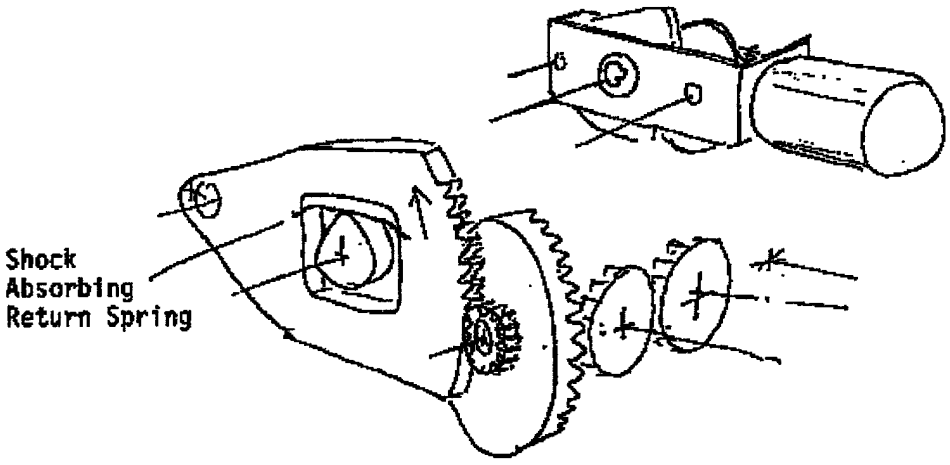

Figure 3-3. Cam and spring mechanism.

An even simpler and less costly solution was still needed. This was achieved by using a drive mechanism that used simple friction to spin the generator shaft. The friction surfaces had to provide a positive drive force without excessive drag on the mechanism. A number of surfaces were investigated, including cork, rubber, sandpaper and plastic. Figure 3-4 shows one of the test assemblies using a sandpaper surface.

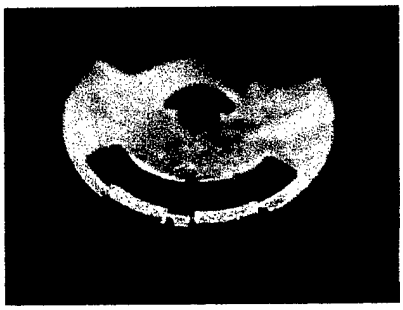

Figure 3-4. Doorknob generator drive cam assembly.

None of these proved satisfactory, and another design evolved that used a fine-tooth rack and pinion arrangement. The periphery of the cam was fitted with a curved row of teeth, and a simple gear was placed on the shaft of the motor. The resting position of the doorknob assembly is in

the center position. When the knob is turned in either direction, the gear engages the cog on the shaft, and turns the generator and simultaneously winds a spring. When the knob is turned about 30 degrees, which is before the latch is disengaged, the row of teeth is disengaged from the cog, and the spring is released. The generator then spins freely back in the other direction. If the doorknob is turned fast enough on the opening sequence, the generator will cause the transmitter to send a signal on the initial movement, as well as on the return. If the doorknob is turned slowly, then the free-spinning generator will fire the transmitter on the return movement. Figure 3-5 shows the five components of the rack and pinion drive for the doorknob sensor.

Figure 3-5. Rack and pinion drive components for doorknob sensor.

This mechanism has proven to be reliable, silent and most importantly, very low cost to manufacture. There are only 5 parts involved, including the spring, and the two circular cams are exactly alike. The two screws in the upper left corner are used to connect the two circular cam sections. The metal parts can be stamped or made of cast metal, and the estimated cost in large quantities is only *11 cents*. Including the generator and transmitter, the total cost of the doorknob mechanism should be less than $5.00.

3.4 DOORJAMB DRIVE MECHANISMS.

A doorjamb mechanism was developed based on a spiral, rotary shaft drive. The familiar "Yankee screwdriver" uses this type of drive to convert a linear pushing motion into a rotary motion. As a person presses downward on the handle, a prong engages a spiral cut into the shaft that causes the shaft to spin.

A problem similar to the doorknob drive mechanism is encountered in the rate at which the motion occurs. If the door moves very slowly, then the drive turns correspondingly slowly. An action was added to the drive mechanism to cause the motion to build up spring tension that is released at a point before the door is open sufficiently wide to allow entry or exit.

As this sensor is designed to be installed in the hinge of a door, there is not much linear motion involved. As the door swings open just wide enough to allow entry or exit, there is only about 1 inch of movement. Therefore, the doorjamb drive must be activated with a small amount of linear motion. Fortunately, there is a huge force available near the door hinge point, and the amount of

leverage needed to activate the sensor is not detectable to an intruder. Figure 3-6 shows the completed doorjamb sensor installed in the hinge area of a door. One rod winds the spring mechanism, and the other senses the opening and closing of the door, which releases the spring drive to spin the generator.

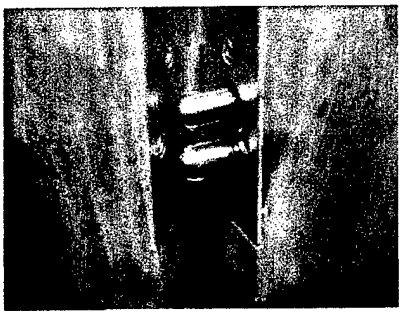

Figure 3-6. WASP doorjamb sensor installed behind a door hinge.

3.5 WINDOW SENSOR DRIVE MECHANISMS.

There are two applications for a window sensor drive mechanism. One is for a drive that is based on the bottom or top of a window, so that when the window is opened, a linear motion is present. However, if the window is already partially open, then the action is not present at the top or bottom of the window.

If a sensor is desired to be installed at the top of bottom of a window that is normally closed, then the same "Yankee screwdriver" drive mechanism that is used in the doorjamb can be employed. However, for a sensor that will work whether the window is open or closed, then a different type of drive is required. The motion is linear, but the drive uses a sliding motion as the window moves past the sensor.

A drive mechanism was designed and constructed that employs a rubber roller wheel that presses up against the window frame, such that when the window moves, the rubber wheel turns and spins the generator. A high gear ration is used to ensure that the generator here spins rapidly enough to power the transmitter.

A mounting frame is used to support the sensor behind the window frame of either side of the window, and a metal sleeve encompasses the sensor and the drive mechanism. The metal sleeve has a spring to keep tension on the wheel against the edge of the window as the window is moved up or down. Figure 3-7 shows the window frame sensor and drive mechanism, without the metal sleeve for clarity. A window sensor was mounted in a miniature window frame constructed especially for this program to test and demonstrate the operation of the sensor.

Figure 3-7. Window frame sensor.

In summary, we developed and successfully reduced to practice three versions of the mechanics for the WASP sensor under Phase II. These include (1) the doorknob device shown in Figure 3-5, (2) the doorjamb device shown in Figure 3-6, and (3) the window frame sensor shown in Figure 3-7.

SECTION 4
WIRELESS LINK TRANSMITTER AND RECEIVER

4.1 INTRODUCTION.

The concept for the Wireless and Self-Powered (WASP) sensor is based on a wireless link that is powered solely by the motion of the intruder. The wireless link is designed to be a short-range system. The distance that can be covered is a function of a myriad of variables, such as the building structure (concrete, wood frame, metal, etc.), the type of door and door frame (metal or wood), and the location of the receiver.

It was visualized that a number of sensors could be located in a small area, and be served by a single receiver, such as in a home installation. For this reason, the transmissions are coded to identify which sensor has sent an alarm. The receiver can be a stand-alone annunciator, or can be integrated with a central alarm system where the transmissions are time-tagged and logged, and the location of the alarm indicated on an annunciator panel.

In Phase I, a simple prototype transmitter was used that exhibited a higher false alarm rate than was acceptable, as well as a limited number of discrete codes (less than 20). For this reason, alternative transmitters and encoding techniques were investigated extensively.

4.2 FREQUENCY BAND OF OPERATION.

The Phase I wireless transmitter and receiver operated near 50 MHz, in the old cordless telephone and garage door opener band. Licensing by the FCC is not required under Part 15 for this type of operation. This frequency band and the components were chosen in Phase I due to easy availability and low cost. A severe limitation on this band is the restriction on the number of discrete channels or coding available to handle more than a few collocated sensors. Due to the heavy use of this band, interference is also a concern, which can lead to both false alarms and missed signals.

Investigation showed that three other license-free bands are good candidates. These are in the region of 300 MHz, and in the 900 MHz Industrial, Scientific and Medical (ISM) band, and in the 2.4 GHz ISM band. The goal was to select a frequency band for operation that is acceptable on a worldwide basis. Different countries, and even different regions of some countries, control radio frequency usage under their own guidelines. An investigation by Mr. Antonio D'Angelo, associated with the DSWA sponsor office, found that the 300 MHz region is acceptable on nearly a worldwide basis, particularly at US Army bases.

Mr. D'Angelo also indicated that the army controls spectrum usage very tightly – more so than, say, the FCC. Spectrum users must be registered centrally, allocated globally, and assigned locally before each user can operate. He met with the Joint Spectrum Center and discussed frequency selection for our program, and received information that the 300 MHz band happens to

be a very good choice as it is broadly available worldwide, and the power levels are within acceptable limits.

The registration process will require additional information. If DSWA decides to go forward with the application process, Mr. D'Angelo will likely be involved in the process, and anticipates no problems. At a Program Review in Orlando on May 9, 1996, it was concluded that the 300 MHz band would be the best choice, and that future developments would focus on that region. The other frequency bands were investigated as alternatives, both as primary sensor links and a potential wireless relay link.

4.3 MODULATION AND SENSOR ENCODING.

A series of encode/decode devices were located that provided sufficient coding to uniquely identify the sensors in any anticipated deployment scenario. Devices manufactured by Holtek, for example, use pulse width modulation and are available on 8 or 12-bit configurations. Variable address and data bit lengths are also available.

Holtek provided a working demonstration model of the device using a 310 MHz surface acoustic wave (SAW) transmitter and receiver on small circuit boards. The transmitter provided an output of about 2 milliwatts (mW). The demonstration models were used to test compatibility with the WASP Sensors.

Work at the Rochester Institute of Technology led by Dr. Joseph DeLorenzo concerned the development of algorithms, components and hardware available for use in the ISM bands at 900 MHz, 2.4 GHz and above. A portion of this investigation involved the use of ALTERA chip technology and Gold code spread spectrum techniques such that each user in a network has their own addressable code. CDMA techniques are used to provide sufficient access channels. The work focused on baseband circuits and components. Construction of sample wireless components was then undertaken.

This investigation led to further work in spread spectrum communications techniques. A number of specific objectives were set forth, including the following:

- Determine methods of generating coding structures that have the following properties
    - Applicable (efficiently) to systems that have both small and large numbers of users.
    - Have good correlation properties (low cross correlation properties between signals within its own structure as well as other signals anticipated to be in the environment). Gold codes and Bent codes were studied.
- Develop analytical methods to design, analyze and simulate the performance of the code structures.

- Ensure compatibility of code structures with programmable hardware that is within the low power and size constraints of personal communications devices.

- Determine the applicability of the developed concepts to a broad array of PCS multiple access problems.

The results of these studies were published in program quarterly reports, and are included in this report as Attachments B "Design and Generation of Orthogonal Pseudo-Noise Sequences for Application to Code Division Multiple Access", and C "Investigation of an Indoor Digital Wireless System at 900 MHz."

The salient results of the investigation were:

1) It was shown that Gold codes have good correlation properties relative to signals in its structure and can be implemented using programmable hardware (Altera EPM5032).

2) Analytical methods to design, analyze and simulate the performance of the code structures have been developed.

3) A study of system design problems and some model development relative to methods of dealing with indoor propagation attenuation at 900 MHz was carried out.

The Statement of Work (SOW) called for ANRO to investigate newly developed techniques, which could support the development of the WASP sensors. As discussed in the proposal and at subsequent meetings, low transmitter power consumption and a low radiated power level are desirable for system reliability and covertness. These requirements are balanced against the need for a low false alarm rate, and a high probability of detection of valid alarms.

The selection of the operating radio frequency band is affected by a number of factors, including government regulation (licensing), interference, and size of the components, principally the antenna. For the initial prototype units, it was decided at the 6-month design review to proceed with the nominal 300 MHz band, and pulse width modulation.

Other frequency bands and modulation techniques are potentially available, the most applicable of these are the ISM bands. These bands are attractive due to the higher radio frequency (900 MHz and above), and the resulting small antenna size. In addition, the market forces for use in these bands for cellular telephones, for example, is driving the availability of components upward rapidly, while driving down costs. The principal concern with the ISM bands is interference, due to the rapidly increasing numbers of users. Multipath signals are also a concern at the higher frequencies.

Spread spectrum coding techniques, coupled with the ISM hardware, appear to be a sound point for addressing these concerns. The continued investigation into the suitability of off-the-shelf PCS components to provide small, reliable, low-cost wireless communications for self-powered

sensors is considered warranted as a back-up or alternate means of alarm transmittal. In addition, this technology has broad applications in dual-use markets.

The investigation into the use of low-cost wireless components coupled with spread spectrum coding structures for reliable, low-cost, short-range data transmissions indicates that this technology offers significant advantages and an opportunity for use in a very broad range of applications.

4.4 300 MHZ BAND TRANSMITTERS AND RECEIVERS.

At the Program Review meeting in November 1996, the 300 MHz band transmitter and receiver, and sample motors were presented to Advantor for further testing and development, and for integration with the transmitter and generator. The specific frequency was 315.0 MHz.

Advantor generated a configuration of the motor with the transmitter mounted on two circular circuit boards sandwiched on the rear of the generator. The circuit boards are the same diameter as the motor, and extend the length of the motor by only about 5/8-inch. Figure 4-1 shows the two components of the surface mount miniature 315 MHz transmitter and the two components stacked and mounted on the end of the generator. The antenna extends beyond the circuit boards.

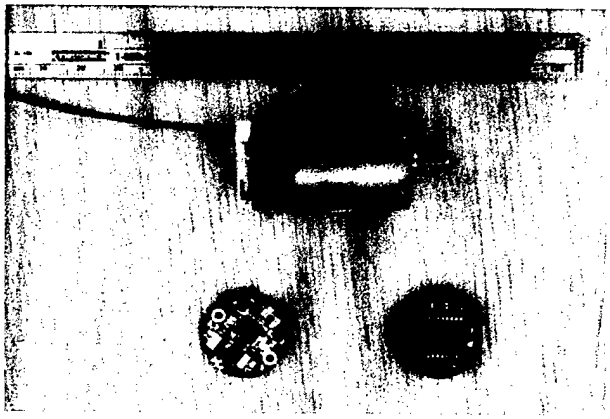

Figure 4-1. Surface mount 315 MHz transmitter and generator assembly.

A total of 35 surface mount technology 315 MHz transmitters were built by Advantor for evaluation and use on this program. These transmitters have an output of less than 10 mW. The field strength is highly dependent upon the antenna, and the output field strength can potentially exceed the maximum allowed by the FCC under Part 15, unlicensed operations. In the applications for the WASP sensor, however, the antenna will normally be in a nonoptimum configuration, and the output field strength will not exceed FCC rules.

Part 15 of the FCC rules allow for intermittent operation of transmitters. The anticipated operation of the transmitters is much less than a 1% duty cycle. Each door activation, for example, sends a coded message with duration of less than ¼ second. Typically, four pulse trains are sent per activation to increase the probability of reception by the receiver. The individual pulses are either 1 or 0.5 ms in duration (pulse width modulation), and are sent at intervals of 1.5 ms. There is approximately a 20 ms pause between each of the for transmission bursts.

Four doorknob sensors were built and demonstrated at the Department of Defense (DoD)-sponsored Force Protection Equipment Demonstration (FPED) held at Quantico Marine Base, Virginia in September 1997. In spite of the very heavily congested radio frequency (RF) environment during the event, not a single false alarm or missed signal occurred, demonstrating the robustness of this modulation technique.

A Ming companion receiver to the transmitter has been evaluated for operation and was important to prove the concept. It has a range of about 125 – 150 feet together with the present transmitter design. A different receiver (TRF 1400 Marcstar) was received from Texas Instruments to evaluate for additional sensitivity and therefore, range. Surface mount technology (SMT) is used in this receiver, which has been assembled and was tested. It exhibited a range in excess of 500 feet. A third receiver built by Telecontri, and Italian firm using a super regenerative technique exhibited a range of 375 feet. The Texas Instruments unit, which has a cost on the order of $20, was selected as the best choice.

Each of the deliverable hardware sensors on the program utilizes the 315.0 MHz wireless link, and the pulse width modulation.

4.5 900 MHz BAND TRANSMITTER AND RECEIVER.

In parallel with the pulse coded communications system discussed above, ANRO conducted a separate and parallel investigation into the use of spread spectrum technology for use in the WASP program. Spread spectrum techniques are used frequently in higher frequency bands, and offer advantages such as jamming and multi-path resistance and covertness. The principal objectives and activities associated with this investigation were:

- Determine methods of generating coding structures that have the following properties:
  - Efficient systems that have both small and large numbers of users
  - Have good correlation properties (Gold and Bent codes were investigated).

- Develop analytical methods to design, analyze and simulate performance of code structures.

- Ensure compatibility of code structures with programmable hardware that meets size and low power constraints of WASP and personal communications system (PCS) devices.

The requirements developed for the WASP communications system are presented below. Current products with performance parameters similar to those specified were investigated. The product that most closely matched our requirements was the Spreadnet system manufactured by C&K systems. We purchased system components from C&K and evaluated their product. This 902-928 MHz spread-spectrum system can be disabled by a spread-spread cordless telephone operating in the vicinity, thereby eliminating this type of system from consideration.

The 315 MHz communications link utilizing the Ming hardware was duplicated in Rochester. The FCC requirements for such a system were determined and compared to the operation of the Ming boards. As there are fewer FCC restrictions on output power and supervision in the unlicensed 902-928 MHz band, a 916.5 MHz narrow-band solution was designed and built.

A promising solution to our problem is a spread-spectrum system. Originally, the 902-928 MHz unlicensed band was considered for this purpose due to the availability of low-cost components in this band. After considering the poor performance of the Spreadnet system and the fact that this band is not universally accepted throughout the world, the 2.4 GHz band was targeted. With the proliferation of PCS and WLAN systems throughout the United States and Europe, the availability of low-cost, high-performance chip-sets for this band is on the rise. The following system requirements were used as guidelines in the investigation.

Table 4-1. System Requirements.

Transmitter @ 2.4 GHz	Low cost (~$30 per pair)
	Small physical size
	Very low power consumption
	Programmable for at least 1024 separate sensors
Receiver @ 2.4 GHz	Detect and identify/decode sensor data
	Automatic notification of an event or failed check-in
	Does not have low power consumption or small physical size constraints.
False-alarm reduction	Send multiple messages for each event, and receive more than one to signal an alarm condition
	Use spread spectrum techniques to spread over interference
Low probability of intercept/detection	Short transmission time
	Low signal power in any given bandwidth
	Spread spectrum techniques to reduce detection and jamming
Supervisory capability	Adjustable check-in times
	Self-powered or long-life battery
Resistance to interference	Spread spectrum techniques to create a large bandwidth, with low power density per given frequency spectrum

The two issues above that presented the most risk were low power and sensor power. We strived for the lowest possible cost while not sacrificing product performance. We are confident that the transmitter can be implemented utilizing small, high-capacity batteries (similar to Tadiran TL-2150/S) and obtain battery lifetimes on the order of 5 years. Currently, we do not believe that such a transmitter can be powered solely from the current self-powered generator. We focused on two approaches, one utilizing batteries (~100 mW output power) and one using only the sensor for power (~5 mW output power).

4.5.1 Candidate Wireless 900 MHz Systems.

To avoid duplication, an extensive investigation of off-the-shelf products was conducted. Product information on existing products that meet many of our system requirements is given below.

1. C&K Systems – Spreadnet product line
- Wireless security sensors/systems
- Sensor transmitter cost is $30-40 (for simple sensors – panic buttons, door/window switch)
- 5 year battery life
- 902-928 MHz, Direct Sequence Spread Spectrum
- 10mW (pendant), 100 mW output power
- Supervisory as often as every 30 seconds to 5 minutes (or never)
- 7.6ms on-air time per transmission
- Range (published): 1 mile (open line of sight, 8 feet high)

2. Inovonics – Frequency Agile ™ product line
- Wireless security sensors/systems
- Sensor/transmitter cost is $40-50 (for simple sensors – panic buttons, door/window switch)
- 1 to 8 year battery life (8 year battery life = no supervision)
- 902-928 MHz, Spread spectrum
- Supervision every 10, 60 seconds

3. Adcon Telemetry – Micro-T
- Micro transceiver for the sensor industry
- 902-928 MHz, spread spectrum (also available in the 433 and 418 MHz bands)
- 10mW output power
- Range: Up to 1 mile
- Tx power req: 5VDC, 30 mA
- Built-in network protocols
- RS-232/RS485 and SPI bus
- Data rates to 2000bps
- $595 unit cost.

The Speadnet product offered by C&K Systems came very close to meeting our requirements and is fairly inexpensive. We purchased system components and evaluated this product. Our data shows the following:

- Outdoor line-of-sight range:
  >898 feet, 10mW transmitter (12dB S/N)
  >2006 feet, 100mW transmitter (13 dB S/N)

- Indoor line-of-sight range (RIT building 09, concrete block construction, metal doors):
  >350 feet, 10mW transmitter (18dB S/N)
  >434 feet, 100mW transmitter (32dB S/N), building hallway limit

- Indoor obstructed path (RIT building 09, 3rd floor) range:
  >109 feet, 10mW transmitter (22dB S/N)
  >147 feet, 100mW transmitter (16dB S/N), physical limitation.

However, as mentioned earlier, the Spreadnet system performance is significantly degraded by the operation of a 902-928 MHz spread-spectrum cordless telephone in the vicinity of the receiver. By using a 902-928 MHz spread-spectrum cordless telephone, we can degrade system performance by 50 dB (50dB rise in the noise floor as seen by the Spreadnet system) by choosing the proper "channel" on the phone. This is most likely not due to receiver overload as the phone can be several rooms away. The pseudo noise (PN) code sequence that the Spreadnet system uses may be too short. This would produce a repetitious correlation envelope in the presence of interference (the cordless telephone). This problem has been brought to the attention of the Spreadnet engineers.

4.5.2 FCC Part 15 Requirements.

The average FCC emissions limit for periodic operation about 70 MHz is given in Part 15.231. At 310 MHz, this limit at a distance of 3 meters is[6]:

$$5.9\frac{mV}{meter} * \frac{100}{duty\_cycle(\%)}$$

Assuming a 50% duty cycle yields a field strength of 11.8mV/meter which yields ~ 42 μWatts at the transmitter assuming an isotropic radiator with unity gain.

A comparison of various parameters regarding data transmission at 310 MHz and in the 902-928 MHz band is given in Table 4-2.

[6] Note that there is a peak maximum radiated field strength of 20dB above this specification. Accordingly, 59mV/meter is the maximum peak field strength allowed at 3 meters. This corresponds to a peak output power of ~ 1mWatt and a 10% duty cycle.

Table 4-2. Comparison between 300 and 900 MHz Systems.

Parameter	315 MHz narrow-band link	900 MHz narrow-band link	900 MHz spread spectrum link
Max power (FCC limit)	42 μW – 50% duty cycle (1 mW, peak)	0.75 mW	1 W
¼ λ	9"	3"	3"
Minimum check-in interval (FCC)	60 min	No limit	No limit
Max on-air time (FCC)	5 seconds	No limit	No limit
Range (open line of sight)	430 feet	396 feet	>2000 feet (100mW) >898 feet (10mW)
Range (in building)	80 – 165 feet	154 – 240 feet	109 – 350 feet (10mW) 147->434 feet (100mW)

The 315 MHz range data was taken with the Ming transmit/receive boards and ¼ wave antennas. The 900 MHz narrow-band range data was taken using a 900 MHz cordless telephone (output power of ~ 300 μW). The 900 MHz spread-spectrum range data was taken using Spreadnet system components (both a 10mW and 100mW transmitter). The in-building data was taken with and without obstructed paths (several concrete walls, door) at RIT in building 09.

For better in-building range and no restriction on the check-in interval, the next logical step for WASP communications was operation in the 902-928 MHz unlicensed band. We built a 916.5 MHz (narrow-band) transmitter and receiver using surface-mount technology and hybrid components. The transmitter is designed to interface with the Ming encoder board and the receiver is designed to interface with the Ming decoder board. This transmit/receive pair was successfully tested.

Table 4-3. System requirements and measured results.

Description	Requirements	Measured
Frequency of Operation	Between 902 and 928 MHz	916.415 MHz
Data Rate	1 kbps	1kbps (tested to 3 kbps)
Outside LOS range	2,500 Feet	2,693 Feet
Oscillator Input Power	Less than 25 mW (5V line) for 100 msec	16.15 mW peak, ~4 mW average for 91 msec
Oscillator Output Power	~750 μW (radiated FCC limit)	825 μW into the antenna

4.6 2.4 GHZ SPREAD SPECTRUM.

The following details the 2.4 GHz spread-spectrum communications system that was investigated for this program.

Transmitter:

- DSSS, 2.4 GHz unlicensed band (battery-less, 5 mW, battery, 100 mW)
- Low-power (Design goal of 25 mW power consumption)
- Physically small (surface mount components)
- Programmable for at least 1024 ID numbers
- Supervised only with a battery installed, programmable time delay between check-ins
- Short on-air time with data repetition (<50 msec).

Receiver:

- Designed to receive one transmission at a time (short transmit time, low probability of collision)
- Sliding correlator
- Not low power or small in size.

We chose the 2.4 GHz band due to the large number of services and wide variety of equipment in and near the 902-928 MHz band. In addition, the 2.4 GHz band is widely accepted both in the US and Europe. The portion of this band that we have chosen is also accepted in Japan and is above the frequency used by microwave ovens. Figure 4-2 depicts the 2.4 GHz, direct sequence spread spectrum wireless link.

2.4 GHz, Direct Sequence, Spread Spectrum Sensor Communication System

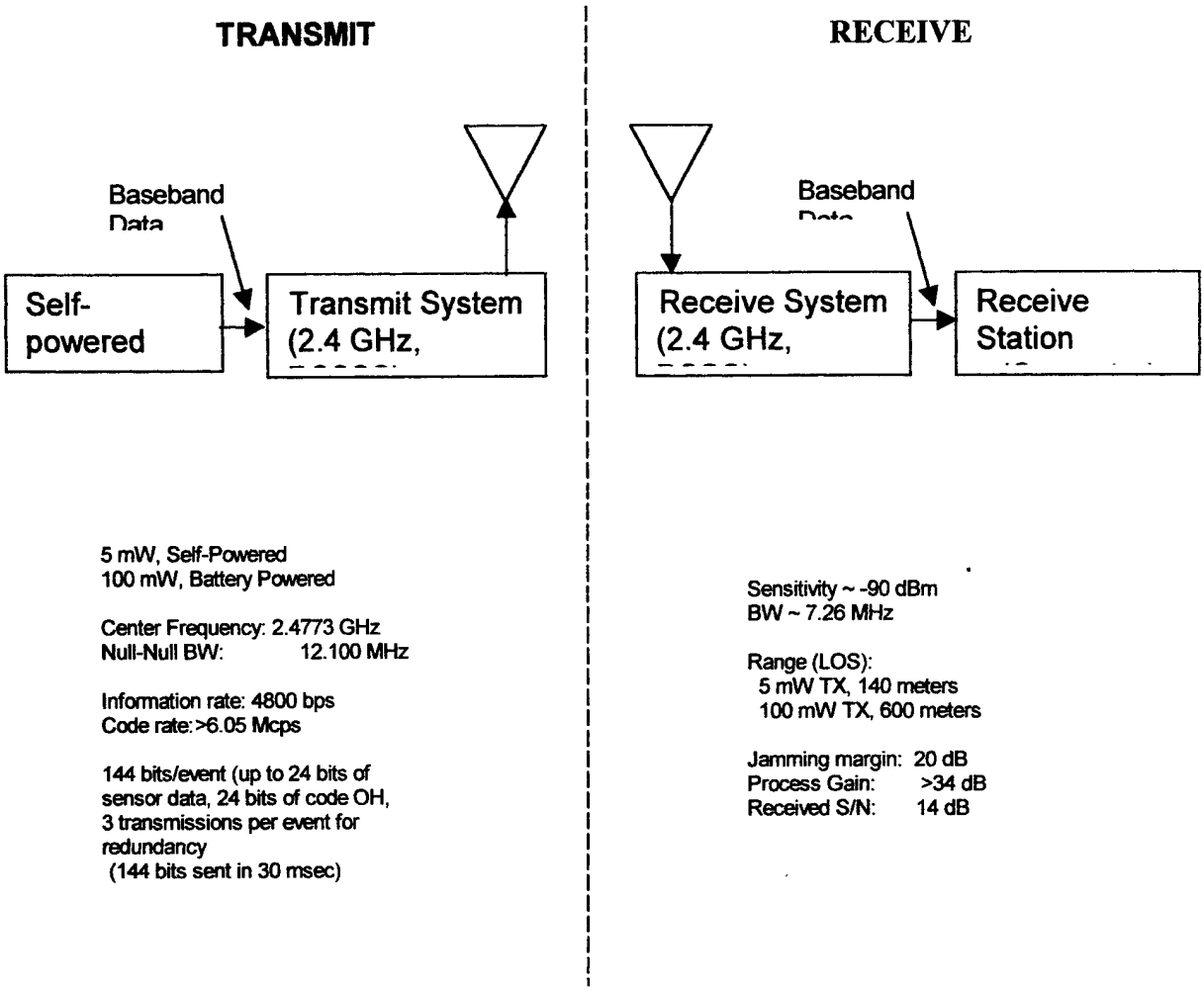

Figure 4-2. 2.4 GHz spread spectrum link parameters.

A MATLAB program was used to generate Gold Codes that were downloaded into the spread spectrum transmitter. In a spread spectrum system, to implement multiple access techniques (multiple transmitters using the same radio frequency band at the same time), the pseudorandom sequence utilized by each transmitter must have a low cross correlation with the other transmitted signals, while having good autocorrelation properties with its own desired circuit. While linear maximal length sequences have very good autocorrelation properties, the cross-correlation between two codes is not, in general, well defined. Gold code sequences are generated by modulo-2 addition of two specifically chosen maximal length sequences, called a preferred pair.

These sequences have well-defined and bounded cross-correlation properties in addition to good auto-correlation characteristics. A pair of n-stage shift registers can generate $2^{(n-1)}$ Gold codes.

The MATLAB simulation program was used to simulate the system. The transmitter baseband hardware was built and tested. A 64-bit file was loaded into an electronically-erasable programmable module (EEPROM) in conjunction with a microcontroller. The first 8 bits of the sequence were used as identification data, then mixed with the pseudorandom sequence. The demodulator performs the opposite action to extract data. This system provides the basis for a low-cost, spread spectrum wireless system for use in the WASP program, or as a relay for remote monitoring.

In summary, WASP-type sensors on Phase II were designed to operate at 315 MHz after consulting with government sponsors. The sensors were also tested with 900 MHz transmitters and receivers because of the availability of components because of the cell phone market. Because this frequency band is not used in Europe, we then investigated the 2.4 GHz band where many of the new cell phone spread spectrum systems are now operating. Because of the smaller size and shorter antenna lengths required, this is the recommended band for at least short-range applications (e.g., less than 300 feet).

All units operating at 310 MHz were coded (8-12 bit configurations) to permit the use of at least 256 different sensors. Each of the frequency bands evaluated on the Phase II program (e.g., 315 MHZ, 902-928 Hz and 2.4 GHz) were performed under FCC Part 15 regulations where licensing is not required.

SECTION 5
ANTENNA DEVELOPMENT

5.1 INTRODUCTION.

Certainly, the simplest and often the most efficient antenna, is the dipole (including the half-dipole or monopole) antenna. Indeed, the very first experiments with electromagnetic radiation were conducted by Hertz using an antenna of this type. it follows that the use of another type of antenna for a particular application must be justified by special requirements such as high directivity or environmental-physical constraints.

For the present application, near isotropic radiation characteristics are desired. If the environment - door, window, and the closer frames for these, etc., are non-metallic non-conductors, a dipole, appropriately configured for covertness and ease of installation is clearly the first antenna of choice. Under Phase I, two forms of dipole antennas were designed and constructed and tested for use with the 50 MHz transmitter using the components employed in cell phones. Later versions developed in Phase II used different transmitters operating at 315 MHz.

When the door is metallic or laminated with sheet metal, as is often the case in commercial-warehouse and military installations, an electric dipole mounted on the surface of the door would be short-circuited by the conducting material and could not radiate. Consequently, a different antenna type is necessitated by this environment. The parallel plane structure of the metal lamination suggests the use of a stripline, patch antenna in this environment. While such antennas represent relatively recent innovations, the design principles governing their performance are now quite well understood. Design formulas for patch antennas appropriately configured for the door application were developed under Phase I, but no construction of this antenna proceeded, as total effort was focused on antennas for wooden doors.

5.2 DIPOLE ANTENNAS.

The primary consideration governing the design of the antenna used in the Phase I doorknob at 50 MHz was the covert placement of a sufficiently large dipole. In this application, the very severe limitation on the available primary power demands an efficient radiator. No radiator (in particular, no dipole radiator) much smaller than one-half free-space wavelength radiates efficiently. At 50 MHz a free-space-wavelength computes to three meters. A given conductor length can effectively be *doubled* through the use of a large conductive ground place - the monopole configuration. This option is evidently available in conjunction with metal or metal laminated doors.

A particularly intriguing means for increasing the effective length of a short antenna, an antenna whose static length is only the length of a doorknob, utilizes the dielectric properties of the door opener (person) to effectively increase the length. In Phase I, a circumferential halfwave dipole at 50 MHz antenna was constructed by constructing 3/4" pine strips to simulate a doorframe.

The vertical frame was placed proximal to the PM generator/gear train and electronics assembly. Propagation from the sensor was reviewed each time the mock-up door was opened and closed. A second similar dipole placed in the laboratory received signal levels at 50 MHz, as measured using a wideband scope as indicated in Table 1. When we operated the transmitter using a fixed dc supply, the results were the same.

Table 5-1. Measurement of radiated signal.

Spacing between antennas (ft)	Scope voltage, p-p (mv)
4	220
8	200
15	180

Using a specifically designed receiver and monopole, we were able to receive the signal at least 2000 feet through the ANRO laboratory and building structure in the vicinity of the National Guard Armory on Bedford Street in Lexington, MA. We used a gated 150 ms duration supply to simulate the opening and closing of a door for this experiment.

A novel means for increasing the effective length of a short antenna, an antenna whose static length is only the length of a doorknob, utilizes the conductive properties of the human in contact with the door handle. This is further described in the improvement patent filed as a result of the Phase I effort.

The person-antenna interaction has recently received detailed attention in the literature.[7] Although the particular study cited focused on hand-head interactions with portable cordless phone antennas at 900 MHz, the principles of person-antenna interaction studied and described as well as the computational techniques employed are clearly applicable at 50 MHz.

The range of the doorknob antenna appeared to be about 100 feet with no one holding the knob. When the knob is held, the range is substantially greater than 150 feet but it is difficult to quantify within a building structure because it depends upon the body orientation as well as the contact with the knob. The antenna is also effective when an intruder is wearing a medical glove, because of the capacity coupling between the hand and the doorknob at 50 MHz; at higher frequencies the coupling is even greater.

An interesting observation to make here is that if the knob can be conveniently insulated from a metal frame door, then it should make an effective alternative to the patch antenna. This requires operating at higher frequencies; for example, 300 MHz and higher.

[7] M.A. Jensen and Y. Rahmat-Samii, "EM Interaction of Handset Antennas and a Human in Personal Communications." Proceedings of the IEEE, Vol. 83, No. 1 pp. 7-16, January, 1995.

5.3 COVERT MICROSTRIP ANTENNA.

For metal laminated doors, a form of microstrip antenna has been designed that conforms to the door geometry and is readily concealed. This type of antenna can (but does not necessarily) use the outer metal door covering as an integral part of the antenna as shown in Figure 5-1. The pattern of the radiation from the slit aperture is that of a horizontal magnetic dipole. Note that the dimensions for a patch antenna at approximately 900 MHz will only be about 6 inches in length.

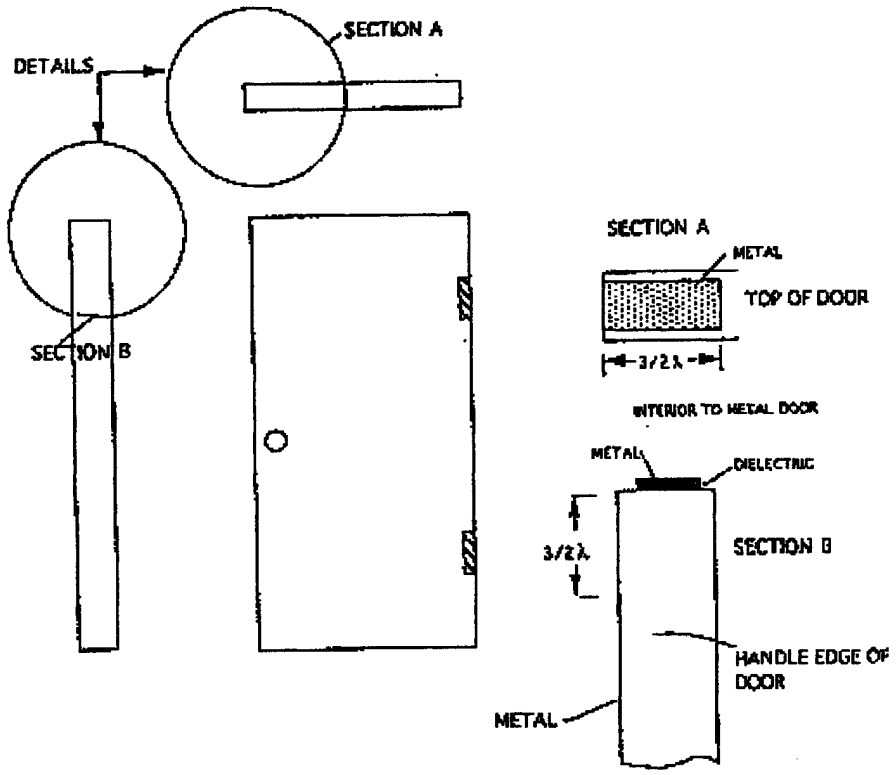

Figure 5-1. Totally flush patch antenna for metal door installation.

5.4 THE MONOPOLE ANTENNA.

During Phase II, efforts were made to reduce the size and the cost of the embedded sensor placed in the doorknob. To this end, a frequency of 315 MHz was chosen for the transmitter because off-the-shelf coded transmitters that were available. At this frequency we found that a convenient means to radiate the energy was by using a single wire (i.e., a form of monopole) above a small ground plane. The wire was cut to be $\frac{\lambda 0}{4}$ at 315 MHz (e.g., about 10 inches long). For hollow core doors, this wire simply extends directly into the open cavity between the front-end backside of the door. For solid core doors the mounting hole that must be drilled to imbed the transmitter is extended 10 inches to contain the #10 wire.

This must be done using an electricians bit (i.e., used for snaking wires between floors). The drill must be mounted in a special clamp mounted on the edge of the door to ensure a centered hole. The use of a 900 MHz transmitter would only require a 3-inch hole, but might result in a shorter range within a building. The wire attaches directly to the load containing the surface mounted components constituting the transmitter.

Finally, some comment on other antenna types should be made. A monopole antenna (i.e., a length of wire) is the simplest form of antenna. When space becomes a factor (e.g., the requirement for a 10-inch hole to be drilled in a solid core door), another type of antenna element might be possible. Namely, a coil of wire wound on a ferrite core increases the effective length of the antenna in two ways; one by the foreshortened length of the bobbin and secondly, by the square root of the permeability of the core material. Unfortunately, there was not sufficient time on the program to evaluate this type of antenna.

A whip antenna cut to be $\frac{\lambda 0}{4}$ is also used in the receiver. The range measured in an open field was greater than 600 feet. The range within a building is expected to be much less; perhaps, 150 feet.

SECTION 6
MARKET ANALYSIS

6.1 INTRODUCTION.

An objective of all Small Business Innovative Research (SBIR) programs is introduction of technology into the commercial arena, in addition to the defense applications. Phase III programs are intended for commercialization of the products developed in Phases I and II.

To accomplish this goal, ANRO enlisted as a program team member the Advantor Corporation, located in Orlando, FL. Advantor is a well established home, commercial, and defense security systems supplier, with an excellent manufacturing, marketing, and system engineering capabilities.

6.2 MARKET RESEARCH.

Advantor performed a complete market research analysis, to include all three market areas, over a period of 12 months. Most of the market research focused on the commercial and residential markets and several key features that are necessary to be a viable player in this arena.

6.2.1 Government Markets.

The government market is described as primarily a retrofit of existing annunciators or upgrades as opposed to introduction of new sensors. The following points were found.

- The size of new system installations is decreasing vs. increasing at existing military bases. Options for new installations are confined to new construction or replacement of human security with electronic security.
- Historically, the military has expressed greater interest in annunciator upgrades than in new sensor installations.
- Sensor supervision is a must. Semi-supervised or unsupervised sensor systems greatly limit the potential of the system to meet any given requirement.
- Price elasticity is great, meaning that a $20 unit price is not important in this market.
- Other applications can include both tactical deployment and covert operations.

However, in spite of the above rather limited market in the government sector, it is recognized that the wireless and self-powered (WASP) sensor is an entirely new type of sensor and the potential applications and acceptance has not yet been fully explored or recognized.

6.2.2 Commercial and Residential Markets.

The elimination of the need for a battery that must be replaced on regular intervals, like a smoke detector, is a strong point for the commercial and residential markets. Users can forget to replace the batteries on a timely basis, and batteries can fail unexpectedly.

Another strong feature is the avoidance of wiring in existing structures. Homeowners and some business locations do not want unsightly wires to be exposed and the expense and time required to retrofit wiring within walls or ceilings can be a burden. The wireless aspects of this system are therefore very appealing. The monitor annunciator can be simply placed in a central location, and the sensors installed in a hidden fashion, and the system is completely unobtrusive.

A principal goal for the WASP sensors is an ability to be installed simply and quickly in existing structures by untrained personnel and using simple hand tools. It is envisioned that for the residential market, that kits would be sold at the neighborhood hardware stores, and be installed by the homeowner, just like chain locks on doors.

To meet the residential market, and to some extent the commercial market, the component price must be low. Considerable effort has been expended on this program to achieve this goal, particularly for the doorknob sensor. The estimated product component manufacturing price for the doorknob sensor is now under $5.00.

6.2.3 Special Opportunities for Hotel Application.

It is important to note that the elimination of a battery, a non-maintenance feature, offers a very key selling point in many applications. An extension of this technology is it application to hotel keyless door locks. Most hotels today use a magnetic coded card to open a hotel room door, eliminating the metal key. The room "key" code can be changed as each customer checks out, preventing unauthorized re-entry into the room. The loss of property or exposing the guests to dangerous situations places the hotel at risk.

And perhaps most importantly, the hotel keyless entry systems today use batteries to read the card and to unlatch the door. A dead battery means that the magnetic key does not work, and the guest is unhappy. A self-powered hotel keyless lock is an important market for the WASP technology. The wireless transmitter is not required for this application. All the power generated is used to read the magnetic card strip and to declutch the door lock mechanism.

6.3 SUPERVISION.

A high percentage of wireless systems available today incorporate some sort of supervisory capability, ranging from simply a low battery alert to a fully supervised system. Full supervision implies that the wireless system can automatically test itself on a regular basis to make sure that all sensors and receivers in the system are fully functional continuously as well as for signal

circumvention. A semi-supervised system does not constantly require the sensors to check-in with the receiver, and requires manual testing.

Sensor supervision is critical in most of today's market. In the commercial, residential and government markets, this feature is very important.

ANRO developed and tested a form of semi-supervision. The power generation capability of the system is in excess of that needed to power the wireless transmitter. This excess power can be stored in a "super capacitor" that functions like a battery that is recharged each time the sensor is activated. This method will work satisfactorily to test the electronics alone in applications where the door or window is activated on a regular basis. For other applications where the door, for example, is not opened over long periods of time, then this form of semi-supervision will not be effective. For fully supervised systems, it is recommended that a small lithium ion battery be included within the system, but the sensor still features the wireless aspects of the WASP system.

6.4 RADIO FREQUENCY ALLOCATION.

Most security systems today operate in the 900 MHz range, causing some concern about crowding in this band. Some systems go even further, relying on spread spectrum technology to achieve greater reliability in hostile or difficult radio environments. Another concern that surfaced was that a higher power level was needed in the 900 MHz band, which places a greater burden on the self-powered generator.

The military clearly prefers to operate in the 300 MHz band, or higher. This frequency is also favored because of its simplicity and low cost of parts. But, neither the 300 nor 900 MHz bands are accepted universally worldwide. Hence, ANRO and Advantor pursued operational capabilities in other bands including operations in the 2.4 GHz band. ANRO favored operation at 3.5 MHz because of the availability of inexpensive components as well as the extended range within buildings. It is tempting to consider operating at higher frequencies because of the reduced antenna size. Later work in the WASP area will investigate the higher frequencies as an option.

SECTION 7
CONCLUSIONS AND RECOMMENDATIONS

7.1 CONCLUSIONS.

ANRO has successfully completed the task of embedding WASP sensors in a doorknob, doorjamb, and a window mounting. Embedding a generator and transmitter in a doorknob was identified by the Advantor Corporation, a subcontractor tasked to do a market survey on this program, as the most commercially potential product. After considerable effort, we concluded that we could embed a generator, transmitter and antenna in a low-cost (Kwikset) lockset, adapt it to other locks, and keep the additional cost of a keyset manufactured in a production containing this technology for less than $10.

The WASP sensors developed on this program do not include a "supervision" feature. Supervision implies the capability to verify the operation of the sensor, for example, each hour. We concluded that by adding a so-call "super capacitor" we could excite our transmitter once per hour after normal working hours to verify its operability. But this feature would increase the volume of the present electronics as well as cost and does not perform full monitoring. For example, the electronics may be still working, but it does not check the generator source. A better form of quasi-supervision would be to check door openings and closing during normal working hours and correlate this data via computer software with other sensors to assure operation of the WASP sensor.

The success of the WASP program just completed suggests a new form of device of use in hotels, motels and secured facilities. It is hard to find any hotel/motel today that still uses a key for entry. Almost all facilities use keyless entry systems; namely, the use of an ID card that, when drawn through or pushed into a slot, declutches the lock. Energy is required to also read the card as well as activate the solenoid to open the door. This power is currently supplied by a battery which must be replaced often, and if it fails unexpectedly, creates problems for the guests and the hotel. We believe that the generation sources developed under WASP are directly applicable to solve this problem. The market for a batteryless hotel lock is huge. A large manufacturer that we visited indicated to us that they ship 10-15,000 keyless locks a week.

We compromised on a frequency of 315 MHz for use with the WASP program. Originally, to demonstrate feasibility of the concepts on Phase I, we operated around 50 MHz to use available cordless telephone technology. We have also studied using 900 MHz as well for doorknob and doorjamb and window applications, but propagation, as well as cost considerations helped us conclude that 315 MHz was the frequency of choice. Repeaters were studied for use at 2400 MHz.

Before concluding, some mention should be made of the reliability of the three different WASP sensors developed on this program. We have calculations on the reliability of the solid state transmitter, coding module and the receiver. The joint reliability of these components over a wide temperature range is 0.98 or higher. At this writing, we do not have sufficient data to

estimate the reliability of the mechanical linkages and spring forming part of the energy conversation source. We have operated 18 devices in doorjambs, doorknobs and in window locations without any failures. Our conclusion is that these sensors have a high degree of reliability, but we cannot state a number without a mechanical analysis of the componentry that has not been performed.

7.2 RECOMMENDATIONS.

ANRO is aggressively pursuing new commercial opportunities for use of WASP sensors in commercial and home security systems. It is recommended that the government study their current and future needs and contract with ANRO to initiate work to improve the security at selected facilities using ANRO's WASP technology.

It is recommended that the government fund additional work in developing batteryless keyless lock systems to save on maintenance and the cost of batteries. ANRO is currently investigating commercial opportunities in this are as well.

SECTION 8
DESCRIPTION OF THE APPENDICES

Appendix A describes the investigation that was accomplished regarding the use of digital and spread spectrum techniques in the 900 and 2400 MHz bands. A functional 915 MHz transmitter and receiver were built and tested for use as an alternative to the 315 MHz system. Both the 315 and 915 MHz transmitters use exactly the same form factor, and are thus direct replacements. An outside range of over ½ mile was demonstrated using the 915 MHz system. Coverage within a 3-story brick and concrete block building was nearly complete, with only a few "holes" or shadow areas. These can be easily eliminated by prudent placement of the receiver antenna. The 915 MHz transmitter draws very low input power, less than 750 μA from a 5-volt source due to the low duty cycle. This system can be easily adapted to transmit additional information, which makes it useful for any kind of remote monitoring. For example, a wireless thermostat, humidity sensor, etc.

To reduce multipath fading and increase range a spread spectrum modulation system could be employed. More importantly, a spread spectrum system reduces the probability of intercept and detection (or jamming). The lowest frequency band where unlicensed operation is allowed is located around 2.45 GHz. In the US, FCC Part 15.247 specifies spread-spectrum operations from 2400 to 2483.5 MHz.

A spread spectrum communication link is suggested as the next logical step to provide more robust communication. A system level design was accomplished, and simulations were performed to create PN sequences belonging to a family of Gold codes. Up to 101 simultaneous users can be assigned using this technique. This type of system can also serve as a repeater for deployed sensors.

Appendix B describes the work performed to investigate the use of PN sequences to generate CDMA spread spectrum communications systems. This technique allows users of the system to use the same RF bandwidth without interference. Additionally, the technique reduces the likelihood of detection and jamming. A design method was successfully completed to determine the necessary code length of the PN sequence, based on the required number of users and the anti-jam performance.

Appendix C describes the design considerations for an indoor wireless communications system operating in the 902 to 928 MHz region, utilizing spread spectrum and CDMA techniques.

A major obstacle in the system design for a wireless intrusion detection system is the characterization of the communication path. In interior environments, path losses are greater due to the variability in a building's interior construction and the number of floors. Additional loss is experienced by shadowing and multipath interference.

The benefits of spread spectrum techniques are discussed in Appendix B, and include interference suppression (both accidental and intentional), the removal of time and frequency assignment constraints (all users have access to the channel all the time), energy density reduction (lessens interference), and reduction of multipath interference.

APPENDIX A

DEVELOPMENT OF A DIGITAL WIRELESS COMMUNICATION SYSTEM FOR SECURITY SENSOR APPLICATIONS

28 January 1998

Author:

Steven M. Ciccarelli

CONVERSION TABLE

Conversion factors for U.S. Customary to metric (SI) units of measurement.

MULTIPLY →	**BY** →	**TO GET**
TO GET ←	**BY** ←	**DIVIDE**
degree Fahrenheit	$t_k = (t°f + 459.67)/1.8$	Kelvin (K)
erg/second	1.000 000 X E –7	watt (W)
foot	3.048 000 X E –1	meter (m)
mile (international)	1.609 344 X E +3	meter (m)

TABLE OF CONTENTS

Section Page

CONVERSION TABLE A-1

FIGURES A-4

TABLES A-5

1 ABSTRACT A-6

2 INTRODUCTION A-7

3 SYSTEM DESIGN A-9

3.1 SYSTEM REQUIREMENTS. A-9
3.1.1 Transmitter Data Rate A-9
3.1.2 Transmitter Power Requirements. A-9
3.1.3 System Range and Receiver Sensitivity. A-10
3.1.4 Requirements Summary A-11
3.2 TRANSMITTER DESIGN. A-11
3.2.1 RF Oscillator. A-11
3.2.2 Encoder A-22
3.2.3 Aggregate Transmitter. A-23
3.3 RECEIVER DESIGN A-24
3.3.1 Decoder. A-24
3.3.2 Receiver Assembly A-25
3.3.3 Aggregate Receiver. A-31

4 SYSTEM PROTOTYPE PHASE A-33

4.1 TRANSMITTER. A-33
4.1.1 RF Oscillator. A-33
4.1.2 Oscillator Experimental Results. A-37
4.1.3 Transmitter Prototype. A-39
4.2 RECEIVER. A-41
4.2.1 Receiver Assembly. A-41
4.2.2 Receiver Assembly Experimental Results. A-42
4.2.3 Receiver Prototype. A-43
4.3 RANGE TESTING. A-44

5 DISCUSSION A-47

6 RECOMMENDATIONS A-50

6.1 SPREAD-SPECTRUM SYSTEM DESIGN A-50
6.1.1 Transmitter A-52
6.1.2 Receiver A-53
6.1.3 PN Sequence Generation. A-54

TABLE OF CONTENTS (Continued)

Section		Page
7	CONCLUSIONS	A-65
8	REFERENCES	A-67

FIGURES

Figure Page

A-3-1. Colpitts oscillator. A-12
A-3-2. Frequency domain oscillator simulation. A-16
A-3-3. Phase plot. A-16
A-3-4. Gain plot. A-17
A-3-5. Time domain oscillator simulation. A-17
A-3-6. Voltage at Q1-C, 200nS span. A-18
A-3-7. Voltage at Q1-c, 44.2nS span. A-18
A-3-8. Oscillator with load. A-20
A-3-9. Voltage across R1, 200nS span. A-21
A-3-10. Voltage across R1, 69.7nS span. A-21
A-3-11. Oscillator with load, Q1-C. A-22
A-3-12. Encoder circuit. A-23
A-3-13. Transmitter schematic. A-24
A-3-14. Decoder circuit. A-25
A-3-15. Receive system block diagram. A-29
A-3-16. Receiver schematic. A-32
A-4-1. Prototype oscillator. A-34
A-4-2. Complete oscillator circuit. A-36
A-4-3. Oscillator output power spectrum, 1kbps data rate. A-38
A-4-4. Oscillator output power spectrum, 3kbps data rate. A-39
A-4-5. Prototype transmitter schematic. A-40
A-4-6. RF oscillator. A-40
A-4-7. Prototype transmitter. A-41
A-4-8. Prototype receiver assembly. A-42
A-4-9. Receiver prototype schematic. A-43
A-4-10. Prototype receiver assembly. A-44
A-4-11. Transmitter. A-45
A-4-12. Receiver. A-45
A-5-1. Miniature transmitter. A-48
A-6-1. Spread spectrum system. A-51
A-6-2. Spread spectrum transmitter. A-52
A-6-3. Spread spectrum receiver. A-53
A-6-4. Simulink file to generate b. A-56
A-6-5. Simulink file to generate Gold codes. A-59
A-6-6. Cross-correlation. A-62
A-6-7. Autocorrelation of gold15_1a. A-63
A-6-8. Autocorrelation of gold15_2a. A-63

TABLES

Table	Page
A-3-1. System requirements	A-11
A-3-2. Receive system parameters	A-30
A-4-1. Initial oscillator parameters A-34	
A-4-2. Oscillator circuit parameters	A-36
A-5-1. System requirements and measured results	A-46

SECTION 1

ABSTRACT

This report details the investigation of wireless, self-powered (WASP) sensors communicating to a receive station utilizing the unlicensed bands authorized by the Federal Communications Commission (FCC). In this report, a digital wireless communication system operating in the 902-928 MHz Industrial, Scientific and Medical (ISM) band is specified, designed, and analyzed. The purpose is to transmit sensor identification (ID) data from several low-cost, self-powered sensors to a single receive station located up to 2,500 feet away. Personal Simulation Program with Integrated Circuit Emphasis (PSPICE) simulation is used where appropriate and a complete transmitter and receiver have been built and tested. Experimental results are presented.

A spread-spectrum system is specified at the end of this report and suggested as the next logical step in developing a low-cost, robust communication system. The spread-spectrum system is suggested in order to minimize interference and increase the range of the communication link. Due to complexity of the circuitry, the spread-spectrum transmitters would require battery or wired power and therefore would act as repeaters to increase the range and robustness of the WASP communications link developed for this program. The repeater link is designed to operate in the 2.45 GHz unlicensed band, but could easily be adapted to other frequency bands. Simulink and Matlab are used to develop and verify various system parameters.

SECTION 2

INTRODUCTION

Wireless devices that are used to transmit small amounts of data over a short distance such as car alarm remotes, security systems, garage door openers and RFID tags generally utilize the upper portion of the VHF or lower portion of the UHF spectrum. The allowed output power in this portion of the spectrum is very limited and the Federal Communications Commission (FCC) limits supervisory intervals as well. For simplicity and to keep costs low, modulation is very often on-off Keyed (OOK).

FCC part 15.231 specifies the radiated field strength limit *for "Periodic operation in the band 40.66-70 MHz and above 70 MHz."* The maximum radiated field strength allowed is 12,500 uV/m (measured at a distance of 3 Meters) for operation above 470 MHz. Since the regulations specify average power, one can transmit a larger peak power as long as the average power requirement is met. For OOK modulation, the average power is determined by the peak output power and the duty cycle of the modulating function. Part 15.231 references section 15.35 that limits the peak radiated emissions to be no higher than 20 dB above the allowed average emissions. Therefore, the peak allowed field strength above 470 MHz is 12,500 uV/m + 20 dB = 125,000 uV/m. Assuming an isotropic radiator with unity gain [1]:

$$P_T = \frac{4 \cdot \pi \cdot d^2 \cdot E^2}{\eta_0} \qquad \text{(A-2.1)}$$

where

P_T = total received power in watts (W)
d = distance from the source in meters (m)
E = specified field-strength in volts/meter (V/m)
η_0 = impedance of free-space in ohms

At the specified distance (d) of 3 meters in free-space (η_0=377 ohms) and a field strength (E) of 125,000 uV/m, the peak allowed transmitted power is 4.687 mW. The average output power would have to be (using E = 12,500 uV/m) 46.874 uW. For OOK modulation, the duty cycle would have to be less than 10% to be in compliance. At frequencies below 470 MHz, where many of these systems reside, the average radiated emissions limit is as low as 1,250uV/m which corresponds to an output power of 468.7 nW average or 46.87 uW peak. Furthermore, FCC part 15.231 allows check-in intervals for transmitters in the system no more than once per hour, and limits the length of any transmission to five seconds or less.

The FCC allows operation in the 902 - 928 MHz ISM band that is more flexible than that allowed for by part 15.231. FCC part 15.249 specifies the radiated field strength limits for *"Operation within the bands 902-928 MHz, 2400-2483.5 MHz, 5725-5875 MHz, and 24.0-24.25 GHz."* For operation from 902 - 928 MHz, the radiated field strength limit is 50 mV/meter which corresponds to an output power of 749.98 uW (average or peak). This is significantly better than the 46.874 uW allowed under part 15.231. In addition to higher output power, additional benefits include no limitation on the length or type of transmission and a smaller antenna. If one wishes to transmit with higher power in this band, two options are available. The first is to operate under part 15.231 and use a larger peak power (up to 4.687 mW) but much lower average power (less than 46.874 uW). The second, more complicated but less restricted option is to use spread-spectrum transmission.

Given the small amount of output power allowed for narrow-band transmission, these systems must work with small signal-to-noise (S/N) ratios and are susceptible to intentional and non-intentional interference. They are also limited in range and flexibility.

SECTION 3

SYSTEM DESIGN

The system described in this report is a wireless security system. There exists one receiver for many transmitters. When an event takes place, such as a break-in, the sensor/transmitter will send an identification word, and if appropriate, data defining the event.

3.1 SYSTEM REQUIREMENTS.

The communications system will operate in the 902 - 928 MHz ISM band for timing flexibility (no limitation on check-in times or length of transmission) and to allow a fair amount of output power. In addition, the transmitter must be small, inexpensive and programmable for 1,024 separate sensor ID combinations.

3.1.1 Transmitter Data Rate.

The ANRO self-powered sensor supplies 5 volts for 100msec when an intruder is detected. A data-rate of 1kbps allows 100 bits to be transmitted during an event, which is more than sufficient to represent the sensor ID and send redundant data to increase the robustness of the communication link. The low data-rate will allow for a simple transmitter oscillator configuration and for OOK modulation.

3.1.2 Transmitter Power Requirements.

The transmitter input power is limited to 25 mW (5V, 5mA), the available power from the ANRO self-powered sensor. The RF output power of the transmitter (into the antenna) must be slightly over the allowed radiated FCC limit of 749.98 uW. This allows for some loss in the antenna while radiating near the limit to achieve the greatest range.

3.1.3 System Range and Receiver Sensitivity.

Most wireless systems, even those designed to be used inside, use an outside line-of-sight (LOS) range measurement under ideal conditions as a benchmark. The transmitter and receiver are mounted on six or eight feet high platforms and separated on flat, unobstructed land until effective communications are no longer possible. For this project, an outside LOS range of 2,500 feet is set as the goal. This distance will allow the system to pass data from one building to another in an office park environment and allow for good overall coverage of a standard residential dwelling or one floor of commercial office space. This range is comparable to some of the newer cordless telephones working in the same band and therefore, is achievable with fairly low-cost hardware.

Most of the system complexity will reside in the receiver. Since the output power is defined by the FCC, the receiver sensitivity has to be great enough to receive a transmitted signal with power of 750 uW 2,500 feet away. To determine the received power given a 750 uW source at a distance of 2,500 feet (762 meters) and assuming ideal omnidirectional antennas, equation (A-3.1) is utilized [2]:

$$P_r = P_t \frac{G_r \cdot G_t \cdot \lambda^2}{(4 \cdot \pi \cdot r)^2} = 750uW \frac{1 \cdot 1 \cdot \left(\frac{c}{915 \cdot 10^6}\right)^2}{(4 \cdot \pi \cdot 762)^2} = 877.88fW \qquad \text{(A-3.1)}$$

Where:

P_r = the received power (W)
P_t = the transmitted power (W)
G_r = the receive antenna gain (linear)
G_t = the transmitter antenna gain (linear)
λ = the wavelength in meters (c/f)
r = the distance between the receiver and the transmitter in meters

Converting 877.88 fW to dB referenced to 1 mW (0 dBm):

$$P_{dBm} = 10 \cdot Log\left(\frac{P_W}{1mW}\right) = 10 \cdot Log\left(\frac{877.88fW}{1mW}\right) = -90.57dBm \qquad \text{(A-3.2)}$$

The receiver must be able to demodulate arriving signals at this power level. Therefore, the noise-floor of the receiver must be significantly lower than this number. Assuming that at least a 10 dB S/N ratio is required for robust communications, the receiver noise-floor must be less than or equal to -100.57 dBm which corresponds to 87.7 fW.

3.1.4 Requirements Summary.

Table A-3-1. System requirements.

DESCRIPTION	REQUIREMENT
Frequency of Operation	Between 902 and 928 MHz
Data Rate	1 kbps
Receiver Noise-Floor	-100.57 dBm (87.7 fW)
Oscillator Input Power	25 mW from 5 volts for 100 msec
Oscillator Output Power	750 uW (FCC limit)
Number of Tx allowed	1024

3.2 TRANSMITTER DESIGN.

The transmitter will consist of two sections, the encoder and the RF oscillator. The encoder will encode ID data to identify the transmitter and use this data to OOK the oscillator. To make the system as flexible as possible, the encoder section will be implemented on a standard engineering bread-board or *superstrip*. The oscillator will require a good RF printed wiring board (PWB) layout for proper operation. Therefore, the oscillator will be implemented on a PWB using surface-mount components.

3.2.1 RF Oscillator.

Since the system may contain many transmitters, the simplest design that will achieve the results necessary is desired to keep costs low. To achieve reasonable frequency

stability a surface acoustic wave (SAW) resonator is selected since simple quartz crystals are typically useful only to about 200 MHz [3]. In the 902 - 928 MHz band, a search of various manufacturers' products yields few choices. For this project, an RP1285 (916.55 MHz) SAW resonator manufactured by RF Monolithics (RFM) is chosen. The center frequency (@ 25°C) is given as 916.55 MHz, +/- 150 kHz. Temperature stability is specified as 0.037 ppm/°C and frequency aging is given as less than or equal to 10 ppm/yr for the first year. The cost is low at $2.07 per piece in quantities of 100 pieces and goes lower with increasing quantity.

The next choice to make is the oscillator configuration and modulation type. Since RFM manufactures a receiver hybrid IC that works at 916.5 MHz that uses AM detection and may help simplify the receiver tasks, OOK modulation is selected. A simple oscillator configuration utilizing the SAW resonator is the Colpitts configuration shown in Figure A-3-1.

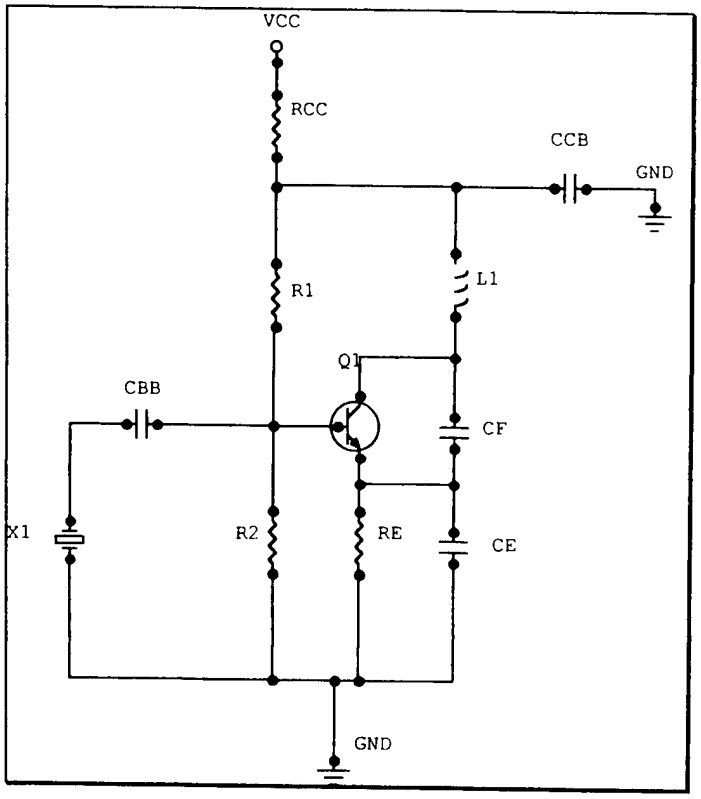

Figure A-3-1. Colpitts oscillator.

In this circuit, R_{CC} helps stabilize the operating point of the transistor and provides a simple means to measure the total current flowing into the circuit. R1, R2 and R_E set up the bias conditions for Q1. C_{BB} blocks DC to the SAW resonator (X1). C_{CB} provides an RF ground at the top of L1. The resonant frequency of the combination of L1, C_F, and C_E is set to a value slightly above the SAW frequency using equation (A-3.3) [4]. The RF output is taken at the junction of L1 and C_F through a coupling capacitor and fed to an antenna.

$$F_R = \frac{1}{2 \cdot \pi \cdot \sqrt{\frac{L1 \cdot C_F \cdot C_E}{C_F + C_E}}} \qquad \text{(A-3.3)}$$

In addition to the SAW resonator, a suitable RF inductor and transistor are necessary. For the RF inductor, the 1206CS series from Coilcraft, Inc. is a good candidate. This series of chip inductors contains values from 3.3 nH to 1200 nH. In addition, these parts have self-resonant frequencies (SRF) of up to 6 GHz, good quality factors (Q) at RF frequencies and are available in tight tolerances. The transistor chosen for the oscillator is an NEC 68133. This part has an F_T of 9 GHz. In addition, it has over 14 dB of gain at 1 GHz with V_{CE} = 2.5 V and I_C = 3 mA. Since the oscillator design goals specify 5 V as the power supply for the oscillator and a low "on" current of 5 mA (max), it is a reasonable choice.

The bias point for Q1 is chosen as V_{CE} = 3.0 V, IC = 4.0 mA. This keeps the power dissipation below the 25 mW specified and allows a fairly large voltage swing on the collector of Q1 while maintaining V_E at 1.25 V for improved stability over temperature. Bias point calculations are given below:

$$R_E = \frac{V_E}{I_E} \approx \frac{V_E}{I_C} = \frac{1.25V}{4.0mA} = 312.5\Omega$$

$$V_B \approx V_E + 0.6V = 1.85V$$

Allowing for a 0.5 V drop across R_{CC} and 250 uA through R1,

$$R_1 = \frac{V_{CC} - I_T R_{CC} - V_B}{I_{R1}} = \frac{5V - 0.5V - 1.85V}{250uA} = 10.6k\Omega$$

$$R2 = \frac{V_B}{I_{R1} - I_B} = \frac{1.85V}{250uA - \frac{4.0mA}{100}} = 8.81k\Omega$$

$$R_{CC} = \frac{0.5V}{I_T} = \frac{0.5V}{I_C + I_{R1}} = \frac{0.5V}{4.0mA + 250uA} = 117.7\Omega$$

The value of C_{BB} is chosen to allow the SAW resonator to look like a low impedance at the resonant frequency. The transistor circuit acts as a grounded-base amplifier with positive feedback. If C_{BB} is too large, the low impedance of C_{BB} in series with the shunt static capacitance of the SAW resonator will cause the circuit to oscillate at the wrong frequency. A value of 33 pF is chosen primarily through experience with similar circuits. The value of C_{CB} is chosen to yield a good RF ground at the junction of L1 and C_{CB} at the intended resonant frequency. A 120 pF capacitor provides an impedance of 1.45 ohms which should be sufficient.

Equation (A-3.3) is used to choose values for L1, C_F and C_E. Assuming resonance at 1.01 GHz (10% higher than 916.55 MHz) and choosing a value of 10 nH for L1 results in a value for the series combination of C_F and C_E of 2.48 pF. Assuming 1 pF of stray capacitance to ground will exist due to the PWB layout, standard capacitor values were chosen that result in 1.4 pF of total capacitance for the C_F, C_E combination. These values also result in a C_E/C_F ratio in the neighborhood of 2.5 to 1 (a rule of thumb for this circuit configuration). The calculated resonant frequency of L1, C_F, and C_E is 1.34 GHz.

L1 = 10 nH
C_F = 2.0 pF
C_E = 4.7 pF

The circuit shown in Figure A-3-2 was simulated using Circuitmaker 5.0. In this circuit, calculated component values have been replaced by the closest standard values except for R5. The value of R5 (100 ohms) was chosen to allow a quick measurement

of the total input current by observing the voltage across it. The RF inductor is modeled as the series combination of L1 and R4 in parallel with C3. From the Q vs. Frequency curves given in the Coilcraft data sheet, the Q of L1 is typically about 80 at 900 MHz. Therefore [5],

$$R4 = \frac{X_{L1}}{Q} = \frac{2 \cdot \pi \cdot F \cdot L1}{Q} = \frac{2 \cdot \pi \cdot 900\,MHz \cdot 10nH}{80} = 0.707\Omega$$

The value of C3 is determined by estimating the SRF of L1 to be equal to the minimum specified SRF for the part, in this case 4.0 GHz.

$$F_R = \frac{1}{2 \cdot \pi \sqrt{L1 \cdot C3}}$$

Rearranging yields,

$$C3 = \frac{1}{4 \cdot \left(L1 \cdot \left(F_R{}^2 \cdot \pi^2\right)\right)} = \frac{1}{4 \cdot \left(10nH \cdot \left(4GHz^2 \cdot \pi^2\right)\right)} = 0.158pF$$

C2 is present to prevent RF leakage onto the power supply line. R1 represents the SAW resonator at resonance. C1 represents the shunt capacitance across the resonator. R2 provides a DC path to ground from the C6/C7 junction (point A) for the circuit simulation engine and has no effect on circuit operation. The function generator across R3 is used to inject an AC signal at the emitter of Q1.

The phase and gain between the emitter of Q1 and point A are plotted as functions of frequency and displayed in Figures A-3-3 and A-3-4 respectively. The positive feedback loop in this circuit is between the emitter of Q1 and point A. The circuit oscillates at the frequency where the phase between these two points crosses zero as long as there is sufficient amplifier gain [6].

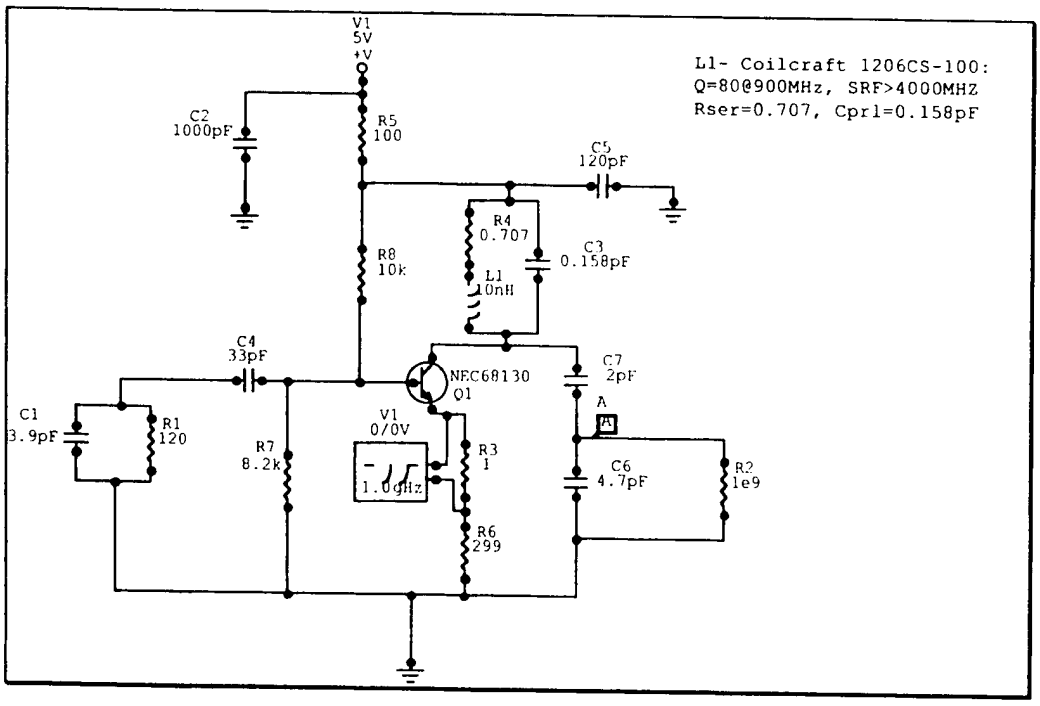

Figure A-3-2. Frequency domain oscillator simulation.

Figure A-3-3 clearly shows that this circuit will oscillate at 1.155 GHz as long as the amplifier has gain at this frequency. Figure A-3-4 shows that the amplifier gain is 10.95 dB at 1.155 GHz. Therefore, the oscillator will oscillate at 1.155 GHz.

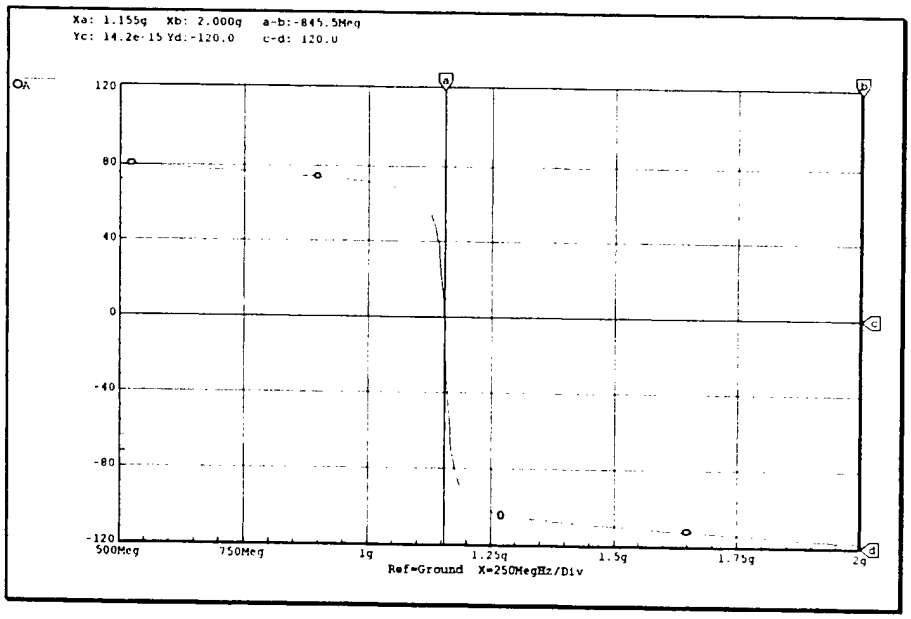

Figure A-3-3. Phase plot.

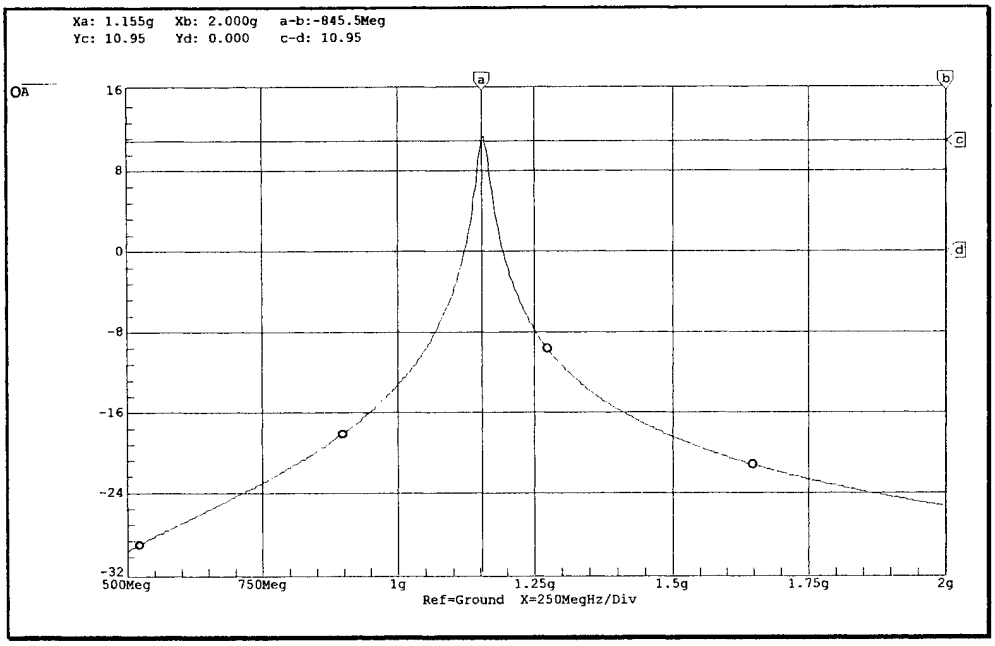

Figure A-3-4. Gain plot.

In Figure A-3-5, the feedback loop is closed and a time domain simulation is performed. The results of this simulation are given in Figures A-3-6 and A-3-7. Both of these figures show the voltage at the collector of Q1 vs. time. Figure A-3-6 shows that the oscillator start-up time is approximately 40 nSec and the voltage at the collector of Q1 is 10.17 Vp-p. Figure A-3-7 shows the frequency of oscillation to be 1.08 GHz (about 6.5 % lower than the predicted 1.155 GHz).

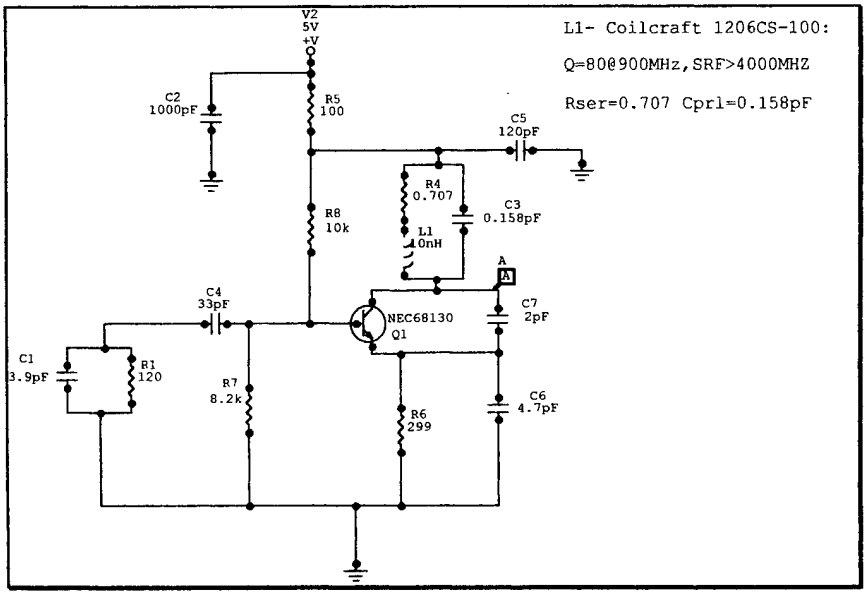

Figure A-3-5. Time domain oscillator simulation.

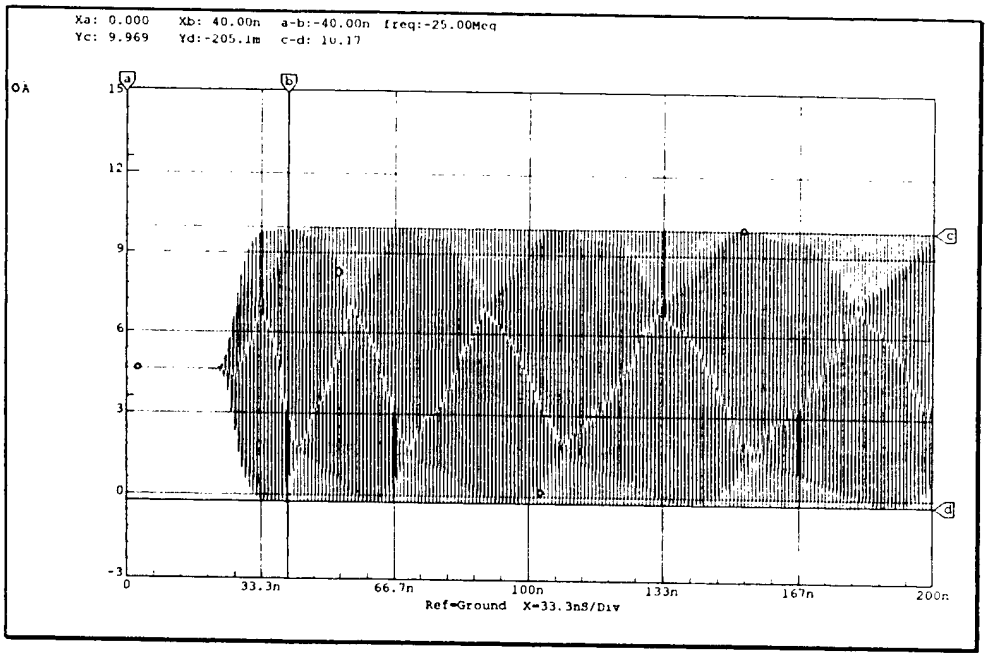

Figure A-3-6. Voltage at Q1-C, 200nS span.

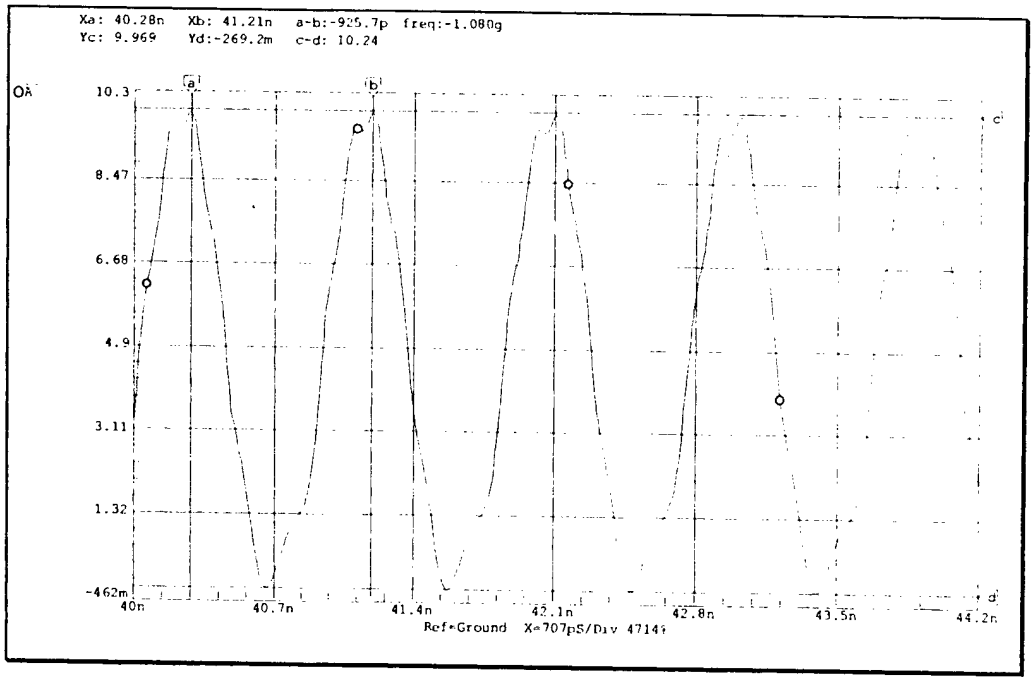

Figure A-3-7. Voltage at Q1-c, 44.2nS span.

The output of the oscillator is taken at the collector of Q1 through a high impedance capacitor to the antenna. The coupling capacitor (C1 in Figure A-3-8) is chosen to load the oscillator circuitry as little as possible but to provide ample power to the antenna. The specified output power of 750 uW corresponds to 193.7 mV RMS into a 50 ohm load. Assuming that C1 will not affect the collector voltage:

$$V_{R1} = V_{Q1\text{-}C} \frac{R_1}{R_1 + X_{C1}}$$

Rearranging and solving for X_{C1} yields:

$$X_{C1} = -R1 \cdot \frac{\left(V_{R1} - V_{Q1\text{-}C}\right)}{V_{R1}} = -50 \cdot \frac{\left(193.7mV - 3.58V\right)}{193.7mV} = 874.1\Omega$$

Therefore, at the intended frequency of oscillation,

$$C1 = \frac{1}{2 \cdot \pi \cdot F \cdot X_{C1}} = \frac{1}{2 \cdot \pi \cdot 916.55MHz \cdot 874.1} = 0.199pF$$

Since it is likely that the C1/antenna combination will load the collector voltage to some extent, a larger capacitor of 1 pF is chosen to allow more output voltage than necessary.

The circuit of Figure A-3-8 was simulated and the output voltage across R1 is displayed in Figures A-3-9 and A-3-10. From Figure A-3-9, it is clear that the oscillator start-up time has increased to approximately 62 nSec and that the output voltage is 1.16 Vp-p which corresponds to 3.36 mW into the antenna. Figure A-3-10 shows that the output frequency has decreased from 1.08 GHz to 931.5 MHz.

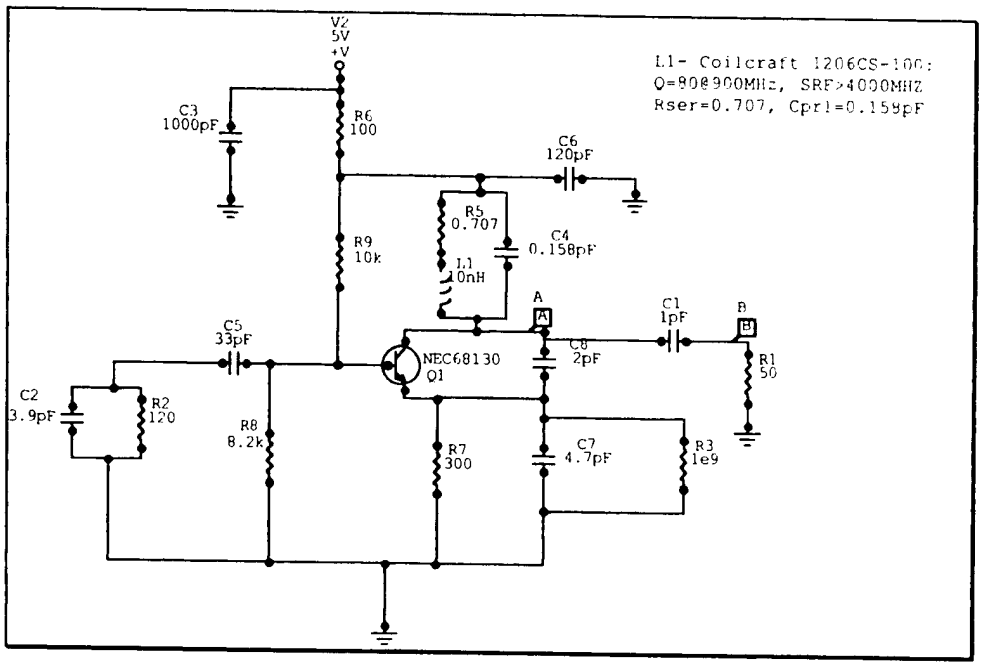

Figure A-3-8. Oscillator with load.

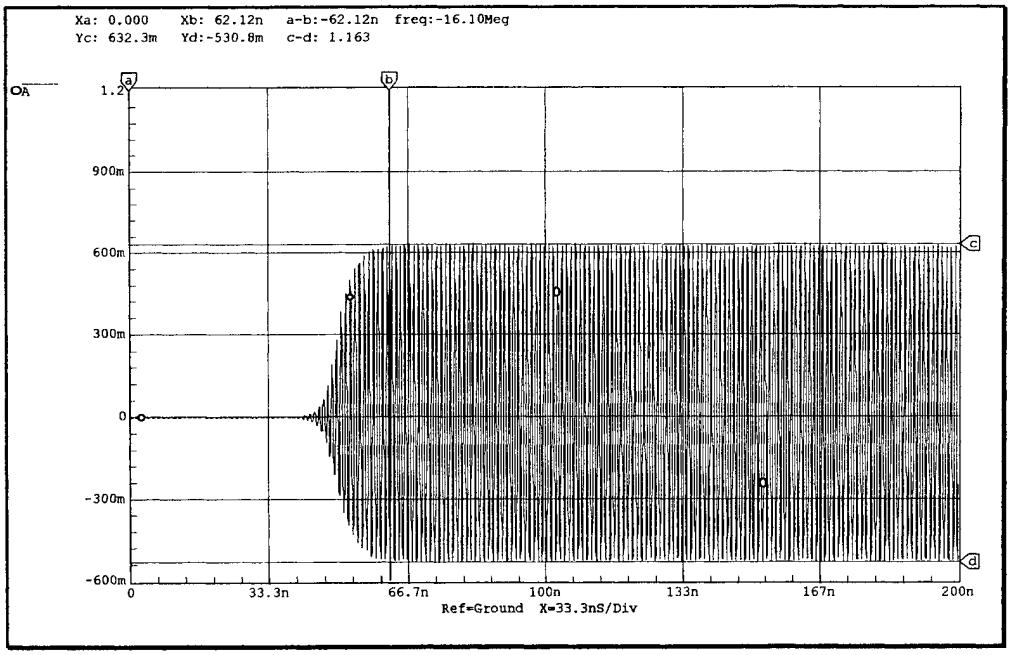

Figure A-3-9. Voltage across R1, 200nS span.

Figure A-3-11 shows that the voltage at the collector of Q1 has decreased from 10.12 Vp-p to 4.09 Vp-p. Therefore, not only did the C1/R1 combination reduce the output frequency, but the gain of Q1 as well.

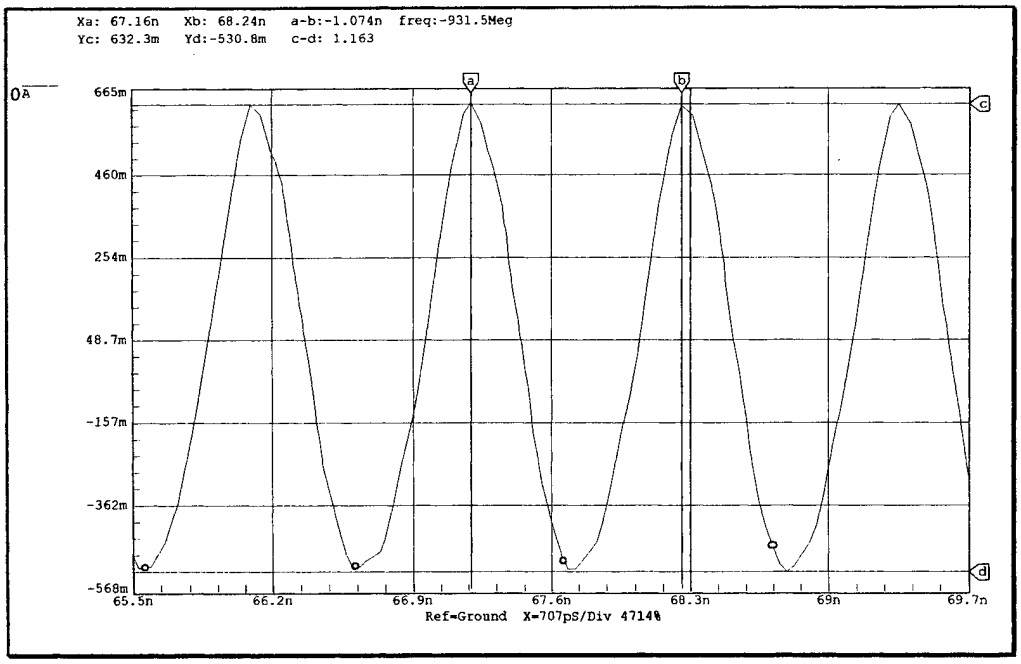

Figure A- 3-10. Voltage across R1, 69.7nS span.

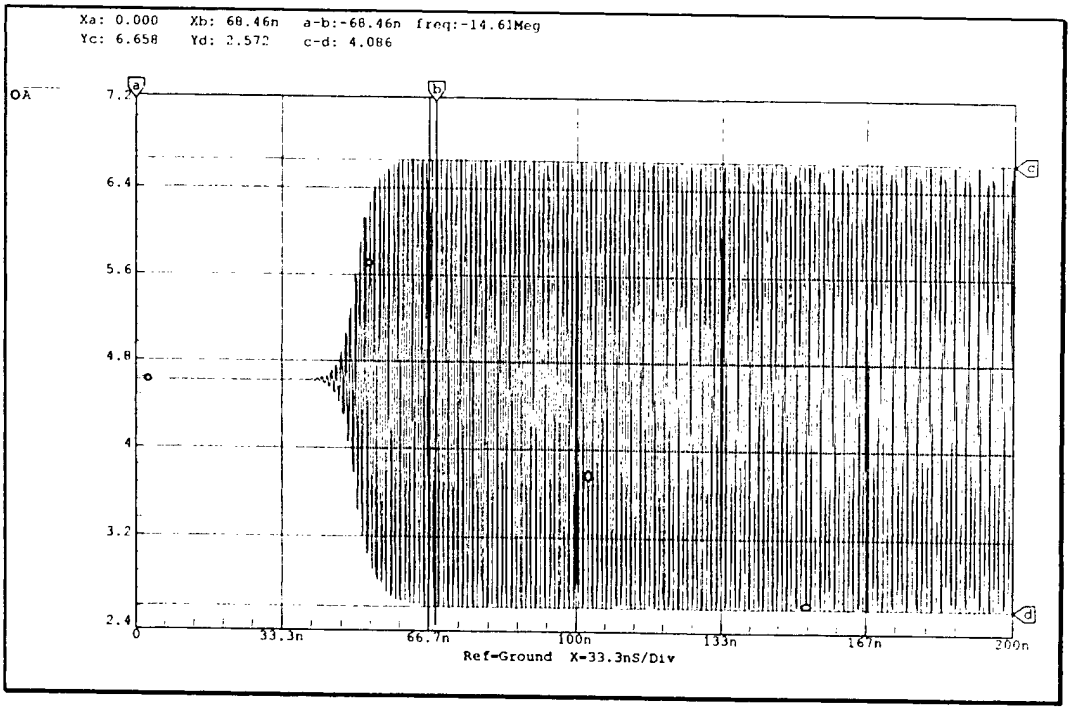

Figure A- 3-11. Oscillator with load, Q1-C.

3.2.2 Encoder.

The encoder on-off keys the oscillator to send ID and sensor data to the receiver. The heart of the encoder is the Holtek HT-12E IC. This IC encodes information consisting of eight address bits and four data bits. By using the four data bits as additional address bits, 4096 sensors can be represented in a system. When the transmission enable line ($\overline{TE}$) goes low, the device sends four words, each composed of thirteen bits. Each word consists of one synchronization bit, followed by eight address bits and four data bits. Each address and data bit takes three clock periods to transmit. A logic *one* consists of a low output on the data out (DOUT) line for two clock cycles followed by a high output for one clock cycle. A logic *zero* is represented by a low output for one clock cycle followed by a high output for two clock cycles. The rate of data transmission is set by choosing the clock frequency using an external resistor. Figure A- 3-12 shows the HT-12E configured to send address data only (as in a security application).

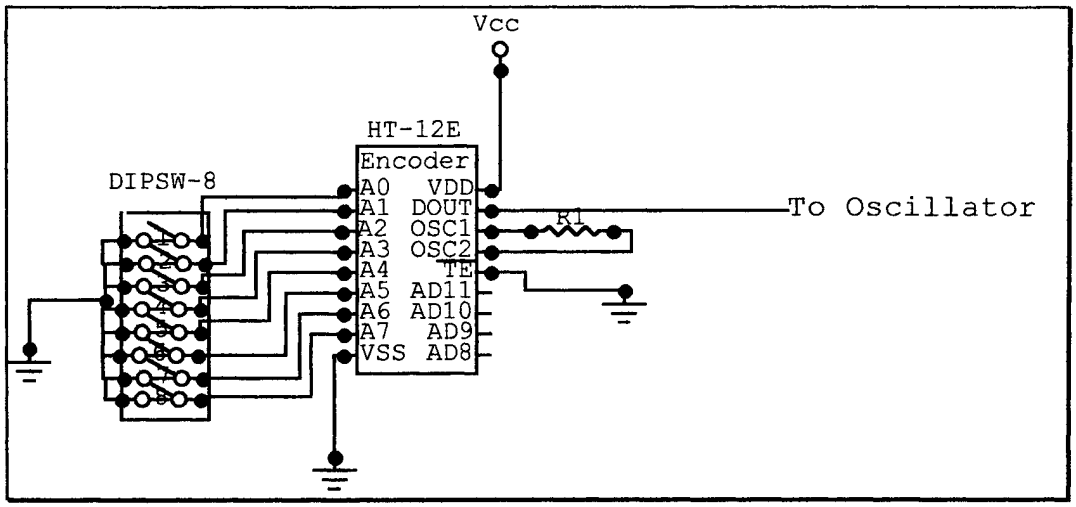

Figure A- 3-12. Encoder circuit.

The eight-bit address to be sent is set using the switch bank. The DOUT line toggles the oscillator on and off.

3.2.3 Aggregate Transmitter.

Figure A- 3-13 shows the schematic for the complete transmitter. The clock frequency chosen for the encoder is 3 kHz. This corresponds to a 1 kbps data rate and is set by choosing the value of R2 in Figure A- 3-13 for a specific power supply voltage from a graph in the HT-12E data sheet. The encoder IC is not capable of driving the oscillator directly since it is made to drive a CMOS load. Therefore, base-drive was added to the oscillator circuit via R1 and D1. The tank circuit at the output (L1 and C1) has been added to attenuate spurious emissions above and below the desired operating frequency.

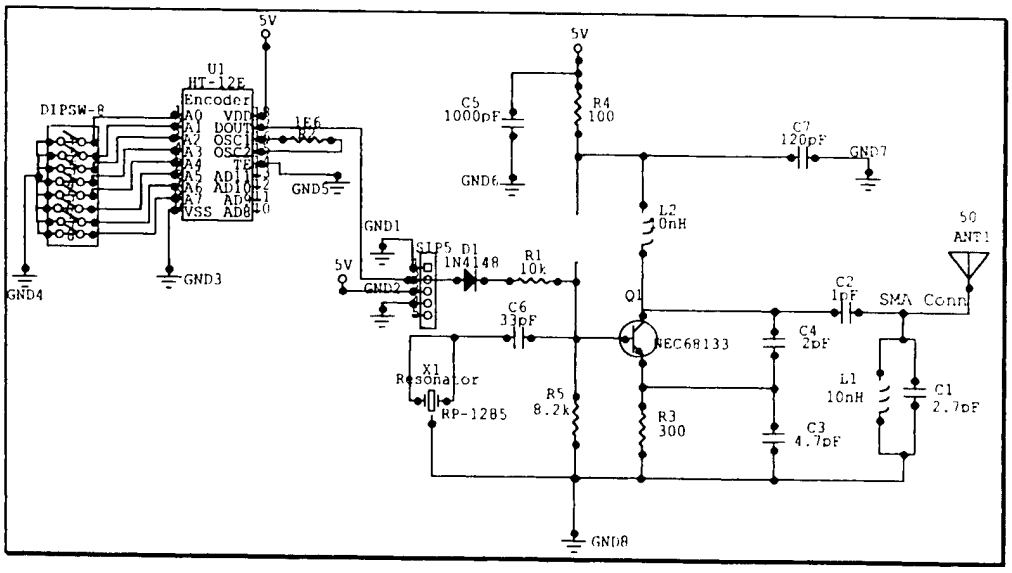

Figure A- 3-13. Transmitter schematic.

3.3 RECEIVER DESIGN.

The receiver consists of two sections, the receiver assembly and the decoder. The receiver assembly contains the RF circuitry necessary to amplify and convert the 916.55 MHz signals to base-band digital data. The decoder interprets this data. To make the system as flexible as possible, the decoder section is implemented on a standard engineering bread-board or *superstrip*. The receiver assembly requires a suitable RF layout for proper operation. Therefore, it is implemented on a PWB using surface-mount components.

3.3.1 Decoder.

The decoder reads the address and data bits received from the receiver PWB and interprets them. The heart of the decoder is the Holtek HT-12D IC. This IC looks for three correct eight-bit addresses (set by the proper levels on the decoder address lines (A0 through A7) in a row. If a valid address is received, the valid transmission line (VT) goes high and the data is decoded and appears on the latched data output pins (D8 through D11). Figure A- 3-14 shows the HT-12D configured to receive address data only (as in a security application).

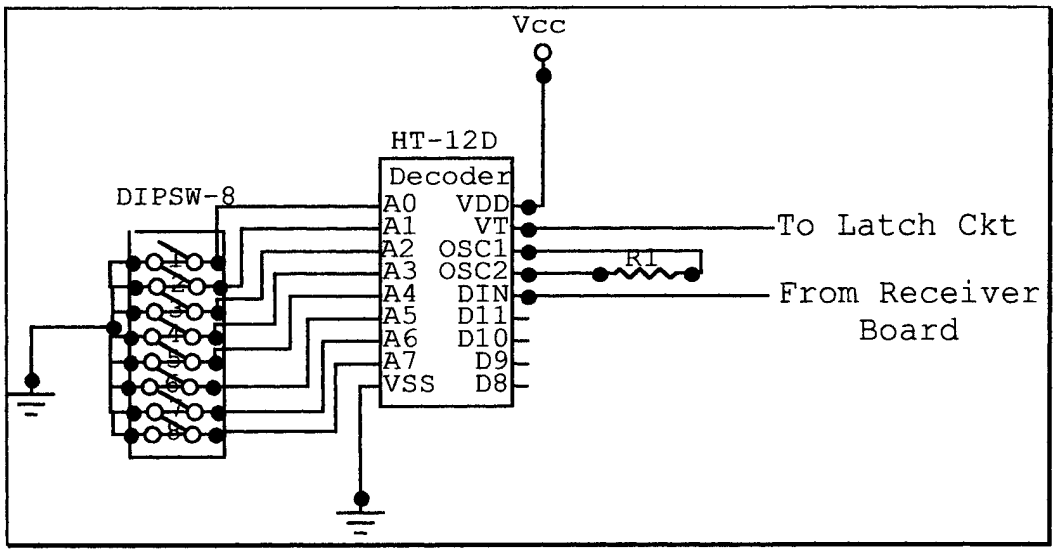

Figure A- 3-14. Decoder circuit.

The eight-bit address that the decoder is expecting is set using the switch bank. The VT line indicates a valid address is being received. Data received is presented at the data output pins (D8 through D11).

3.3.2 Receiver Assembly

The key component on the Receiver Assembly is the RX2010, a 916.5 MHz receiver IC manufactured by RFM. This IC contains approximately 70 dB of gain at 916.5 MHz, an AM detector and filtering at RF and base-band. The input is an AM modulated signal at 916.5 MHz and the output is a base-band digital waveform (the modulating function). If the range requirement were significantly less than 2,500 feet, this IC would be just about the only circuitry on the Receiver Assembly. The sensitivity of this part is given as -80 dBm (typical) and the noise equivalent bandwidth (NEB) is given as 24 kHz. Using this information to determine the part's noise figure [7]:

$$S = N_0 + NBW + NF + SNR \qquad \text{(A-3.4)}$$

where:

S = sensitivity (dBm)
No = theoretical noise floor (dBm/Hz)
NBW = noise bandwidth (10*log(NEB)), (dB*Hz)

NF = noise figure (dB)
SNR = output s/n ratio (dB)

Normally, the sensitivity of a device is given at a specified SNR. Since the sensitivity of the RFM receiver is specified as -80 dBm with no SNR given, it is assumed that -80 dBm is actually the noise-floor of the part (SNR = 0 dB). The theoretical (thermal) noise floor (in a 1 Hz bandwidth) is given as [8]:

$$P_n = k \cdot T \cdot B = 1.38 \cdot 10^{-23} J/K \cdot 298.15K \cdot 1Hz = 4.1145 \cdot 10^{-21} W \qquad \text{(A-3.5)}$$

where

k = Boltzmann's constant, $1.38*10^{-23}$ (J/K)
T = absolute temperature (K)
B = equivalent noise bandwidth (Hz)

Converting to dBm:

$$N_0 = Pn_{dBm} = 10 \cdot Log\frac{P_n}{1 \cdot 10^{-3}} = 10 \cdot Log\frac{4.1145 \cdot 10^{-21} W}{1 \cdot 10^{-3} W} = -173.86 dBm/Hz$$

Determining the NBW:

$$NBW = 10 \cdot Log(NEB) = 10 \cdot Log(24kHz) = 43.8 dB \cdot Hz$$

Therefore, rearranging equation (A-3.4) and substituting values yields:

$$NF = S - (N_0 + NBW + SNR) = -80dBm - (-173.9dBm + 43.8dB + 0dB) = 50.1dB$$

Now that the noise-figure is known, the sensitivity of the part for a specific SNR can be determined. In this application, the encoder sends four data packets, each consisting of one synchronization bit, eight address bits and four data bits. The four-packet sequence takes 91 msec to transmit. The decoder must receive (at a minimum) the synchronization bit and the eight address bits three times in a row out of the four times that they are sent in order to indicate a valid transmission. If one bit is in error out of the 52 bit sequence sent, the decoder will still receive a valid transmission. If two bits are in error, it is possible that these bits are contained in two separate address packets and therefore, a valid transmission will not be received. Therefore, as an estimate of the minimum required bit error rate (BER), 1/52 (19.23e-3) is chosen. Since robust

communications are desired, the system is designed for a BER ten times better (a BER less than 1.923e-3). To determine the proper SNR to yield an acceptable BER rate for OOK modulation [9]:

$$BER = 0.5 \cdot erf\left[0.5\sqrt{SNR}\right] \qquad \text{(A-3.6)}$$

A SNR ratio of 12.3 dB yields a BER of 1.78e-3.

The sensitivity of the RFM part is calculated for the desired 12.3 dB SNR using equation (A-3.4):

$$S = N_0 + NBW + NF + SNR = -173.86dBm + 43.8dB + 50.1dB + 12.3dB = -67.7dBm$$

Therefore, to achieve an acceptable BER for this application, the input signal power to the RFM part (RX2010) has to be at least -67.7 dBm

Converting to watts:

$$P_W = 1mW \cdot 10^{\frac{P_{dBm}}{10}} = 1mW \cdot 10^{\frac{-67.7dBm}{10}} = 169.82pW$$

To determine the expected range knowing that the transmitter output power is 750 uW (specified) and assuming ideal omnidirectional antennas as before:

Solving (3.1) for r yields:

$$r = \frac{\lambda \cdot \sqrt{P_t \cdot G_t \cdot G_r}}{4 \cdot \pi \cdot \sqrt{P_r}} = \frac{\frac{c}{916.55MHz} \cdot \sqrt{750uW}}{4 \cdot \pi \cdot \sqrt{169.82pW}} = 54.7m \qquad \text{(A-3.7)}$$

This corresponds to 179.5 feet, significantly less than the specified range of 2,500 feet (762 meters). Therefore, the RFM part can not be used alone in this application.

Knowing that the operating frequency is 916.55 MHz, and recalculating the necessary received power (from equation A-3.1) yields:

$$P_r = P_t \frac{G_r \cdot G_t \cdot \lambda^2}{(4 \cdot \pi \cdot r)^2} = 750uW \frac{1 \cdot 1 \cdot \left(\frac{c}{916.55 \cdot 10^6}\right)^2}{(4 \cdot \pi \cdot 762)^2} = 874.9fW$$

This corresponds to -90.58 dBm. To determine the necessary receive system noise figure:

$$NF = S - (N_0 + NBW + SNR) = -90.58dBm - (-173.9dBm + 43.8dB + 12.3dB) = 27.22dB$$

It is possible to improve the noise figure of a receiver by inserting high gain, low-noise amplifiers (LNAs) at the front-end of a receive system. The cascaded noise figure equation is [10]:

$$F_{IN} = F_1 + \frac{F_2 - 1}{G_1} + \frac{F_3 - 1}{G_1 \cdot G_2} + \ldots + \frac{F_n - 1}{G_1 \cdot G_2 \cdot \ldots \cdot G_{n-1}} \qquad \text{(A-3.8)}$$

where

F_{IN} = the equivalent input noise factor

$F_1, F_2, F_3, \ldots, F_n$ = the noise factors of stages 1, 2 and 3 respectively

$G_1, G_2, \ldots, G_n$ = the linear gains of stages 1 and 2 respectively

The relationship between noise-figure (NF) and noise-factor (F) is:

$$NF_{dB} = 10 \cdot Log(F) \qquad \text{(A-3.9)}$$

or

$$F = 10^{\frac{NF_{dB}}{10}} \qquad \text{(A-3.10)}$$

The relationship between linear power gain and power gain in dB is identical.

It is desirable to add gain only at the intended frequency of operation between the receive antenna and the RFM receiver IC (RX2010). Adding wide-band amplification will increase the amplitude of undesired signals as well as desired signals at the input to the RX2010. This could result in receiver desensitization caused by nearby signals (cellular phones, cordless telephones, etc.) which would limit the system range. Therefore, a filter is placed between the antenna and amplifiers. Figure A-3-15 illustrates one system that will reduce the receiver noise figure below the necessary 27.22 dB.

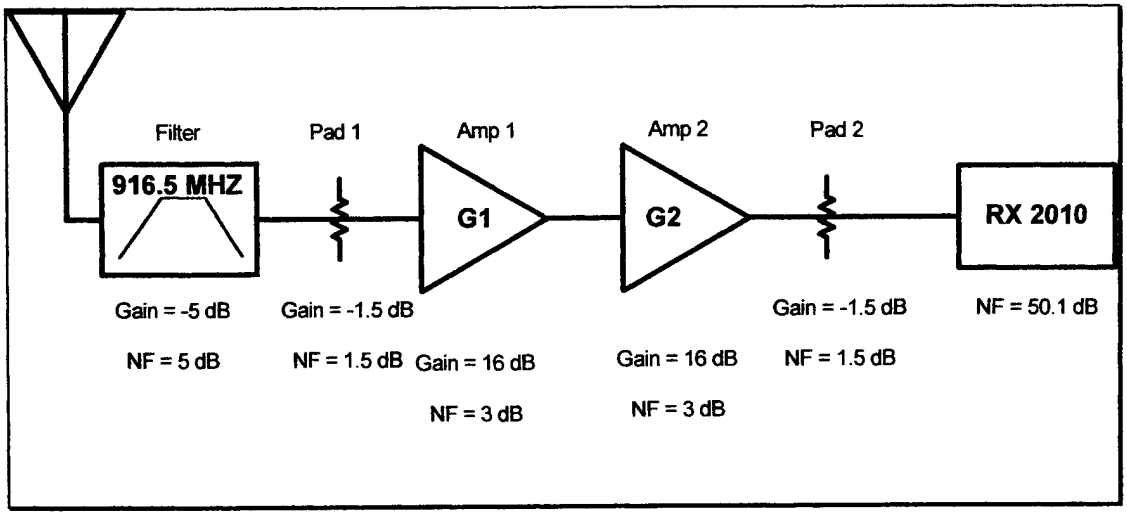

Figure A- 3-15. Receive system block diagram.

The filter is an RF1181 SAW filter manufactured by RFM. It has a typical insertion loss of 5 dB and rejection of at least 30 dB 10 MHz away from the center frequency. Pad 1 and Pad 2 are standard resistive attenuators that serve as buffers between the RF1181 and Amp1 and between Amp2 and the RX2010. They are necessary since the amplifiers require a reasonable 50 ohm termination at their inputs and outputs over a wide range of frequencies. The RF1181 and the RX2010 present a 50-ohm impedance at 916.55 MHz, otherwise the impedance of these two devices varies significantly. Amp1 and Amp2 are MAR-6SM surface-mount amplifiers manufactured by Mini-Circuits. They have gain from DC to over 2 GHz, a low noise-figure and require 16 mA at 3.5 VDC to operate. Converting the noise-figure and gain values from dB to linear form to be used in equation (A-3.8) yields:

Table A- 3-2. Receive system parameters.

Parameter	Value (dB)	Linear Value
Filter noise figure	5	3.162
Filter gain	-5	0.316
Pad noise figure	1.5	1.413
Pad gain	-1.5	0.708
Amplifier noise figure	3	1.995
Amplifier gain	16	39.811
RX2010 noise figure	50.1	102,330

Applying these values to equation (A-3.8) yields:

$$F_{IN} = 3.162 + \frac{1.413-1}{0.316} + \frac{1.995-1}{0.316 \cdot 0.708} + \frac{1.995-1}{0.316 \cdot 0.708 \cdot 39.811} + \frac{1.413-1}{0.316 \cdot 0.708 \cdot 39.811 \cdot 39.811} + \frac{102.330-1}{0.316 \cdot 0.708 \cdot 39.811 \cdot 39.811 \cdot 0.708} = 416.63$$

This corresponds to a receive system noise figure of 26.2 dB. Substituting this noise-figure into equation (A-3.4) to determine the receiver's sensitivity (with a 12.3 dB SNR):

$$S = N_0 + NBW + NF + SNR = -173.86dBm + 43.8dB + 26.2dB + 12.3dB = -91.56dBm$$

This power level corresponds to 698.23 fW. Using equation (A-3.7) to determine the range of the system yields:

$$r = \frac{\lambda \cdot \sqrt{P_t \cdot G_t \cdot G_r}}{4 \cdot \pi \cdot \sqrt{P_r}} = \frac{\frac{c}{916.55MHz} \cdot \sqrt{750uW}}{4 \cdot \pi \cdot \sqrt{698.23fW}} = 852.98m$$

Therefore, the expected range of this system is 853 meters or 2,799 feet.

3.3.3 Aggregate Receiver.

Figure A- 3-16 shows the schematic for the complete receiver circuit. L1, C1 and L2, C2 match the SAW filter to the 50-ohm RF path impedance at 916.55 MHz. The 1.5 dB attenuators (R1, R19, R20 and R21, R22, R23) are in a standard pi configuration and yield 1.5 dB of wide-band power loss. These pads isolate the SAW filter (FL1) and the receiver hybrid (U3) from the termination sensitive low-noise amplifiers (U1, U2). The bias to U1 and U2 is determined by the voltage drop across R2 and R3 respectively. Each amplifier requires 3.5 VDC at a nominal current drain of 16 mA. Therefore, the 150 ohm resistors allow 16.7 mA of bias current for each part. R5 and D1 form a simple voltage regulator to power U3 and U5. The analog output of the receiver is passed to U4A and the associated resistors that form an amplifier circuit (Av=20) and level shifter. Once the signal is amplified, a peak detector converts the level into a DC voltage that is applied to the Schmitt trigger consisting of U4B and associated resistors. The trigger level is controlled by R16. During the prototyping phase, a fixed value is chosen for R16 such that large input signals cause the Schmitt trigger to fire, acting as an overload detect circuit.

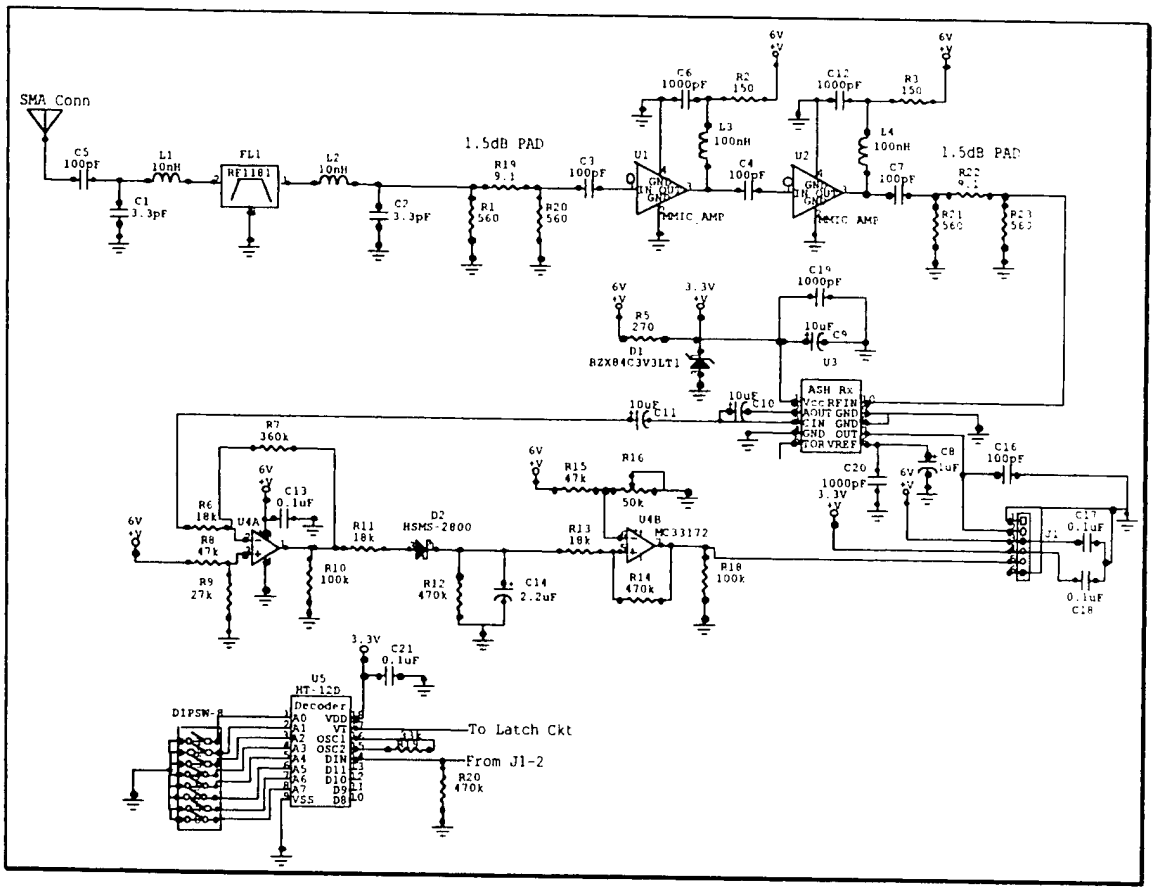

Figure A- 3-16. Receiver schematic.

SECTION 4

SYSTEM PROTOTYPE PHASE

4.1 TRANSMITTER.

The RF oscillator portion of the transmitter was implemented on a PWB. Traxmaker 5.0 software was utilized to develop a suitable RF layout and Alberta Printed Circuits was contracted to manufacture the PWB. The oscillator was built in sections similar to the design process documented earlier until a functional oscillator with low spurious emissions and the proper output power was developed. The encoder circuitry was added afterwards for range testing.

4.1.1 RF Oscillator.

The circuit shown in Figure A- 4-1 was built using surface-mount components on a PWB.

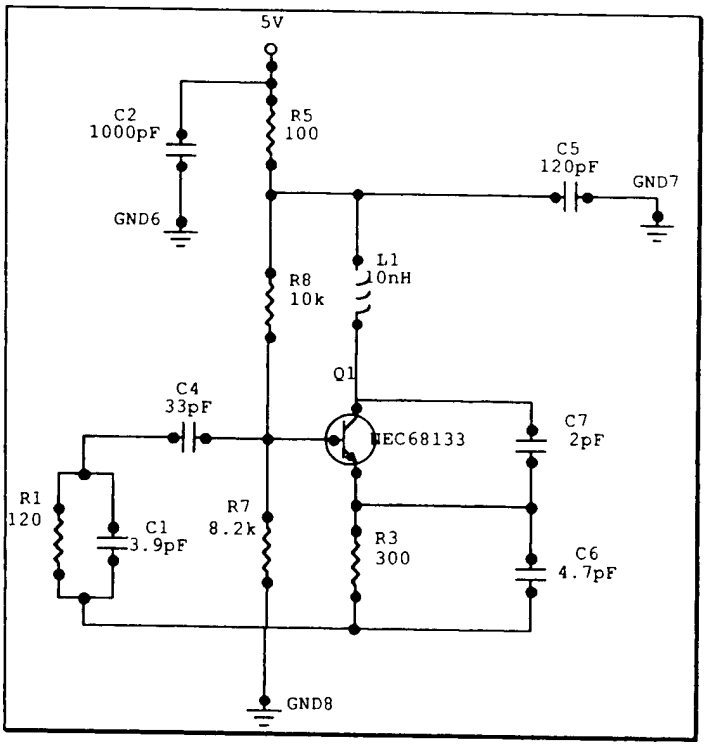

Figure A- 4-1. Prototype oscillator.

With +5.0 VDC applied, the following parameters were measured:

Table A- 4-- 1 Initial oscillator parameters.

Parameter	Value
Input Current (through R5)	5.15 mA
Collector Voltage	4.57 VDC
Emitter Voltage	1.33 VDC
Base Voltage	1.81 VDC
RF at the collector	578.125 MHz, 3.08 VRMS

The transistor bias levels and the total circuit input current are close to the designed levels. The frequency of oscillation is much lower than expected. After careful examination of the PWB layout, it was determined that there is stray inductance

between the RF ground at GND7 and C5. To increase the frequency of oscillation to the designed value, the value of L1 was reduced as follows:

The resonant frequency of L1, C6 and C7 is given by equation (A-3.3) which is repeated here for convenience.

$$F_R = \frac{1}{2 \cdot \pi \cdot \sqrt{\frac{L1 \cdot C_6 \cdot C_7}{C_6 + C_7}}}$$

This can be restated as the simple L-C resonance condition:

$$F_R = \frac{1}{2 \cdot \pi \cdot \sqrt{L \cdot C}}$$

The desired frequency of operation is approximately 1.6 times the current resonant frequency. Therefore, the new value for L1 must be at least the square of 1.6 or 2.56 times smaller. This gives a new value of 3.91 nH for L1. L1 was replaced by 3.3 nH since it was the closest standard value in the series of RF inductors on hand. The resonant frequency increased to 759 MHz, which is much closer to the design frequency but still too low.

C7 was reduced from 2.0 pF to 0.5 pF to further increase the frequency of oscillation. The oscillator frequency increased to 997 MHz. Next, a 1 pF coupling capacitor was added at the collector of Q1 and connected to the input of a spectrum analyzer (50 ohms input impedance). The oscillation frequency shifted to 902.75 MHz and the output power was measured to be -19 dBm. In addition, a parallel tank circuit was added at the output consisting of a 3.3 nH inductor and a 4.7 pF capacitor. The oscillation frequency shifted to 895.5 MHz at an output power of -13 dBm.

Since the coupling capacitor and tank circuit at the output reduced the frequency of oscillation, C6 was reduced to 3.9 pF to increase the oscillation frequency. In addition, another 120 pF capacitor was added in parallel with C5 to establish a better RF ground at the L1, C5 junction. This caused the output frequency to increase to 1.02 GHz and

the output power to increase to 6.8 dBm. After increasing C7 to 1.0 pF, the output frequency was 963 MHz and the output power was -1.1 dBm or 776 uW.

Now that the frequency of oscillation and output power were close to the specified values, R1 and C1 were replaced by the RP1285 SAW resonator. The oscillator output frequency did not lock-in to 916.55 MHz as expected but increased to 985.5 MHz and the circuit yielded an output power of -0.28 dBm. To reduce the oscillation frequency to 916.55 MHz, C6 was increased to its original design value of 4.7 pF and C7 was increased to 1.5 pF. The oscillation frequency decreased to 916.415 MHz at an output power of 3.04 dBm. This frequency is within the 916.550 MHz +/- 150 kHz limits given in the specifications for the RP1285. The output power is significantly higher than necessary. Therefore, R3 was increased to 470 ohms. This reduced the output power to -0.51 dBm at a supply current of 3.23 mA.

The final oscillator circuit is shown in Figure A- 4-2.

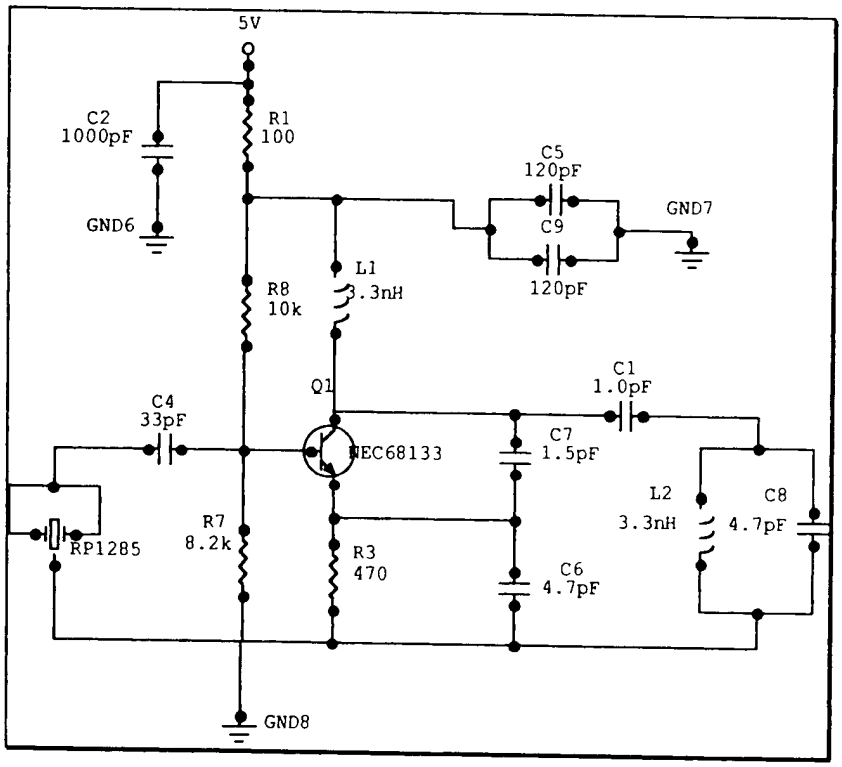

Figure A- 4-2. Complete oscillator circuit.

4.1.2 Oscillator Experimental Results.

Table A- 4-2. Oscillator circuit parameters.

Parameter	Value
Input Current (through R1)	3.23 mA
Collector Voltage	4.68 VDC
Emitter Voltage	1.40 VDC
Base Voltage	1.92 VDC
RF at the output (into 50 ohms)	916.415 MHz, -0.51 dBm

The output power-spectral density (PSD) is viewed on an HP Spectrum analyzer from 10 kHz to 1.8 GHz. There are no spurious emissions to 66 dBc. This is much better than the required 48 dB limit set by the FCC.

To determine the suitability of this circuit for OOK data transmission, the power supply line is powered by a signal generator. The signal generator is adjusted to supply a square-wave with a 50 % duty cycle, a peak voltage of 5 V and a peak-peak voltage swing of 5 V. Figure A-4-3 shows that there are spurious emissions approximately 57 dBc at 923.75 MHz for a data rate of 1 kbps. Figure A-4-4 illustrates that these emissions are approximately 57 dBc at 921.5 MHz for a 3 kbps data rate. These emissions are below

the FCC limit and are the only observed spurs from 10 kHz to 1.8 GHz.

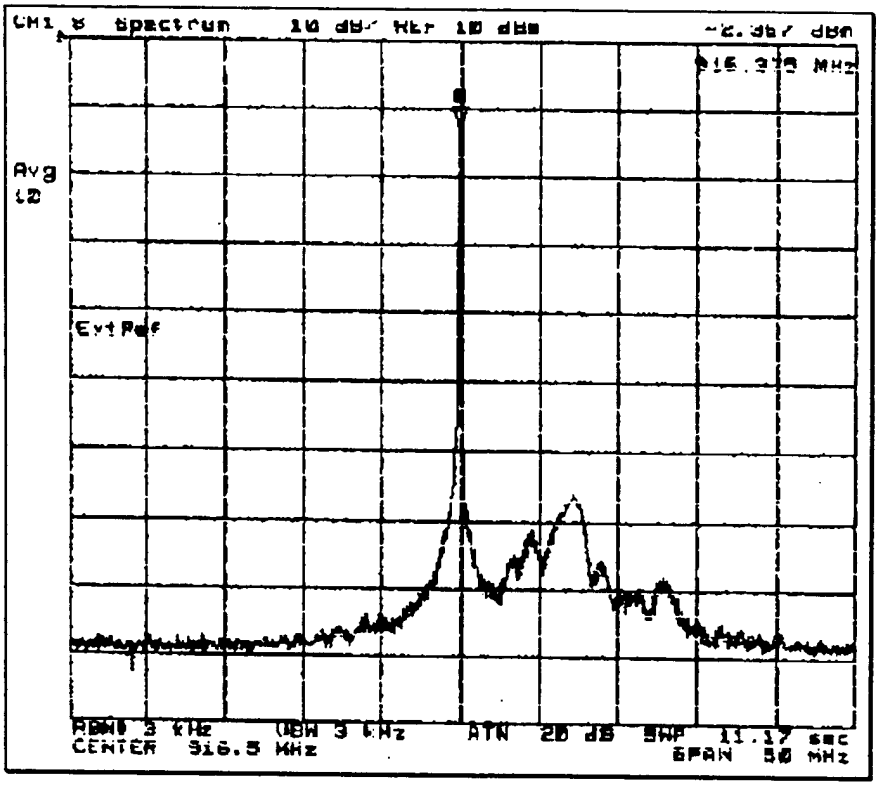

Figure A- 4-3. Oscillator output power, 1 kbps

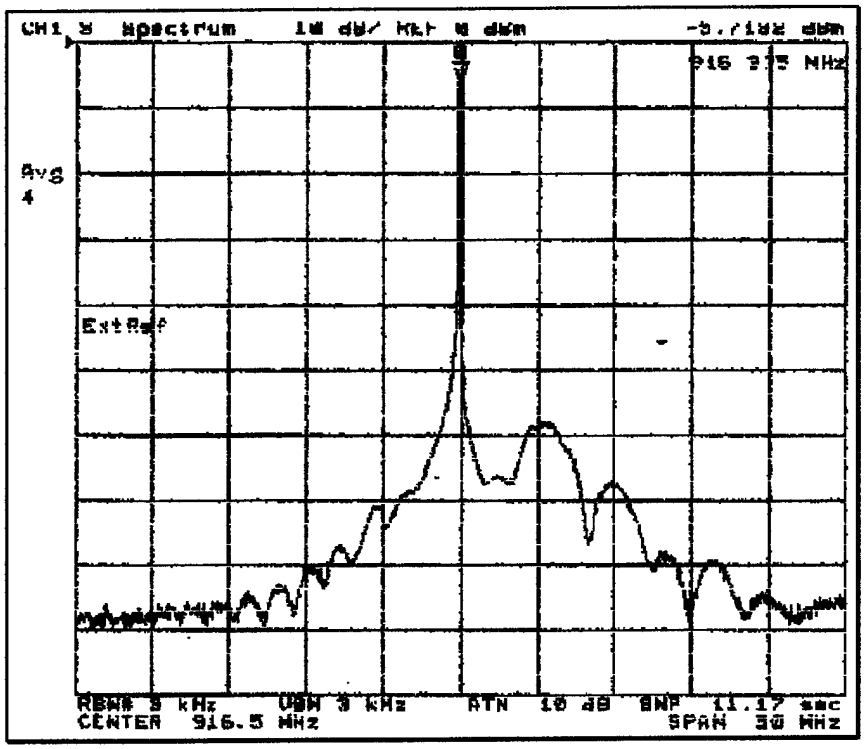

Figure A- 4-4. Oscillator output power spectrum, 3kbps data rate.

4.1.3 Transmitter Prototype.

Figure A- 4-5 is a schematic of the complete transmitter including the encoder and power supply. When the transmitter is turned-on, the encoder on-off keys the oscillator to send ID data. The peak output power was measured as -0.84 dBm in this configuration which is 0.41 dB higher than the allowed radiated field strength. It is assumed that at least this much loss exists in the antenna system. The circuitry to the left of J1 was implemented on a *superstrip* while the RF circuitry (to the right of J1) was implemented on a double-sided PWB using surface-mount components. The RF output is connected to a 1/4 wave antenna through a short piece of 50 ohm coax cable. The antenna length was adjusted to achieve a VSWR of 1.07:1 at 916.50 MHz.

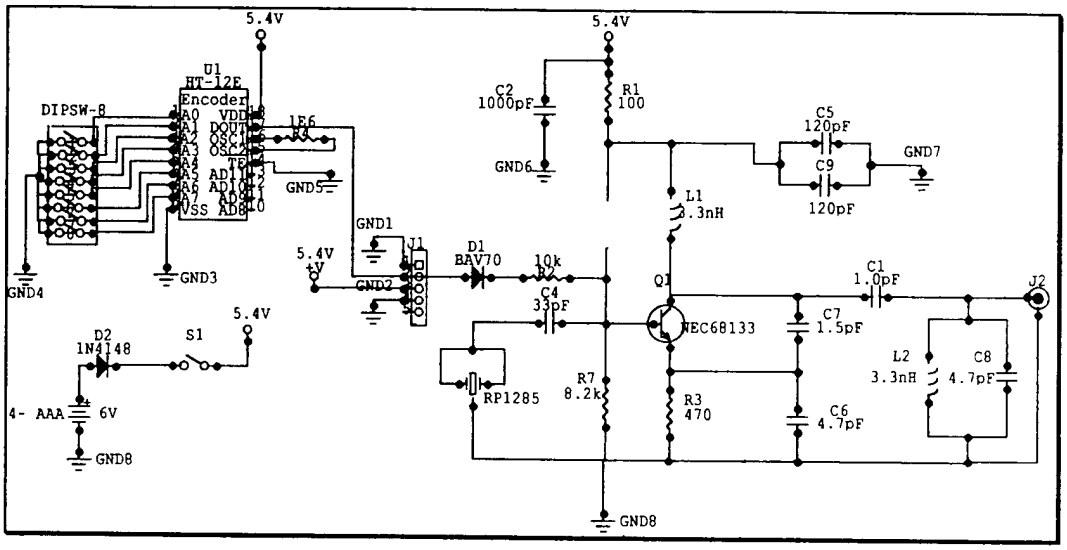

Figure A- 4-5. Prototype transmitter schematic.

Figure A- 4-6 is a photograph of the PWB that contains the RF oscillator. Figure A- 4-7 is a photograph of the inside of the completed transmitter showing the *superstrip* circuitry as well as the RF oscillator and the power supply.

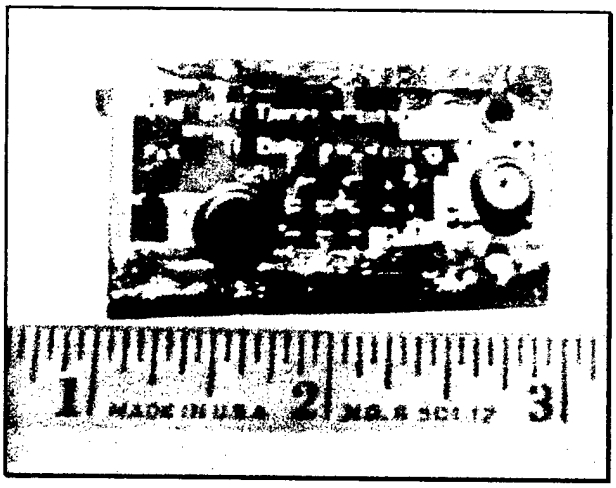

Figure A- 4-6. RF oscillator.

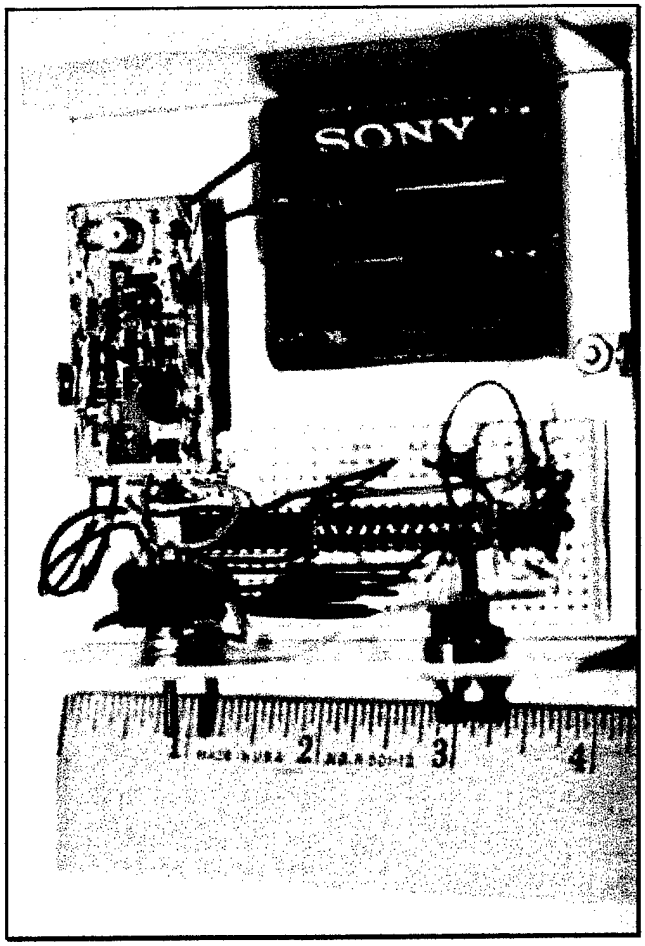

Figure A- 4-7. Prototype transmitter.

4.2 RECEIVER.

4.2.1 Receiver Assembly.

The following circuit was implemented on a double-sided PWB:

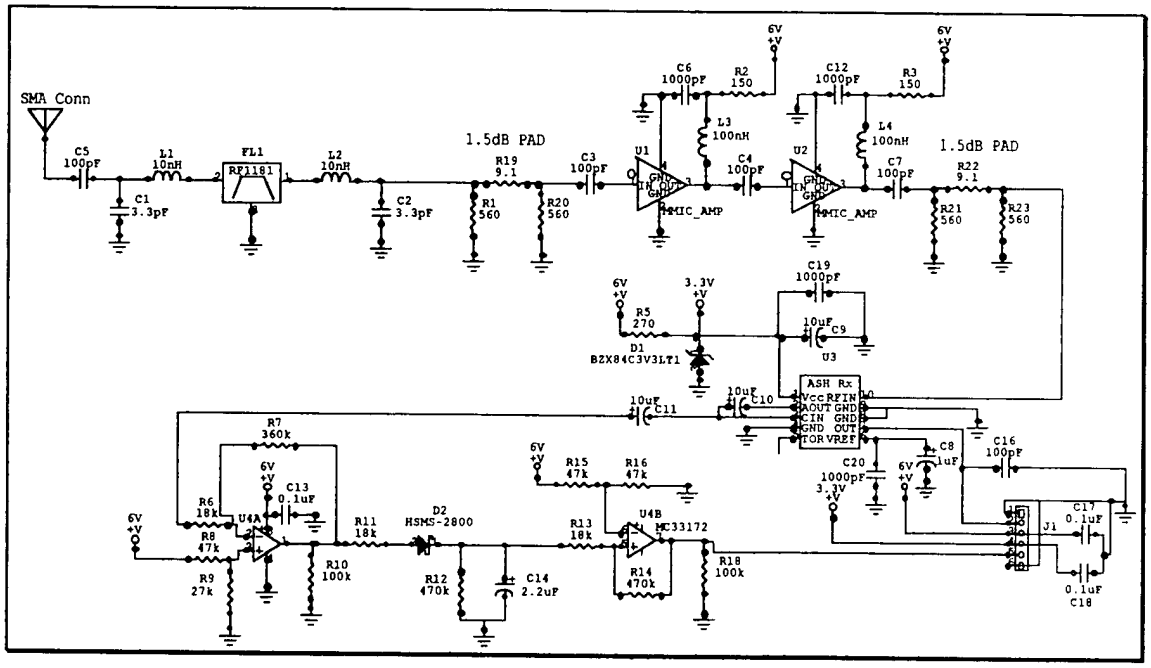

Figure A- 4-8. Prototype receiver assembly.

4.2.2 Receiver Assembly Experimental Results.

To check the RF circuit gain a -60 dBm carrier is injected at the input to the RF path through C5 using an HP RF signal generator. Using a 10x high-impedance RF probe, the junction of R21 and R22 is monitored. The RF path amplification is 31.2 dB from the antenna port to this point. Therefore, the overall RF path amplification in front of the RX2010 is 29.7 dB. The expected amplification is 24 dB (16 dB for U1 and for U2 minus the two 1.5 dB pads and the 5 dB filter). The SAW filter insertion loss is 5.15 dB. Therefore, the extra amplification is attributed to U1 and U2.

To check the selectivity of the RF path, the response of FL1 (and matching circuitry) is measured on a network analyzer. The insertion loss is 5.15 dB and the selectivity at 5 MHz from the center frequency is between 10 and 12 dB.

To check the receiver's sensitivity, a 916.5 MHz carrier, 100% modulated with a 1 kHz sine-wave is applied to the RF input. At a carrier level of -106 dBm, a base-band signal is barely perceptible at the digital output of U3 (U3-7). This puts the noise-floor of the receiver just below -106 dBm, which is better than the expected receiver noise-floor of -

103.86 dBm (the expected sensitivity of -91.56 dBm plus the SNR of 12.3 dB). As the input power is increased, the output approaches a 1 kHz square-wave.

The trip-point of the Schmitt trigger circuit (U4B) is adjusted by choosing R16 such that a -96 dBm signal (@ 916.5 MHz, 100% modulated by a 1 kHz sine-wave) causes the circuit to trip and indicate an "overload" condition. The input signal level must be reduced by at least 5 dB to cause the overload indication to cease. This level was determined experimentally as it allows for a transmitted signal of the type used in this system to be received at close range without falsely indicating an overload condition.

4.2.3 Receiver Prototype.

Figure A- 4-9 is the schematic of the entire receiver. The decoder circuit, the D-latch and associated circuitry, and Q3 and associated circuitry were implemented on a

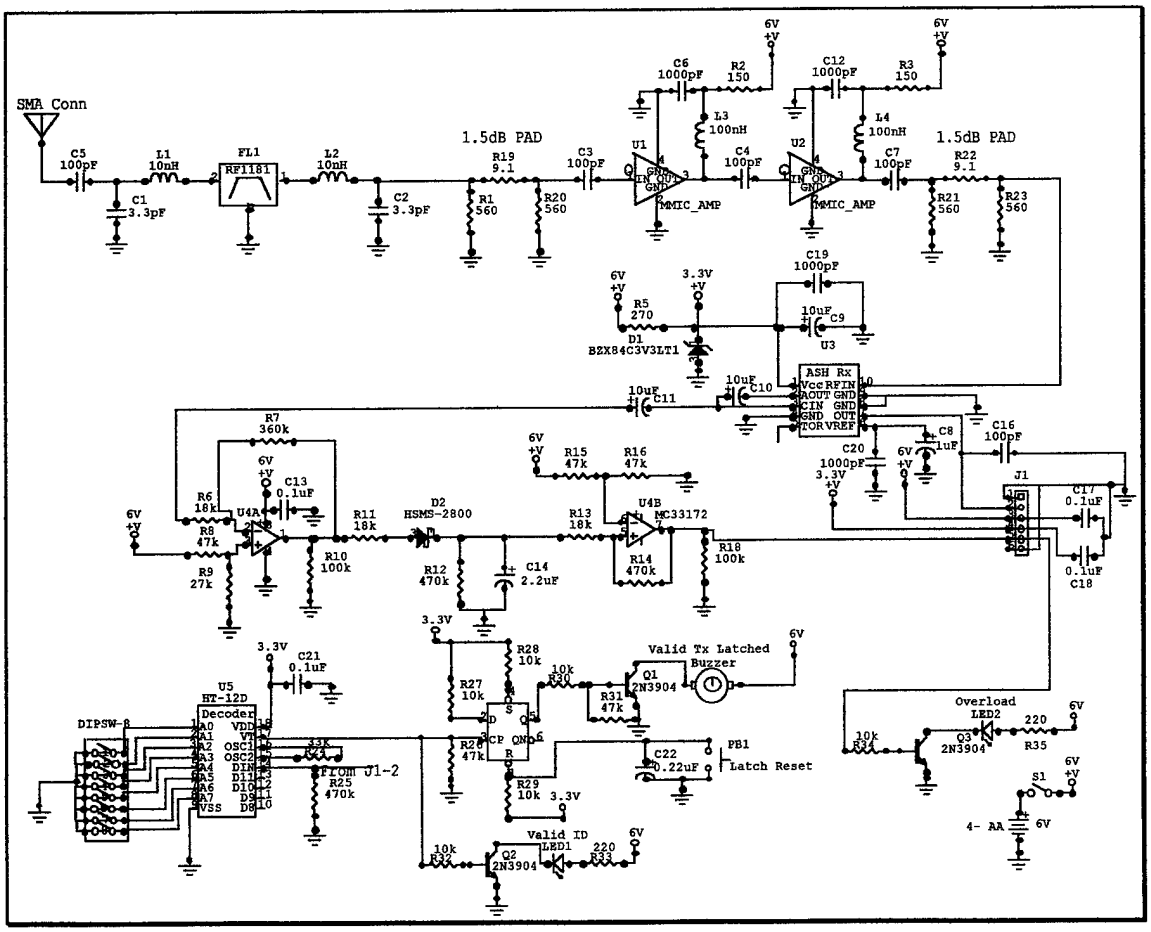

Figure A- 4-9. Receiver prototype schematic.

superstrip. The rest of the receiver was implemented on a double-sided PWB.

Figure A- 4-10 is a photograph of the PWB that contains the Receiver Assembly. The metal fence around the perimeter holds a metal shield that covers the circuitry. This shield reduces the level of stray signals entering the RF path and serves to isolate the antenna from the RFM receiver IC.

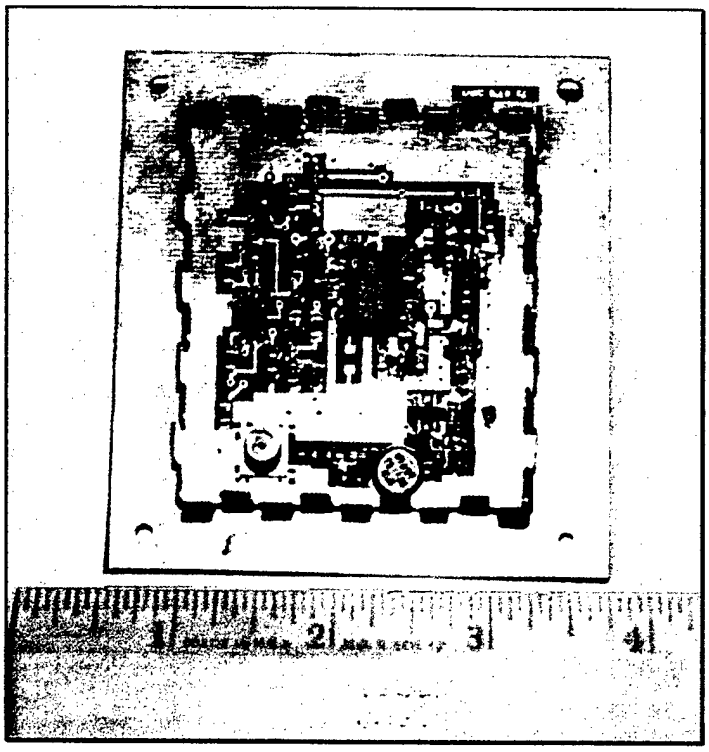

Figure A- 4-10. Prototype receiver assembly.

4.3 RANGE TESTING.

Figures A- 4-11 and A- 4-12 are photographs of the transmitter and receiver prototypes. These units were used to test the range of the communications link outside under close to ideal conditions as well as inside of a standard residential dwelling and in a more commercial type structure.

Figure A- 4-11. Transmitter.

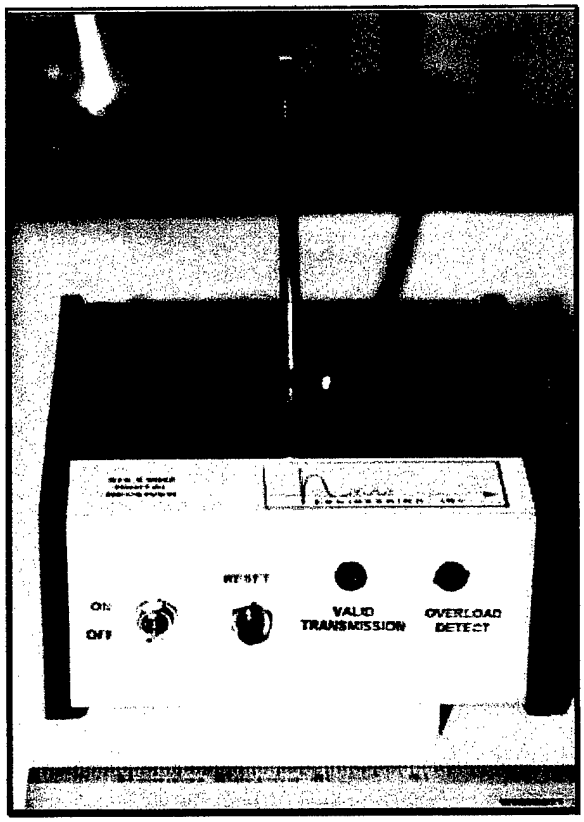

Figure A- 4-12. Receiver.

The outside LOS range of this system was measured by holding the transmitter and receiver approximately six feet above the ground, turning them both on and separating them until successful communications could no longer be established. As the receiver was separated from the transmitter, the valid ID detect LED would flicker. As the separation distance increased, this flickering was more evident. This is caused by multiple paths reaching the receiver from the transmitter at the same time and adding in such a way as to decrease the RF level at the receiver input. Multipath nulls were observed in specific locations. As a null was encountered, leaving the receiver in the same location would usually result in a constant null or lack of communication. If the receiver was then moved a fraction of a wavelength, communications would resume. For the system described in this report, the measured range is 0.51 miles which exceeds the design goal of 2,500 feet and is only slightly less than the expected 0.53 miles.

System operation was also observed inside a standard residential dwelling with excellent results. Very few nulls were encountered and 100 % coverage (about 60 feet and four levels) was achieved. At Rochester Institute of Technology, inside of the engineering building, the transmitter was set-up in the center of the third floor (in a hallway surrounded by brick walls on two sides). The receiver was then walked around the third floor and then the second floor. The distance between the transmitter and receiver varied and was approximately 120 feet at the point of greatest separation. Nulls were encountered approximately 5-10% of the time on the third floor and approximately 10 - 20% of the time on the second floor. The signal penetrated several brick walls and steel doors as well as one floor/ceiling. As before, moving the receiver a small distance after encountering a null resulted in resuming successful communication.

When implementing this type of system, especially indoors, the receiver is usually installed first. Each transmitter is tested as it is installed and moved slightly if it cannot communicate with the receiver due to multipath fading. If the transmitter locations are

fixed in a system installation, reorienting the transmitter antenna is one option to ensure successful communication.

SECTION 5

DISCUSSION

Table A-5-1 below is a brief comparison of the system requirements and measured results:

Table A- 5-1. System requirements and measured results.

DESCRIPTION	REQUIREMENT	MEASURED
Frequency of Operation	Between 902 and 928 MHz	916.415 MHz
Data Rate	1 kbps	1 kbps (tested to 3 kbps)
Outside LOS Range	2,500 Feet	2,693 Feet
Oscillator Input Power	Less than 25 mW (5V line) for 100 msec	16.15 mW peak, ~ 4 mW average for 91 msec
Oscillator Output Power	~ 750 uW (Radiated FCC limit)	824 uW into the antenna

From this table, it is clear that the system requirements have been met. The transmitter output frequency is 916.415 MHz, which is within the receiver passband (916.5 MHz, +/- 200 kHz nominal). Range testing was performed at a 1 kbps data-rate and the transmitter was tested to 3 kbps. The oscillator consumes less input power than specified and radiates at the FCC limit (assuming 0.41 dB loss in the transmitter antenna). The complete transmitter circuit, operating continuously, draws less than 750 uAmps from a 5 volt source due to the low duty cycle.

This system can be easily adapted to transmit additional information that would make it useful for any kind of remote monitoring application, such as a wireless thermostat,

humidity sensors, pressure and temperature sensors, etc. For example, a wireless thermostat, humidity sensors, pressure and temperature sensors, etc. The range can be improved by increasing the sensitivity of the receiver further or by using directional antennas. Since the transmitter input power is so low, one transmitter operating intermittently would last for a long period of time on a couple of watch-type batteries.

A miniature transmitter breadboard was developed for this application. A picture of this transmitter is given in Figure A- 5-1. The two small circular PWBs contain encoder and oscillator circuitry as well as additional interface components for the ANRO WASP sensor. The size of this miniature transmitter circuit (less than 1 inch in diameter and

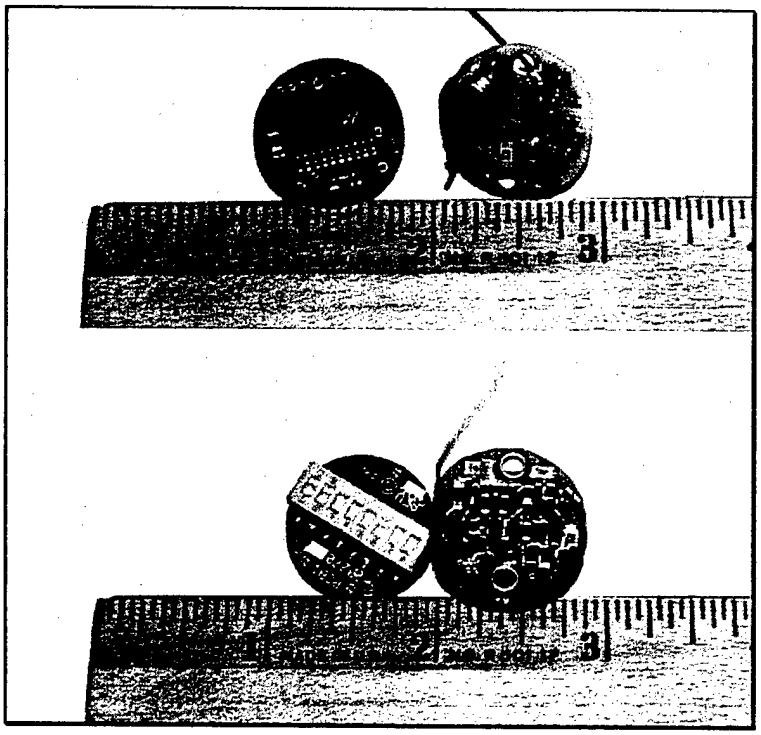

Figure A- 5-1. Miniature transmitter.

less than 5/8 of an inch deep) allows for covert installation in a standard doorknob. Due to the size constraints, surface-mount technology is a necessity in this case.

In quantities of several thousand, the per-unit cost to build these miniature transmitters will be on the order of five to ten dollars. The receiver cost will be much higher at approximately thirty to forty dollars.

SECTION 6

RECOMMENDATIONS

To improve the system range, reduce multipath fading and reduce the probability of interception and detection (or jamming), a spread-spectrum system is suggested as the next logical step. The proposed communication system could be used as a repeater for the ANRO wireless and self-powered sensors or as a battery operated communication link.

6.1 SPREAD-SPECTRUM SYSTEM DESIGN.

Recently, the FCC and regulatory bodies around the world have allowed "unlicensed operation" at higher output powers and spread-spectrum data transmission in various frequency bands. The lowest common unlicensed band is located around 2.45 GHz. FCC part 15.247 specifies spread-spectrum operation from 2400-2483.5 MHz. The regulations describe many characteristics for frequency-hopping and direct-sequence systems. In this report, only direct-sequence systems are discussed. The peak allowed output power is 1 Watt. Therefore, the allowed output power in this frequency band is three to four orders of magnitude higher than that allowed in the narrow-band systems mentioned earlier. Since spread-spectrum transmission is utilized, SNR ratios are much higher due to processing gain. A spread-spectrum system will have a much greater effective range and be more resistant to jamming and interception. The drawback to such a system is added complexity and cost for the additional performance.

Assuming that 24 bits can accurately represent sensor ID and sensor data, and choosing a low data rate of 2400 baud, a complete information packet can be sent in 10 msec. In order to facilitate a system consisting of many transmitters and to increase the probability of reception, the transmitted sequence would be repeated at quasi-random intervals after an initial transmission.

A block diagram of such a system is shown in Figure A-6-1. The code rate of 3.0143 MCPS was chosen to yield a 20 dB jamming margin and 34 dB of processing gain (neglecting system losses). This results in an output S/N ratio of ~14 dB in the presence of a narrow-band jamming signal located the same distance from the receiver as the active transmitter but transmitting with 20 dB more power (10 Watts). Using BPSK modulation, this yields a BER of 6.857E-13. The PN sequence length is chosen as 32,767 chips to allow for greater than 10 mSec of transmit time before the sequence repeats. It is shown later in this report that a 15 stage shift register is required to generate such a sequence. In addition, Gold Codes are used to support code-division multiple access (CDMA) techniques.

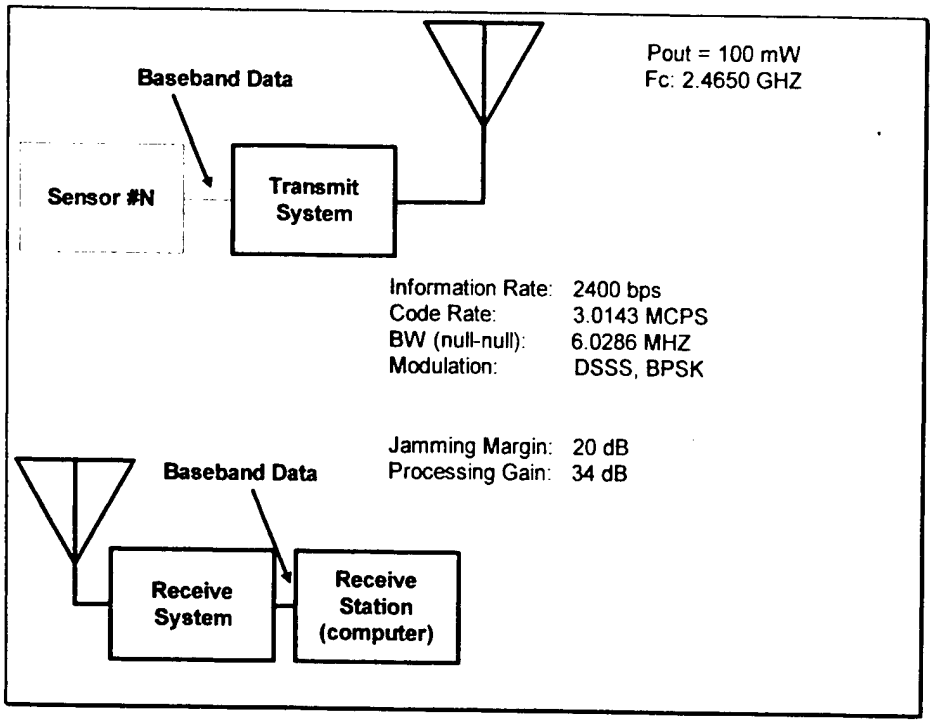

Figure A- 6-1. Spread spectrum system.

The output frequency is chosen as 2.4650 GHz. This frequency is contained within one of the unlicensed bands allocated by the FCC and is available for use in Europe and Japan for spread-spectrum transmission.

6.1.1 Transmitter.

A block diagram of the transmitter is given in Figure A-6-2.

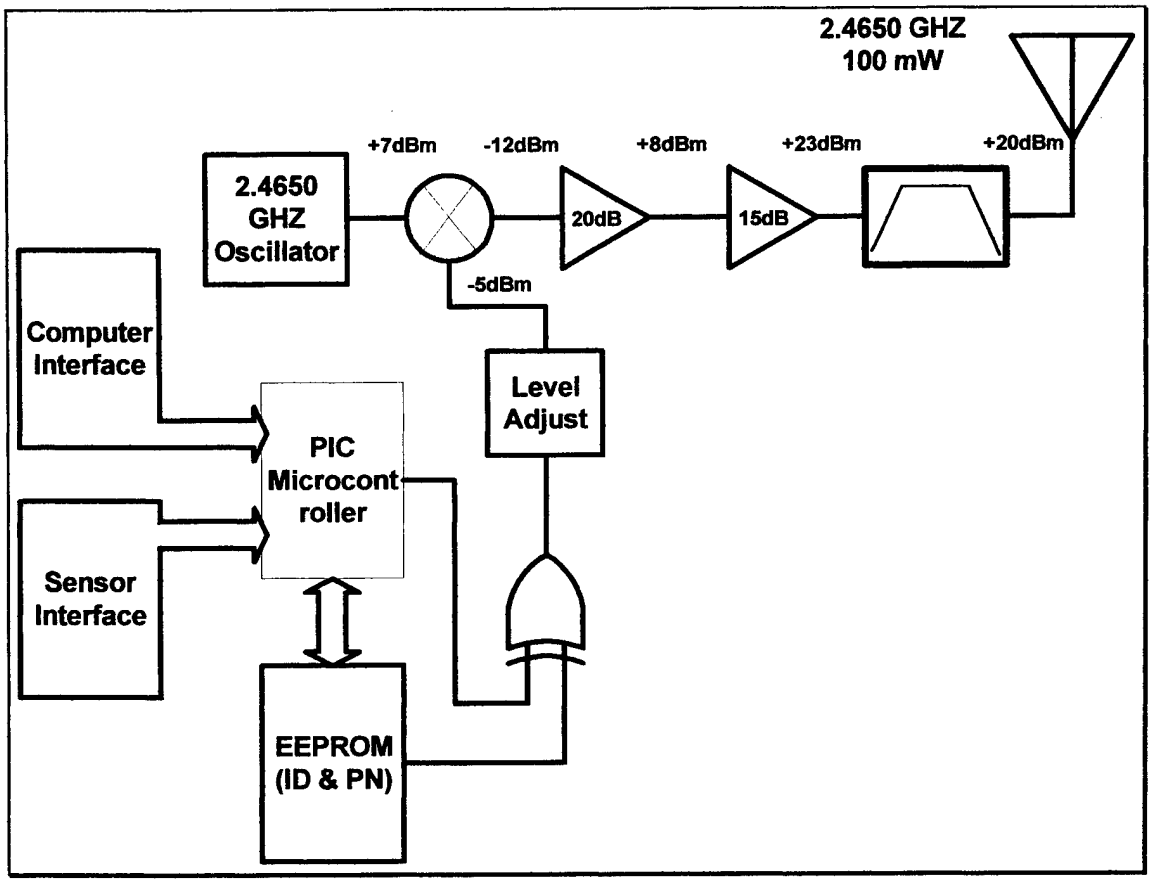

Figure A- 6-2. Spread spectrum transmitter.

The computer interface allows the user to download a transmitter ID and PN sequence into the EEPROM via the PIC microcontroller. The sensor interface allows the PIC to read data from a remote sensor. The PIC microcontroller is the brains of the transmitter while the EEPROM holds the transmitter ID and PN sequence. The 2.4650 GHz oscillator is a highly stable frequency source designed and built using microstrip techniques. The PN sequence (3.0143 Mcps) is code modulated by the transmitter data (2400 bps) by the XOR gate. The output of the XOR gate is level shifted and applied to a passive mixer where it is used to BPSK modulate the 2.4650 GHz carrier. The output of the mixer is then applied to two amplifier stages to increase the output to

+23 dBm (199.53 mW). The signal is filtered by a microwave filter having a maximum insertion loss of 3 dB and a flat passband of at least twice the chip rate (6.0286 MHz) about the center frequency (2.4650 GHz).

This implementation allows the transmitter to have a low part count, and a fairly low price tag. Due to the low part count and the use of surface-mount technology, the transmitter can be implemented in a small amount of physical space.

6.1.2 Receiver.

A block diagram of the receiver is given in Figure A- 6-3.

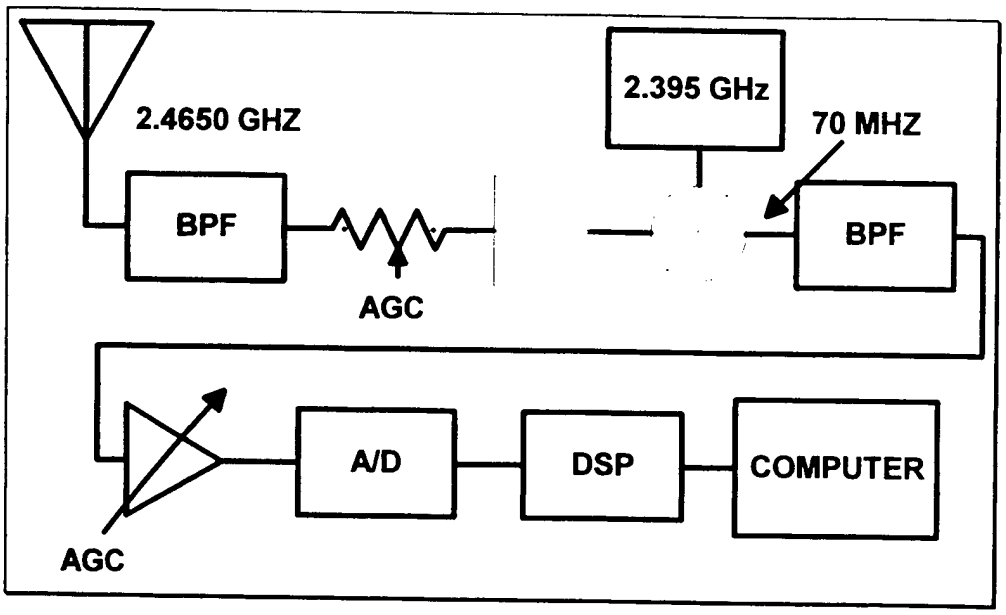

Figure A- 6-3. Spread spectrum receiver.

The input signal is filtered, adjusted in gain and then mixed with a 2.395 GHz local oscillator to reduce the center frequency to 70 MHz. This signal is filtered, level shifted and converted to the digital domain using a high-speed undersampling A/D converter. The A/D converted must have a good track and hold amplifier that works at frequencies up to 70 MHz plus one-half of the null-null bandwidth but needs only to sample at twice the signal bandwidth or more. In this case, the null-null bandwidth of the spread-spectrum signal is equal to twice the chip rate or 6.0286 MHz. Therefore, an A/D

converter running at 20 MSPS would be sufficient. Correlation and demodulation are performed by the DSP engine and the output is viewed and logged on a standard PC.

Assuming a receiver sensitivity that is comparable to that achieved with the 916.55 MHz receiver described previously, the system range would be:

SNR = 14 dB (specified)

The NEB is approximated by twice the chip rate or 6.0286 MHz

Assuming a 26 dB noise-figure as with the 916.55 MHz receiver, equation (A-3.4) yields:

$$S = N_0 + NBW + NF + SNR = -173.86dBm + 67.8dB + 26dB = -80.1dBm$$

This is the receiver sensitivity for an SNR of 34 dB since by using twice the chip rate for the NEB, the full processing gain of the system has been accounted for. Since only 14 dB is required, the receiver sensitivity is -100.1 dBm.

This power level corresponds to 97.7 fW. Using equation (A-3.7) to determine the range of the system with a 100 mW transmitter yields:

$$r = \frac{\lambda \cdot \sqrt{P_t \cdot G_t \cdot G_r}}{4 \cdot \pi \cdot \sqrt{P_r}} = \frac{\frac{c}{2.465GHz} \cdot \sqrt{100mW}}{4 \cdot \pi \cdot \sqrt{97.7fW}} = 9{,}790m$$

This range is ideal outside line of sight and assumes no jamming or interfering signals. If this kind of range was necessary, it would be best achieved through increased output power (1 W is allowed), and directional antennas.

6.1.3 PN Sequence Generation.

An important part of any spread-spectrum system is the pseudo-noise (PN) sequence used to spread the information signal. In a spread spectrum system, to implement multiple access techniques (multiple transmitters using the same channel at the same time), the PN sequence utilized by each transmitter needs to have low cross-correlation with the other PN sequences being transmitted, in addition to good autocorrelation properties. While linear maximal length sequences have very good

autocorrelation properties, the cross-correlation between any two codes is not, in general, low.

Gold code sequences are generated by modulo-2 addition of two specially chosen maximal length sequences, called a preferred pair. They have very low cross-correlation in addition to excellent autocorrelation characteristics. $2^{(n-1)}$ Gold codes can be generated from a pair of n-stage shift registers. By choosing a family of Gold Codes, separate systems can be set up using different codes from this family in the same vicinity without fear of interference.

For the system described earlier, a fifteen stage shift register (n=15) is chosen to generate the first sequence in the preferred pair (designated b). Therefore, the PN sequence will be $(2^{15}-1)$ or 32,767 bits long. For the given code rate of 3.0143 MCPS, the sequence will not repeat itself for 10.87 mSec. Since it will take 10 mSec to transmit the necessary data at 2400 baud, the sequence will not repeat within one "mission lifetime." It is important that the code repetition rate does not lie in the information band [11]. For this case, the code repetition rate is:

$$\mathrm{Re}p\_Rate = \frac{Code\_Rate}{Code\_Length} \qquad \text{(A-6.1)}$$

The code rate is 3.0143 MCPS and the code length is 32,767 bits. Therefore, the code repetition rate is 91.99 Hz, or below the information band.

To generate a family of Gold Codes using 15 stage shift registers, Matlab and Simulink were employed. To generate a preferred pair b and b', the following conditions must be satisfied [12]:

1. $n \neq 0 \bmod 4$; that is, n is odd OR $n = 2 \bmod 4$
2. b' = b[q] where q is odd and either $q = 2^k + 1$ OR $q = 2^{2k} - 2^k + 1$
3. gcd(n,k) = 1 for n odd OR 2 for $n = 2 \bmod 4$

In this case:

n = 15 (condition 1 satisfied)
q = 3, therefore, k = 1 (condition 2 satisfied)
gcd(15,1) = 1 (condition 3 satisfied)

From Table A-3-5 on page 118 [12], a valid octal representation of the generator polynomial for b is [100003]. Expanding this to binary form yields [1 000 000 000 000 011]. This representation reads from right to left: input, tap1, tap2, ...tap14, output. Therefore, to generate the first sequence in the preferred pair, a 15 stage shift register is constructed having feedback from the output exclusively ORed with tap 1 and fed back to the input. This configuration is shown in Figure A-6-4. The output of the first shift register is set to 1 before simulation, all other initial conditions are set to 0. This Simulink file (pn_r15_a.m), generates b, a 32,767 bit sequence and stores it to the file pnr15.mat. To generate b', the Matlab file bprme15a.m is run. This file generates the first 100 bits of b' by decimating b by q and then generates and solves the necessary system of linear equations in binary space. The result is a vector of taps to generate b'.

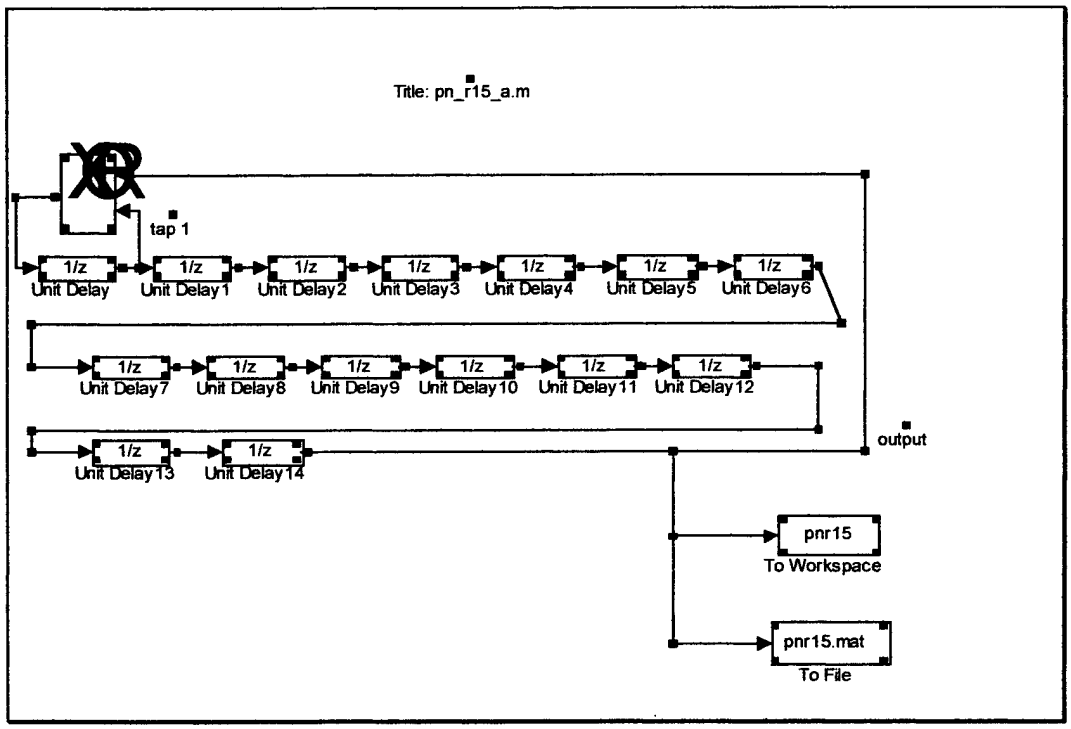

Figure A- 6-4. Simulink file to generate b.

```
% Steven M. Ciccarelli
% File: BPRME15A.M

% This Matlab file loads pnr15.mat containing a 32kBit
```

```
% PN sequence and generates its preferred pair (Gold Codes)
disp('Loading PN Sequence b');
load pnr15.mat

% Remove the time basis from the data
b=pnr15(2,:);

% Finding the first 100 bits of bprime using Q=3
% This routine will only go "through" b twice without error
disp('Generating the first 100 bits of bprime');
NBIT=100;
Q=3;
bprime(1)=b(1);
for i=2:NBIT
 if ((i-1)*Q+1)<=length(pnr15)
  bprime(i)=b((i-1)*Q+1);
 else
  bprime(i)=b((i-1)*Q+1-length(pnr15));
 end
end

% To find the feedback taps for bprime, an r stage shift
% register, r linear equations must be solved.  In this case
% r = 15, so 15 equations are needed
r=15

% Starting with the 50th position of bprime and moving
% forward to develop these equations:
disp('Solving r equations to determine feedback taps for the bprime generator');
init=50;

% The coefficient matrix is

for row=1:r
 count=0;
 for column=1:r
  A(row,column)=(bprime(init-count-1));
  count=count+1;
 end
 init=init+1;
end

% The constant matrix is
init=50;
count=0;
```

```
for row=1:r
  c(row,1)=bprime(init+count);
  count=count+1;
end

% Checking to make sure that the system has a unique answer
%(Don't know how to do this in base 2)
V=det(A);

% Solving the system Ax=C in base 2
disp('Solving for x, vector of taps');
x=gflineq(A,c)

%Yields taps at: 1,5,10,15
```

The output of this program is:

```
Loading PN Sequence b
Generating the first 100 bits of bprime

r =
   15

Solving r equations to determine feedback taps for the bprime generator
Solving for x, vector of taps

x =

    1
    0
    0
    0
    1
    0
    0
    0
    0
    1
    0
    0
    0
    0
    1
```

This result shows taps at the output of registers 1, 5, 10, and 15. To generate Gold codes, the Simulink file goldr15b.m is created. See Figure A-6-5.

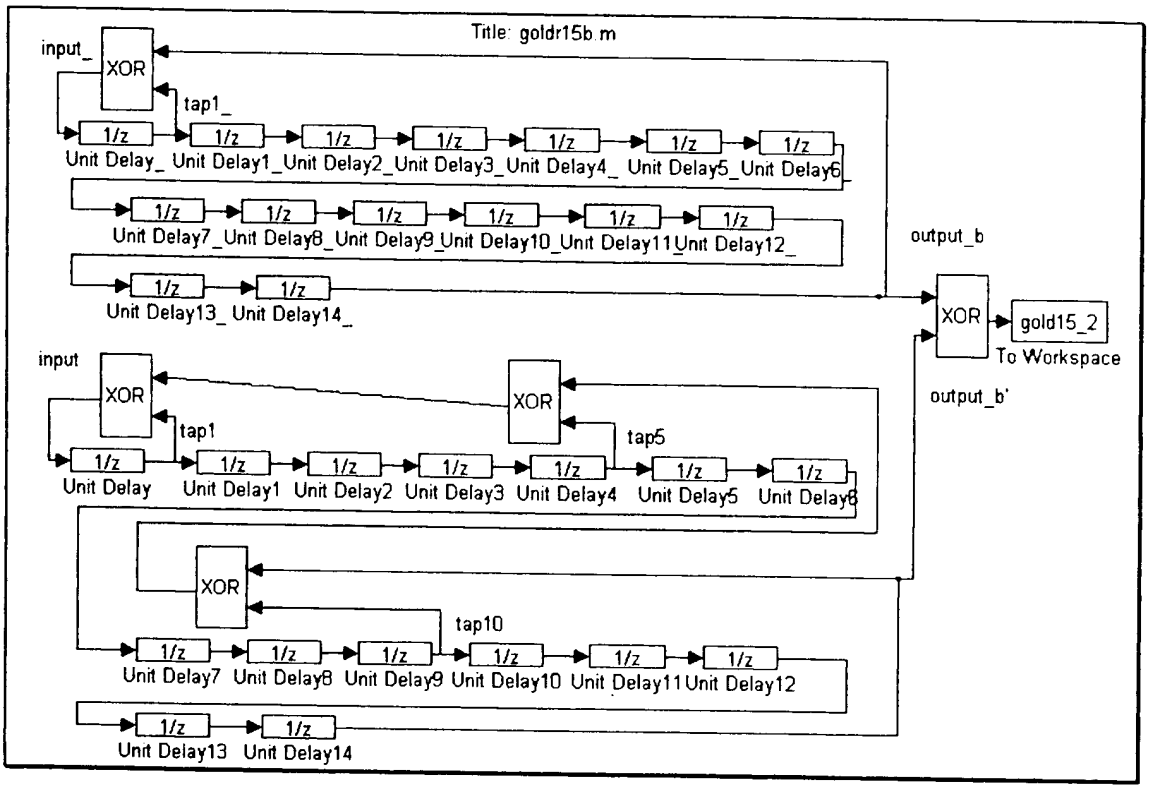

Figure A- 6-5. Simulink file to generate Gold codes.

Using this Simulink file, two 32,767 bit Gold code sequences are generated, gold15_1 (b) and gold15_2 (b'). To generate b, the following initial states are used for the two shift registers:

Top register: 100 0000 0000 0000

Bottom register: 000 0000 0000 0000

To generate b', the following initial states are used:

Top register: 000 0000 0000 0000

Bottom register: 101 0111 1110 0000

These codes are stored in the Matlab file gold15.mat. Each sequence is transformed from standard unipolar binary form (0,1) to bipolar form (-1,1) and saved in Matlab file gold15a.mat. These new sequences are saved as gold15_1a and gold15_2a.

To generate the other members of this 32,767 member family, the initial register values of the top circuit are held constant while the initial register values of the bottom circuit are cycled through all possible states. For each new initialization of the bottom shift-register circuit, the new code is saved.

The cross-correlation spectrum of a preferred pair is three valued. These values are determined by [12]:

$$-\frac{1}{N}\cdot t(n)$$

$$-\frac{1}{N}$$

$$\frac{1}{N}\cdot\left[t(n)-2\right]$$

where

$t(n) = 1 + 2^{0.5(n+1)}$ *for n odd*

or

$t(n) = 1 + 2^{0.5(n+2)}$ *for n even*

and $N = 2^n - 1$, *the code period*

For this case, t(n) = 257 and the three predicted values are:

-7.8433E-3

-30.519E-6

7.7822E-3

As a quick check to ensure that the two sequences generated are in fact a preferred pair, the cross correlation is examined. Using Matlab file ck_xcorr.m, the first fifty cross-correlation values are computed and plotted. From the plot shown in Figure A-6-

6, it is obvious that the cross correlation between the two sequences is three-valued. These three values are identical to the predicted values:

-7.8433E-3

-30.519E-6

7.7822E-3

```
% Steven M. Ciccarelli
% File: ck_xcorr.m

% This Matlab file computes the first fifty cross correlation values
% between the two sequences gold15_1a and gold15_2a contained
% in the file gold15a.mat.

load gold15a.mat

% Compute the first 50 values, save in xcorr
N = length(gold15_1a);
i=0;
for m = 1:50
  gold15_1a = shiftby1(gold15_1a);
  mult = 0;
  mult = (gold15_1a.*gold15_2a);
  xcorr(1,m) = sum(mult)/N;
  i=i+1
end

% Output xcorr to a plot
plot(xcorr);
title('Cross Correlation for gold15_1a and gold15_2a');
xlabel('Sample Number ');
ylabel('Value');
```

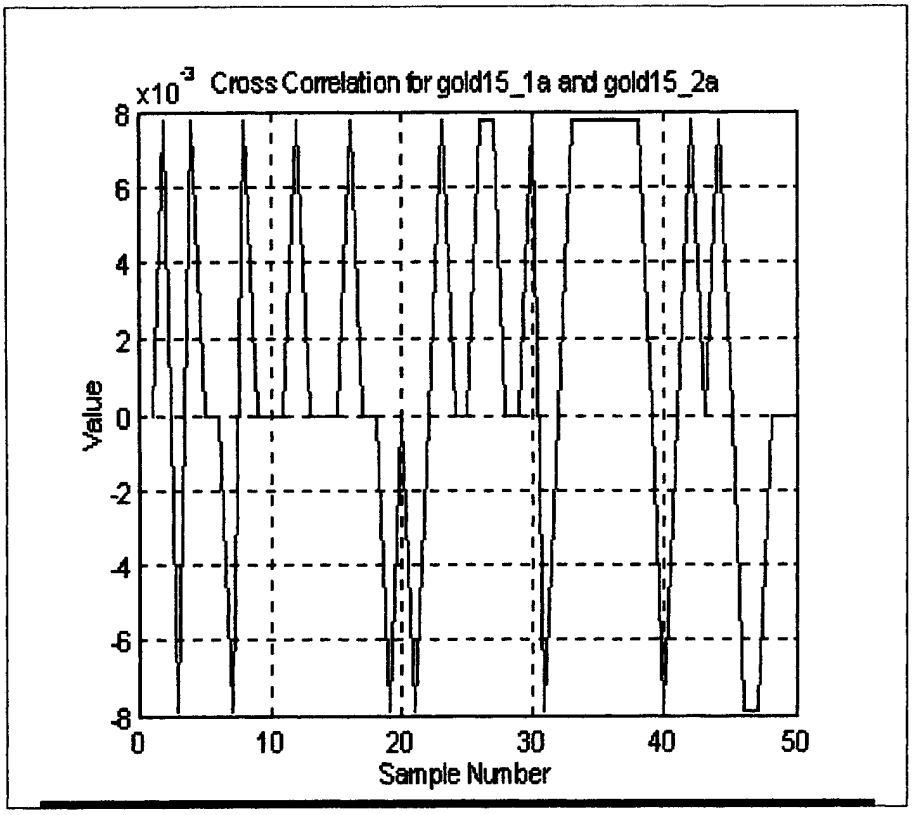

Figure A- 6-6. Cross-correlation.

The autocorrelation of an m-sequence is given as [12]:

1.0, occurs once

-1/N, occurs N times

The Matlab xcorr command is used to view the autocorrelation for each sequence. Figures A-6-7 and A-6-8 show the autocorrelation for gold15_1a and gold 15_2a respectively.

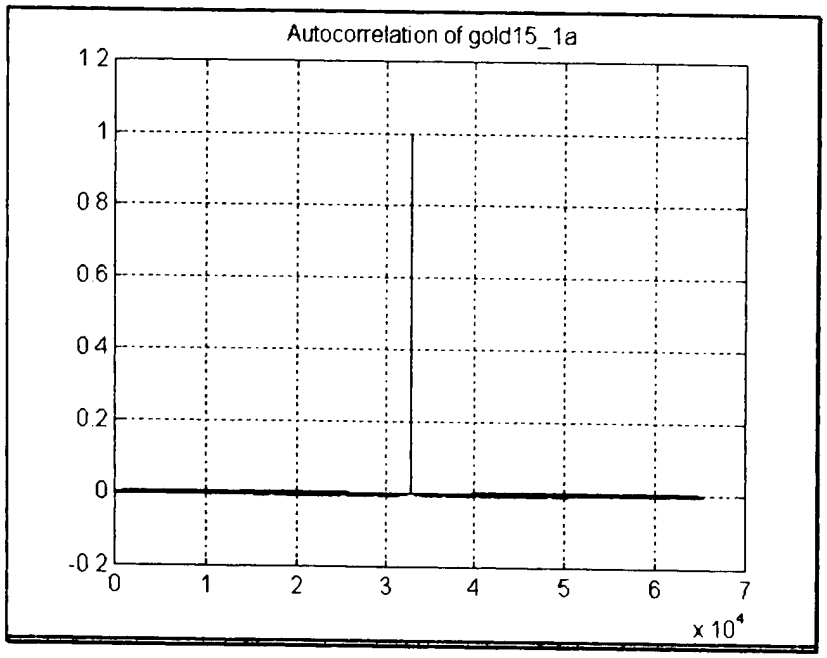

Figure A-6-7. Autocorrelation of gold15_1a.

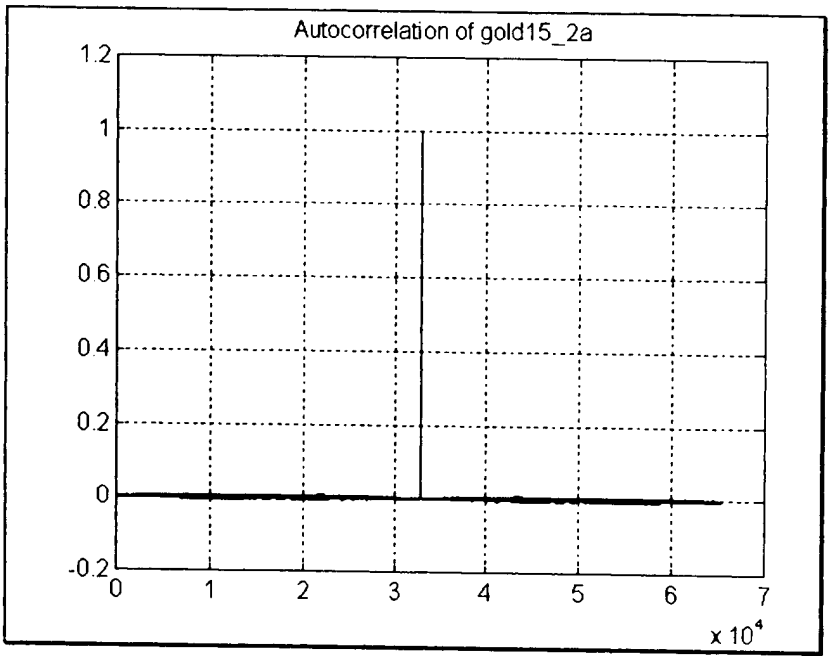

Figure A-6-8. Autocorrelation of gold15_2a.

SECTION 7

CONCLUSIONS

In this report, a digital wireless communication system operating in the 902-928 MHz ISM band was specified and designed. The purpose is to send sensor ID data from a remote location to a centralized receiver located up to 2,500 feet away. One transmitter and receiver were built and tested. The results from testing these units are included as verification of the design.

To implement the transmitter, a Colpitts oscillator using a SAW resonator for frequency stabilization was designed, simulated and then built on a PWB. This 916.5 MHz oscillator was on-off keyed by a Holtek encoder, and sensor ID data was transmitted. The receiver was built around an RFM RX2010 IC. Since the noise-figure of this part is inadequate for the proposed system, low-noise amplifier stages were added along with filtering in the RF path preceding the IC. A Holtek decoder was used to determine whether the received signal indicates a valid address. This system meets the requirements set forth at the beginning of the report.

A spread-spectrum communications link is suggested as the next logical step to provide more robust communication. System level design is presented and Matlab and Simulink are used to create two PN sequences belonging to a family of Gold codes. The maximum number of simultaneous users for this system is estimated as 101 (assuming that the entire jamming margin is available to increase system capacity) [13]:

$$JM = 10 \cdot Log(U-1)\, dB \qquad \text{(A-7.1)}$$

Where:

JM = Jamming Margin (in dB)
U = Number of users

$$U = 10^{\frac{JM}{10}} + 1 = 10^{\frac{20}{10}} + 1 = 101$$

This allows 101 repeaters to operate simultaneously using the same band of frequencies, which would allow for a very large overall system.

SECTION 8

REFERENCES

[1] Earl McCune and Dr. Kamilo Feher, "Near-Far Interference in Digital Wireless Communications," *Applied Microwave and Wireless,* January/February 1997, p. 66.

[2] Peter Vizmuller, *RF Design Guide, Systems, Circuits and Equations,* (Norwood, MA: Artech House, 1995), p. 208.

[3] Randall W. Rhea, *Oscillator Design and Computer Simulation, second edition* (McGraw Hill, 1995), p. 49.

[4] Alexander Glas and Kurt Wacker, "SAW Resonators for RF Keyless Entry Applications," *Microwave Journal,* May 1997, p. 306.

[5] Chris Bowick, *RF Circuit Design* (Sams, 1992), p. 16.

[6] Rhea, p. 30.

[7] McCune and Feher, p.68.

[8] Peter Vizmuller, *RF Design Guide, Systems, Circuits and Equations,* (Norwood, MA: Artech House, 1995), p. 227.

[9] Vizmuller, p. 49.

[10] Vizmuller, p. 228.

[11] Robert C. Dixon, *Spread Spectrum Systems with Commercial Applications, third edition* (New York: John Wiley and Sons, 1994), p. 91.

[12] Peterson, Ziemer and Borth, *Introduction to Spread Spectrum Communications* (New Jersey: Prentice Hall, 1995), p. 135-136.

[13] Joseph Brindisi, "Design and Generation of Orthogonal Pseudo-Noise Sequences for Application to Code Division Multiple Access," (*RIT MSEE paper*, May 1996), p. 33.

APPENDIX B

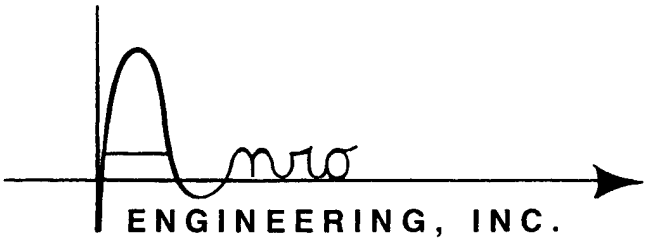

STUDIES & ANALYSIS DIV.
450 BEDFORD STREET
LEXINGTON, MA 02173-1520
TELEPHONE (617) 862-3000
FAX (617) 863-0586
E-MAIL ANROLEX@AOL.COM

TECHNOLOGY & DEVELOPMENT DIV.
1800 SECOND STREET, SUITE 878
SARASOTA, FL 34236-5992
TELEPHONE (941) 957-3080
FAX (941) 957-3082
E-MAIL ANROFL@AOL.COM

Design and Generation of Orthogonal Pseudo-Noise Sequences for Application to Code Division Multiple Access

by

Joseph Brindisi

DEPARTMENT OF ELECTRICAL ENGINEERING

COLLEGE OF ENGINEERING

ROCHESTER INSTITUTE OF TECHNOLOGY

ROCHESTER, NEW YORK

May 25, 1996

For

ANRO ENGINEERING, INC.
Contract #DNA001-95-C-0175

340 RIDGE ROAD
SEDONA, AZ 86336-4022
TELEPHONE (520) 282-7796
FAX (520) 282-7505
E-MAIL anrowest@sedona.net

P.O. BOX 109
CABIN JOHN, MD 20818-0109
TELEPHONE (301) 365-0209
FAX (301) 365-8469

2117 BUFFALO ROAD, #205
ROCHESTER, NY 14624-1507
TELEPHONE (716) 426-1830
FAX (716) 426-7821
E-MAIL cvbn24a@prodigy.com

Design and Generation of Orthogonal Pseudo-Noise Sequences for Application to Code Division Multiple Access

by

Joseph Brindisi

A Graduate Paper Submitted

in

Partial Fulfillment

of the

Requirements for the Degree of

MASTER OF SCIENCE

in

Electrical Engineering

Approved by:

Prof. Joseph D. DeLorenzo
(Graduate Paper Advisor)

Prof. S. Krishnan
(Department Head)

DEPARTMENT OF ELECTRICAL ENGINEERING

COLLEGE OF ENGINEERING

ROCHESTER INSTITUTE OF TECHNOLOGY

ROCHESTER, NEW YORK

MAY 25, 1996

Table of Contents

I.	Introduction	4
II.	Shift Register Sequences	5
III.	Mathematical Properties of Linear Feedback Shift Registers	8
	The A Matrix	8
	The Characteristic Polynomial	10
	The Generating Function	11
	Maximal Length SRG's	13
IV.	Pseudo-Noise Sequences for Spread Spectrum Communications	15
	PN Sequences	15
	The Autocorrelation Function	16
	Direct Sequence Spread Spectrum Communications	18
	Direct Sequence Binary PSK Transmitter	18
	Ideal Channel	20
	Direct Sequence Binary PSK Receiver	21
V.	Gold Code Generators	27
	Physical Description	27
	Preferred Pairs of Characteristic Polynomials	28
	Balanced Gold Codes	29
	Initial Conditions	31
VI.	Gold Code Generators for a CDMA System	33
VII.	Gold Sequence Generator Modulator Implementation	41
	Parallel to Serial Data Converter	44
	Gold Code Generator	47
	PN Sequence Generator/Modulator	52
	Support Circuitry	54
VIII.	Experimental Results	56
IX.	Conclusion	60
X.	References	61

Acknowledgments

I would like to extend my thanks to Dr. J. DeLorenzo for his guidance, encouragement and sharing his immense knowledge on this subject matter as well as making this possible.

I would also like to thank Dr. J. Palmer and Dr. P. R. Mukund for their assistance. Finally, I would like to thank my parents for their support.

I. Introduction

Code division multiple access is an application of spread spectrum communication which requires the use of pseudo - noise (PN) sequences having low cross correlation. This allows users of the system to transmit simultaneously using the same RF bandwidth. This paper presents the theory of the design of orthogonal PN sequences using linear feedback shift registers. An orthogonal PN sequence generator/modulator will be designed using the VHDL hardware description language and used to compare the actual cross-correlation performance of such sequences with the theoretical expectations.

II. Shift Register Sequence Generators

A shift register sequence generator is a set of flip flops connected in series where the output of the generator is the output of the last flip flop. A register containing m flip flops is said to have m stages. All stages are driven by a common clock. The output of each stage is selectively routed to a function which determines the next entry in the in the sequence. The output of the function becomes the input of the first stage. A *Linear Feedback Shift Register* is a shift register generator which the next entry in the sequence is determined by a linear combination of the current register contents. The sequences used in spread spectrum communications are generated using linear feedback shift registers. All shift register generators (SRG) mentioned in this paper hereafter are assumed to be linear.

Figure 1 illustrates a linear feedback shift register. The coefficients $\{a_1, a_2, \ldots a_m\}$ are binary valued (0 or 1). A value of 0 represents an open circuit and a value of 1 represents a

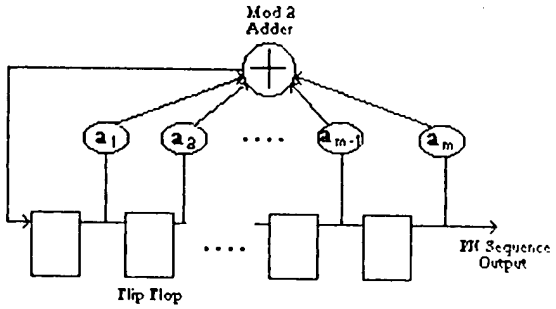

Figure 1: Linear Feedback Shift Register

short circuit. This allows the contents of each stage to be selectively routed to the feedback function. The feedback function is a Modulo 2 adder whose output is routed to

the input of the first stage. This configuration allows the SRG to act as a finite state machine where the current contents of the register is the present state and the output of the adder determines the next state. The output of the SRG is the content of the last stage. The output sequence will be periodic with the period being dependent on the feedback coefficients (or feedback taps). This is illustrated by the following example.

Figure 2 illustrates the effects of a 3 stage register utilizing different feedback configurations. In figure 2a, the feedback is taken from the first and the third stage. By examining the state transition diagram it can be determined that no matter what the initial content of the register is (except for 000) that the period of the sequences generated at the output is 2^3-1 = 7. This sequence is called a maximal length sequence. A *maximal length sequence*[1] is a sequence generated by a SRG with m stages having a period equal to 2^m-1 which is independent of the initial register contents.

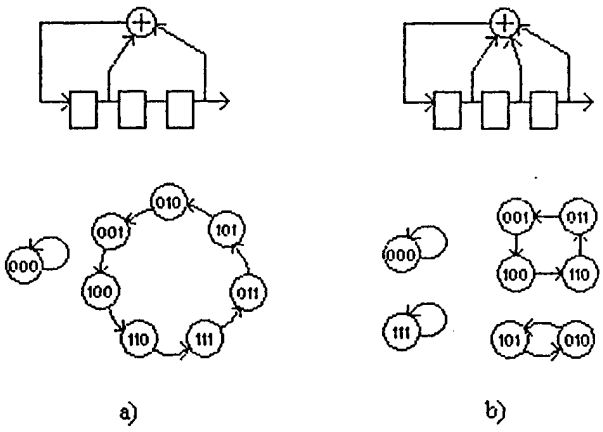

Figure 2: Examples of a 3 stage register utilizing different feedback connections a) [3,1] b) [3,2,1]

Figure 2b shows the same register with feedback taken from all stages. Examination of the state transition diagram shows that two distinct sequences can be generated both having periods less than 2^3-1 and both dependent on initial register

contents. Sequences of this type are *nonmaximal*.[1] Maximal length sequences are of particular interest in spread spectrum communications because they exhibit properties similar to random sequences. These properties will be discussed in a later section.

III. Mathematical Properties of Linear Feedback Shift Registers

This section is included to provide the knowledge foundation necessary to understand the procedure for generating Gold codes which is outlined later in this paper. Holmes[2] provides a more extensive discussion regarding the mathematical theory of SRG's.

The A Matrix

Consider the initial contents of SRG as a m x 1 column vector X(j) where j denotes discrete steps in time.

$$X(j) = \begin{bmatrix} x_1(j) \\ x_2(j) \\ x_3(j) \\ \cdot \\ \cdot \\ \cdot \\ \cdot \\ x_m(j) \end{bmatrix}$$

The shifting operation of the SRG can be described as an m x m matrix multiplying X(j) to produce the column vector X(j+1) which represents the contents of the register after one shift. This matrix is called the A matrix and its general form based on the SRG in figure 1 is

$$A = \begin{bmatrix} a_1 & a_2 & a_3 & \cdots & a_{m-1} & a_m \\ 1 & 0 & 0 & \cdots & 0 & 0 \\ 0 & 1 & 0 & \cdots & 0 & 0 \\ \cdot & \cdot & \cdot & & \cdot & \cdot \\ \cdot & \cdot & \cdot & \cdots & \cdot & \cdot \\ \cdot & \cdot & \cdot & & \cdot & \cdot \\ \cdot & \cdot & \cdot & & \cdot & \cdot \\ 0 & 0 & 0 & 1 & 0 & 0 \\ 0 & 0 & 0 & \cdots & 1 & 0 \end{bmatrix}$$

Construction of the A matrix is as follows. For an m stage register, each column of the first row of the A matrix contains the value of the feedback tap coefficient for the corresponding stage in the SRG. For rows 2 through m, let k represent the current row number. In the kth row, a value of 1 is to be placed in the k-1 column. All other column positions for that row have the value of zero. Therefore, X(j+1) becomes

$$X(j+1) = \begin{bmatrix} a_1x_1(j) + a_2x_2(j) + a_3x_3(j) + \cdots + a_{m-1}x_{m-1}(j) + a_m x_m(j) \\ x_1(j) \\ x_2(j) \\ \\ \\ \\ x_{m-2}(j) \\ x_{m-1}(j) \end{bmatrix}$$

or equivalently

$$\mathbf{X(j+1) = AX(j)}$$

which as was stated before is the contents of the register after one shift. Consequently, the contents of the register after p shifts is obtained by multiplying X(j) by the A matrix p times.

$$\mathbf{X(j+p) = A^pX(j)}$$

The period of the shift register sequence occurs when

$$\mathbf{A^p = I}$$

where I is the identity matrix. This means that

$$\mathbf{X(j+p) = X(j)}$$

stating that the contents of the SRG after p shifts is equal to the initial register contents. For a m stage SRG to produce a sequence of maximal length, it is required that

$$A^{2^m-1} = I$$

The Characteristic Polynomial

The characteristic equation of the A matrix is found by solving for the determinant of the matrix [A - λI] where I is the identity matrix and λ is a variable. Solving for the determinate of the matrix [A - λI] will yield a equation F(λ) which can then be used to find the characteristic polynomial f(λ) of the SRG represented by the A matrix. The characteristic polynomial is a necessary tool for the development of Gold codes. The general form of F(λ) is

$$F(\lambda) = |A - \lambda I| = \begin{vmatrix} a_1-\lambda & a_2 & a_3 & \cdots & a_{m-1} & a_m \\ 1 & -\lambda & 0 & \cdots & 0 & 0 \\ 0 & 1 & -\lambda & \cdots & 0 & 0 \\ \cdot & \cdot & \cdot & & \cdot & \cdot \\ \cdot & \cdot & \cdot & \cdots & \cdot & \cdot \\ \cdot & \cdot & \cdot & & \cdot & \cdot \\ 0 & 0 & 0 & 1 & -\lambda & 0 \\ 0 & 0 & 0 & \cdots & 1 & -\lambda \end{vmatrix}$$

Solving for the determinant |A-λI| and simplifying yields

$$F(\lambda) = \lambda^m + a_1\lambda^{m-1} + a_2\lambda^{m-2} + \cdots + a_{m-1}\lambda + a_m$$

or

$$F(\lambda) = \sum_{k=0}^{m} a_k\lambda^{m-k} \qquad a_0 = 1$$

Reference [2] defines the *characteristic polynomial* of a SRG in terms of the characteristic equation.

$$f(\lambda) = \lambda^{2k-m} \cdot F(\lambda)$$

or

$$f(\lambda) = \sum_{k=0}^{m} a_k \lambda^k \qquad a_0 = 1$$

As an example, consider the SRG in figure 2a. There is feedback being taken from the first and the third stages which translates to a characteristic polynomial of

$$f(\lambda) = 1 + \lambda + \lambda^3$$

The Generating Function

This section focuses on using the characteristic polynomial to study the output sequence of the SRG. The initial register contents for a register with m stages can be expressed as a binary polynomial

$$g(X) = b_{m-1}X^{m-1} + b_{m-2}X^{m-2} + \cdots + b_1X^1 + b_0$$

where the coefficients $\{b_{m-1}, b_{m-2}, \ldots b_0\}$ are binary valued (0 or 1) representing the initial

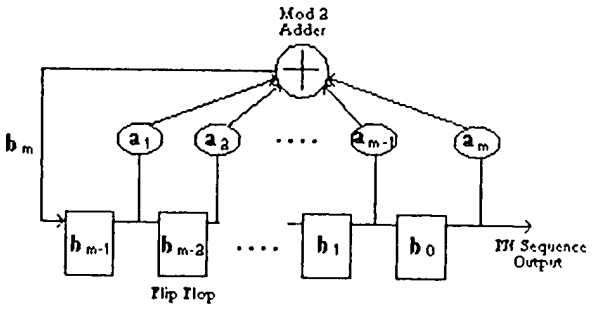

Figure 3: SRG in figure 1 showing initial register contents

register values. The output sequence of the modulo 2 adder can be expressed as a binary polynomial G(X) defined to be

$$G(X) = \frac{g(X)}{F(X)}$$

where g(X) is the binary polynomial describing the initial register contents and f(X) is the characteristic polynomial describing the feedback tap connections. f(X) is equal to f(λ) with λ replaced by X for convenience. G(X) is called the *generating function* and is of the form

$$G(X) = G_0 + G_1X + G_2X^2 + \cdots$$

where the coefficients of G(X) represent the sequence generated at the output of the adder. Therefore, G(X) can be written as

$$G(X) = b_m + b_{m+1}X + b_{m+2}X^2 + \cdots$$

Consider for example the SRG shown in figure 4. The output sequence can be determined by finding the coefficients of the generating function and then rotating the output sequence so the first 3 digits match the initial conditions.

$1 + X + X^3$

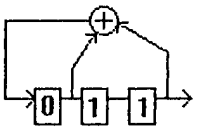

Figure 4: Maximal Length SRG Showing Initial Conditions

The characteristic polynomial describing the maximal length SRG is $f(X) = 1 + X + X^3$. The binary polynomial describing the initial register contents is $g(X) = X + 1$. The generating function can then be found by long division.

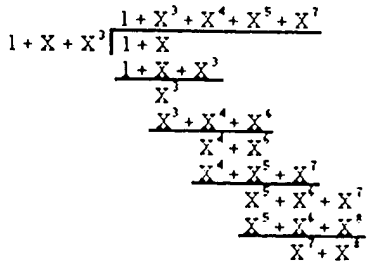

The generating function is

$$G(X) = 1 + X^3 + X^4 + X^5 + \cdots\cdots$$

whose coefficients can be used to find the output sequence of the register. Since the length of the sequence is $n = 2^3-1 = 7$, division need only be performed to determine the coefficients of all powers of X up to X^{n-1}. The output of the register thereafter will be a periodic representation of the first seven coefficients. In this example, the first 7 coefficients are

1 0 0 1 1 1 0

which is a time shifted version of the output sequence of the register. The actual output of the register is obtained by rotating the sequence until the first three terms are the initial conditions themselves. The periodic output of the register becomes

1 1 0 1 0 0 1
1 2 3 4 5 6 7 .....

Maximal Length SRG's

An m stage SRG will produce a maximal length sequence according to the following theorems as stated by Holmes:

> ***Theorem 1:*** *If a SRG produces a sequence of maximal length, its characteristic polynomial will be irreducible.*[2]

Theorem 2: *If the characteristic polynomial is irreducible and of degree m, the period of the sequence will be a factor of 2^m-1.*

If 2^m-1 is prime, then every irreducible polynomial of degree m corresponds to a maximal length sequence generator.

If 2^m-1 is not prime, it is required that the irreducible characteristic polynomial f(X) be primitive, meaning that it divides X^k-1 for no k less than 2^m-1. [2]

References [3] and [4] provide lists of maximal length sequence generators. But, for the generation of Gold codes, it is required that the roots of the polynomials be given as well. Appendix C of reference [5] provides a table of irreducible polynomials of degree ≤ 34 which lists both the polynomial and its root. Generation of Gold codes requires pairs of SRG's with characteristic polynomials known as preferred pairs. The table from [5] will be used to select preferred pairs of primitive polynomials where the criteria for selection is comparison of the roots.

IV. Pseudo-Noise Sequences for Spread Spectrum Communications

The focus up to this point has been the physical and mathematical explanation of SRG's and defining the conditions for which a SRG will produce a sequence of maximum length. Maximal length sequences are of particular interest because they exhibit properties of a *psudeo-random* or *psudeo-noise* (PN) sequences. PN sequences are used as the basis for spread spectrum communications which is the foundation for code division multiple access (CDMA). The PN sequence modulates a binary data sequence at the rate of 1 period/data bit to distribute the power of the data waveform over a larger bandwidth. This allows the data to be successfully transmitted through a channel with a large amount of interference present.

PN Sequences

PN sequences have the following properties:

1) The number of 1's in the sequence is greater than the number 0's by no more than 1. This is known as the *balance* property.

2) For all the runs in the sequence (consecutive occurrences of a 1 or a 0), half the runs are of length one, one-fourth of the runs are of length two, one eighth of the runs are of length three, etc. The number of runs of value 1 for a given run length has an equal number of runs of value 0 for that same length.

3) The autocorrelation function $R(\tau)$ has two reference values

$$R(\tau) = N \quad \text{for } \tau = k \cdot N \quad k = 0, 1, 2, \ldots$$
$$R(\tau) \leq p \quad \text{otherwise}$$

where N is the period of the PN sequence and p is the maximum value of the autocorrelation function when $\tau \neq k \cdot N$. It is true that $N >> p$ provided that the sequence is in polar form (1 = +1 and 0 = -1).

Sequences generated by maximal length SRG's posses the properties necessary to classify them as PN sequences. Figure 5a is the autocorrelation function of a random sequence and figure 5b is the autocorrelation function of a PN sequence both of length 31 shown together for direct comparison.

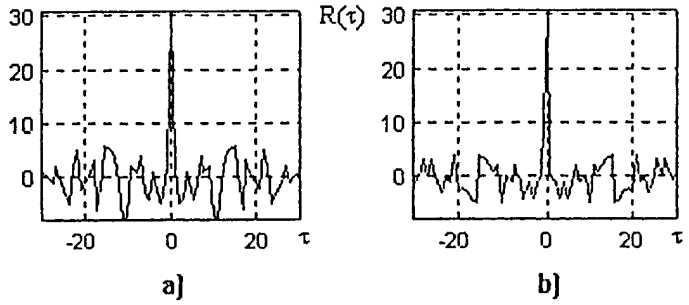

Figure 5: Autocorrelation Function of a Sequence of Length 31
a) Random b) Psudeo-random

Both are at a maximum equal to 31 when $\tau = 0$. Otherwise, the function displays a value much less than 31. It should be noted, however, that a maximal length sequence is periodic and therefore, its autocorrelation function is also periodic.

The Autocorrelation Function

The discrete autocorrelation function of two sequences as defined by [6] is

$$R(\tau) = \sum_{n=1}^{N} c_i(n) \cdot c_i(n-\tau)$$

which measures how similar a sequence is with a time shifted version of itself. Figure 6 is a plot of one period of the autocorrelation function of a PN sequence of length 63.

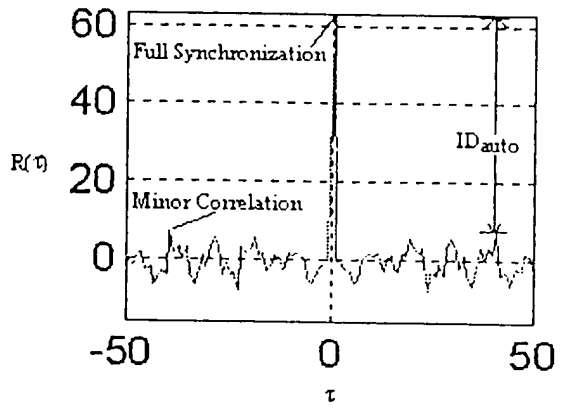

Figure 6: Autocorrelation function of a PN sequence of length 63 illustrating ID_{auto}

The function is at a maximum when $\tau = 0$ corresponding to

$$R(0) = \sum_{n=1}^{N} c_i^2(n) = N$$

which states that the sequence is in full synchronization with itself. The importance of this will become apparent later. By further examination of figure 6, it can be noted that minor correlation can still occur. In a direct sequence spread spectrum communication receivers, detection is performed by means of correlation. Therefore, it is imperative that the magnitude of the minor correlation when $\tau \neq 0$ be much less than N. The *index of discrimination* (ID_{auto}) as defined by [3] is

$$\begin{aligned} \mathbf{ID_{auto}} &= \mathbf{R(\tau = 0) - \max\{R(\tau \neq 0)\}} \\ &= \quad \mathbf{N} \quad \mathbf{- \max\{R(\tau \neq 0)\}} \end{aligned}$$

which is the distance between R(0) and the largest value of $R(\tau)$ when $\tau \neq 0$. This parameter displays the sensitivity of a PN sequence to false synchronization, and should be maximized.

Direct Sequence Spread Spectrum Communications

Spectrum spreading is a communication technique which uses more bandwidth than required by a given modulation technique to transmit information. The advantage is that the transmission can be successful in the presence of substantial interference at the carrier frequency. The most common forms of spectrum spreading are *Direct Sequence*, and *Frequency Hopping*. Both forms utilize a PN sequence generator as the spreading mechanism. Therefore, *Direct Sequence* will be considered here and the details of *Frequency Hopping* will be left for the reader to investigate.

Direct Sequence Binary PSK Transmitter

A block diagram of a Direct Sequence Binary PSK Transmitter is shown in figure 7. The multiplier labeled M1 performs the conversion of the data waveform from a narrowband to a wideband signal, while multiplier M2 transforms the wideband signal from baseband to the carrier frequency.

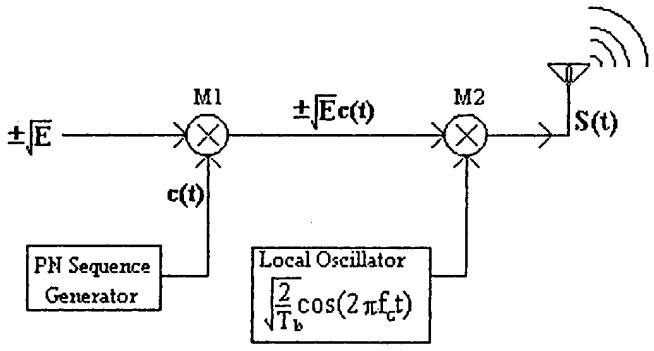

Figure 7: Direct Sequence Binary PSK Transmitter

The data is in the form of a bipolar binary waveform with amplitude of ± the square root of the energy in the signal. The spectrum of a minimum width data pulse is a sinc function

with a maximum of 2 times the square root of the energy of the signal times the bit period T_b. The zero crossings of the spectrum occur at a frequency $f = \pm k/T_b$ where $k = 1,2,3,.....$ This is illustrated by figure 8a and 8b.

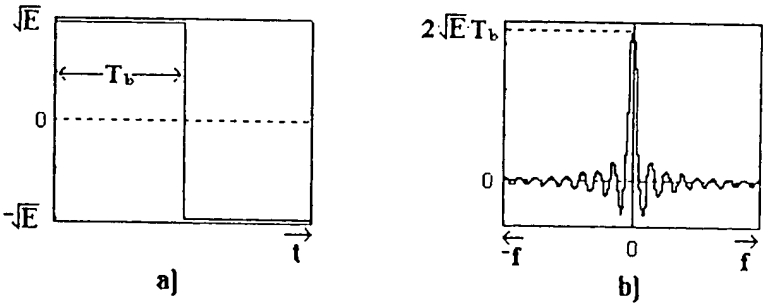

Figure 8: Data Signal a) Waveform b) Spectrum

The data waveform then modulates the PN sequence c(t). Multiplier M1 performs this function. The output of the multiplier is also a bipolar binary sequence with period $T_c = T_b/N$ where N is the period of the PN sequence. Therefore, one period of the PN code occurs for every data pulse. This is shown in figure 9a. This result of this operation is that the spectrum of the minimum width pulse is "spread" over a larger range of frequencies producing a low density power spectra. The spectrum of the minimum width pulse is now a sinc function whose maximum is equal to 2 times the square root of the energy in the signal times the chip rate T_c. The zero crossings occur at the frequencies $f = \pm k/T_c$ where $k = 1,2,.....$ This is shown in figure 9b.

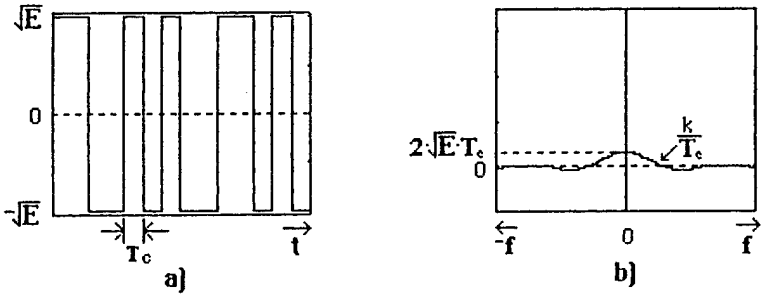

Figure 9: Modulated PN Sequence a) Waveform b) Spectrum

The modulated PN sequence is then used to modulate the basis function

$$\sqrt{\frac{2}{T_b}} \cdot \cos(2\pi f_c t)$$

which shifts the spectrum of the baseband signal in figure 9 to the RF carrier frequency $\pm f_c$. The spectrum is two sided, thus the amplitude is halved. This is shown in figure 10.

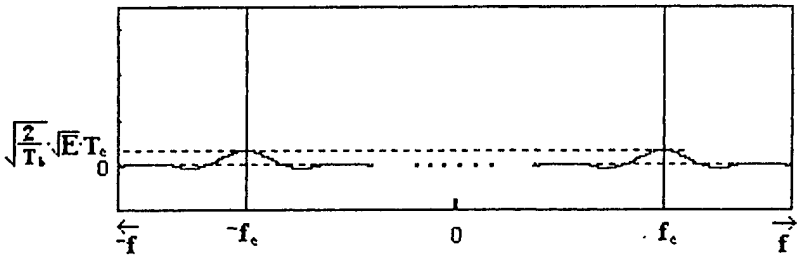

Figure 10: Spectrum of Modulated Carrier

Ideal Channel

The ideal channel will be approximated by the model shown in figure 11.

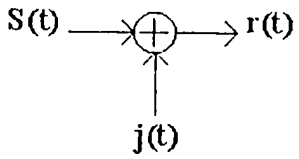

Figure 11: Ideal Channel Approximation

The transmitted signal S(t) is combined with jamming signal j(t), which is the interference in the transmitted band, to produce the received signal r(t)

$$r(t) = S(t) + j(t)$$

where j(t) is intentional or unintentional interference. In a CDMA system, j(t) will be comprised mostly by the other channels in the frequency band identified by their PN sequence

$$j(t) = a_k(t) \cdot \pm\sqrt{\frac{2 \cdot E}{T_b}} \cdot \cos(2\pi f_c t) \qquad k = 1,2,3 \ldots\ldots$$

where the a_k's represent the PN sequences of the respective channels in the system.

Direct Sequence Binary PSK Receiver

Figure 12 is the block diagram of a Direct Sequence Binary PSK Receiver.

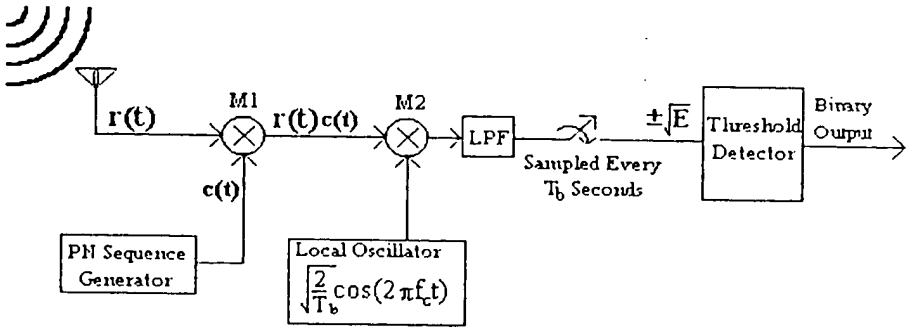

Figure 12: Direct Sequence Binary PSK Receiver

Signal r(t) is multiplied by a local PN sequence to produce

$$r(t) \cdot c(t) = S(t) \cdot c(t) + j(t) \cdot c(t)$$

Substituting yields

$$r(t)\cdot c(t)=\pm\sqrt{\frac{2\cdot E}{T_b}}\cdot\cos(2\pi f_c t)\cdot c^2(t)+a_k(t)\cdot c(t)\cdot\pm\sqrt{\frac{2\cdot E}{T_b}}\cdot\cos(2\pi f_c t)$$

Since c(t) is a bipolar binary waveform with of magnitude of ±1, squaring c(t) results in a constant voltage of +1 which reduces the above equation to

$$r(t)\cdot c(t)=\pm\sqrt{\frac{2\cdot E}{T_b}}\cdot\cos(2\pi f_c t)+a_k(t)\cdot c(t)\cdot\pm\sqrt{\frac{2\cdot E}{T_b}}\cdot\cos(2\pi f_c t)$$

Multiplication of the local PN code results in despreading the spectrum of the channel of interest while spreading the interference of the jamming signal by the same signal. This is true in a CDMA system, provided that the PN sequences are orthogonal and have very low cross correlation function values.

The signal $r(t)\cdot c(t)$ is then multiplied by the local basis function

$$\Phi(t)=\sqrt{\frac{2}{T_b}}\cdot\cos(2\pi f_c t)$$

producing

$$r(t)\cdot c(t)\cdot\Phi(t)=\frac{2}{T_b}\pm\sqrt{E}\cdot\cos^2(2\pi f_c t)+a_k(t)\cdot c(t)\cdot\frac{2}{T_b}\pm\sqrt{E}\cdot\cos^2(2\pi f_c t)$$

Using the identity

$$\cos^2(2\pi f_c t)=\frac{1}{2}\cdot[1+\cos(4\pi f_c t)]$$

reduces $r(t)\cdot c(t)\cdot\Phi(t)$ to

$$r(t)\cdot c(t)\cdot\Phi(t)=\frac{\pm\sqrt{E}}{T_b}+\frac{\pm\sqrt{E}}{T_b}\cdot\cos(4\pi f_c t)+a_k(t)\cdot c(t)\cdot\frac{\pm\sqrt{E}}{T_b}+a_k(t)\cdot c(t)\cdot\frac{\pm\sqrt{E}}{T_b}\cdot\cos(4\pi f_c t)$$

The low pass filter (LPF) performs the integration of the function $r(t)\cdot c(t)\cdot\Phi(t)$ while the sampling of the LPF output waveform every T_b seconds bounds the integration over the range of 0 to T_b.

$$\int_0^{T_b} r(t)\cdot c(t)\cdot\Phi(t)\cdot dt = \int_0^{T_b}[\frac{\pm\sqrt{E}}{T_b}+\frac{\pm\sqrt{E}}{T_b}\cdot\cos(4\pi f_c t)+a_k(t)\cdot c(t)\cdot\frac{\pm\sqrt{E}}{T_b}+a_k(t)\cdot c(t)\cdot\frac{\pm\sqrt{E}}{T_b}\cdot\cos(4\pi f_c t)]$$

All terms which contain the term $\cos(4\pi f_c t)$ will integrate to 0. This reduces the above equation to

$$\int_0^{T_b} r(t)\cdot c(t)\cdot\Phi(t)\cdot dt = \int_0^{T_b}[\frac{\pm\sqrt{E}}{T_b}+a_k(t)\cdot c(t)\cdot\frac{\pm\sqrt{E}}{T_b}]\cdot dt$$

Integrating results in

$$\int_0^{T_b} r(t)\cdot c(t)\cdot\Phi(t)\cdot dt = \pm\sqrt{E}+\frac{\pm\sqrt{E}}{T_b}\cdot\int_0^{T_b}[a_k(t)\cdot c(t)]\cdot dt$$

The second term in the integration calculates the cross correlation function of the interfering PN sequences with the PN sequence assigned to the channel. If the PN sequences used to comprise the system have low cross correlation, this term will be negligible when compared to $\pm\sqrt{E}$. The output of the sampling circuit becomes the input of a threshold detector which determines a binary output value from the polarity of the resulting integration.[6]

It has been shown[7] that the probability of making an incorrect decision is a direct result of the signal to noise (thermal + interference) ratio at the output of the receiver, prior to correlation. Assuming that the interference has a power of J, the signal to noise ratio at the input of the receiver is

$$(SNR)\big|_{IN} = \frac{E_b / T_b}{J}$$

which is the average signal power at the receiver input divided by the equivalent noise variance. The resulting signal to noise ratio at the output as shown by [7] is

$$(SNR)\big|_{OUT} = \frac{E_b}{J \cdot T_c}$$

By solving for $\frac{E_b}{J}$ in the equation for $(SNR)\big|_{IN}$ and substituting into the equation for $(SNR)\big|_{OUT}$, the output signal to noise ratio may be expressed in terms of the input signal to noise ratio.

$$(SNR)\big|_{OUT} = \frac{T_b}{T_c} \cdot (SNR)\big|_{IN}$$

Expressing the above result in decibels results in

$$10 \cdot \log(SNR)\big|_{OUT} = 10 \cdot \log(SNR)\big|_{IN} + 10 \cdot \log\left(\frac{T_b}{T_c}\right) \text{ dB.}$$

Which shows that the output signal to noise ratio is equal to the input signal to noise ratio plus an additional gain in signal to noise ratio which is a result of spread spectrum processing. This is known as processing gain.[7]

If the jamming signal is treated as wideband noise, then the bit error rate for the direct sequence spread spectrum system may be analyzed as that of a binary PSK system having a probability of error

$$P(e) = \frac{1}{2} \cdot erfc\left(\sqrt{\frac{E_b}{N_0}}\right)$$

with noise spectral density of

$$\frac{N_0}{2} = \frac{J \cdot T_c}{2}$$

and bit energy

$$E_b = P \cdot T_b$$

where P is the average signal power and T_b is the bit duration. The bit energy to noise ratio can then be expressed as

$$\frac{E_b}{N_0} = \left(\frac{T_b}{T_c}\right) \cdot \left(\frac{P}{J}\right)$$

which when reformulated results in

$$\frac{J}{P} = \frac{T_b / T_c}{E_b / N_0}$$

The ratio $\frac{J}{P}$ is the jamming margin. This can be related to the processing gain by expressing the equation for $\frac{J}{P}$ in decibels.

$$10 \cdot \log\left(\frac{J}{P}\right) = 10 \cdot \log\left(\frac{T_b}{T_c}\right) - 10 \cdot \log\left(\frac{E_b}{N_0}\right) \quad \text{dB}$$

or

$$(\text{Jamming margin})\big|_{dB} = (\text{Processing gain})\big|_{dB} - \left(\frac{E_b}{N_0}\right)\Big|_{dB}$$

The conclusion to be made from this result is that the signal to noise representation of the processing gain has 2 components. The first component is the minimum $\frac{E_b}{N_0}$ needed to sustain a prescribed probability of error. The second component is the jamming

margin which describes the maximum level of interference which can be tolerated for the system to operate correctly. Since the interference level of a CDMA system is dependent on the number of users, a relationship must be established to describe the necessary jamming margin for a given number of users. [8] states a relationship between the jamming margin JM, and the number of users U as

$$JM = 10 \cdot \log(U - 1)$$

which will allow the designer to determine the necessary code length to accommodate a given number of users.

The PN sequences which have been described up to this point have been realized by the using maximal length shift register sequence generators. However, the cross correlation between pairs of maximal length sequences can be large and therefore are not useful for CDMA applications.[9] Therefore, an alternate method of generating PN sequences must be used. Gold codes[9] can be utilized for CDMA since they posses the proper pseudo-noise properties while having low cross correlation between members of the same set.

V. Gold Code Generators

Physical Description

The physical illustration of a Gold code generator is shown in figure 13. The generation of Gold codes requires 2 maximal length SRG with feedback taps described by different characteristic polynomials. The resulting sequences generated by the individual SRG's are then added together modulo 2 to produce a single Gold sequence.

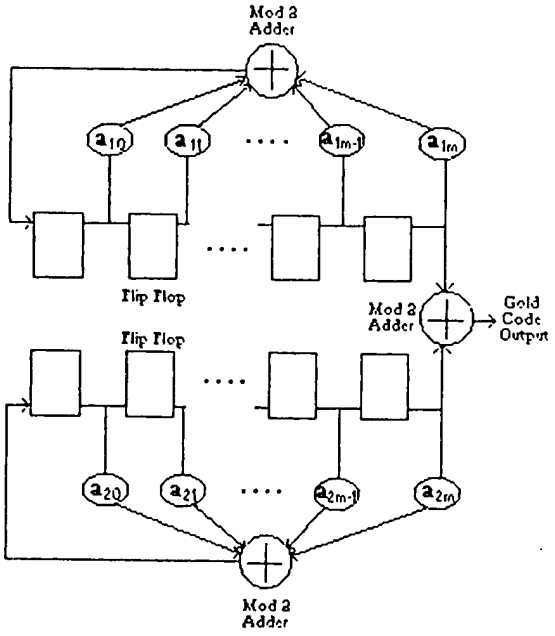

Figure 13: Gold Code Sequence Generator

[2] states the following theorem to explain the effect of the mod 2 sum of sequences generated by SRG's.

> ***Theorem:*** *Let $f_1(X)$ and $f_2(X)$ be characteristic polynomials. Let Q be the sequence which results from the mod 2 sum of the output sequences generated by SRG's described by $f_1(X)$ and $f_2(X)$. Q can be generated by a single shift register generator whose characteristic polynomial is described by $f_1(X)f_2(X)$.*[2]

The following deduction can by made from the result of the above theorem. The sequence which results from the generator in figure 13 is always non-maximal. The same sequence can be generated by a single SRG with an equivalent characteristic polynomial described by $f(X) = f_1(X) \cdot f_2(X)$. Therefore, f(X) is *reducible* into $f_1(X)$ and $f_2(X)$. Recall that a necessary condition for a SRG's sequence to be maximal length is that its characteristic polynomial be *irreducible*.

To generate Gold codes, the SRG's which comprise the Gold code generator must be of maximal length with an equal number of stages. The period of the Gold code will then be equal to 2^m-1 providing that both SRG's have m stages.

Preferred Pairs of Characteristic Polynomials

Up to this point, the properties of the characteristic polynomials of the SRG's have been subject to only two constraints which are that they need to be different and of the same degree. To generate Gold codes, however, an additional restriction must be made. The restriction is that the pair of polynomials must form a preferred pair. A method of determining preferred pairs is outlined by the following theorem.[2]

> ***Theorem:*** Let $f_1(X)$ be a primitive polynomial of degree *m* such that *m* is not divisible by 4. Let α be a root of $f_1(X)$. $f_2(X)$ and $f_1(X)$ form a preferred pair of characteristic polynomials if
>
> $\alpha^{\left\lfloor 2^{\frac{(m-1)}{2}}+1 \right\rfloor}$ is a root of $f_2(X)$ for *m* odd
>
> $\alpha^{\left\lfloor 2^{\frac{(m-2)}{2}}+1 \right\rfloor}$ is a root of $f_2(X)$ for *m* even

Preferred pairs of maximal length characteristic polynomials of degree m when properly added will produce Gold code x. If the generator is *phased*[2], the addition of the output sequences produced by the characteristic polynomials will produce another Gold code y. The discrete cross-correlation of sequences x and y defined by

$$\Psi(\tau) = \sum_{n=1}^{N} x(n) \cdot y(n-\tau)$$

will satisfy the following inequality.[2]

$$|\Psi(\tau)| \leq \begin{cases} 2^{\frac{(m+1)}{2}} + 1 & m \text{ odd} \\ 2^{\frac{(m+1)}{2}} + 1 & m \text{ even} \qquad m \neq 0 \bmod 4 \end{cases}$$

For example, if $m = 6$, the maximum value of the cross-correlation function $\Psi(\tau)$ of two gold codes generated using preferred pairs is $\Psi(\tau) = 17$ which is low when compared with the maximum of the autocorrelation function.

$$R(0) = 2^6 - 1 = 63$$

If maximal length sequences are used for sequences x and y, the maximum value of the cross-correlation function could be much higher.

Balanced Gold Codes

Gold codes generated by the technique stated earlier in this section can be divided into three classes. The first class are codes which exhibit the balance property meaning that the number of ones does not exceed the number of zeros by more than 1. This class of Gold codes are known as balanced Gold codes and are of primary interest because these sequences exhibit the required pseudo-random properties for spread spectrum communications. The other two classes of Gold codes have an excess number of either

ones or zeros and are therefore unbalanced. [2] provides a table which displays the distribution of balanced and unbalanced Gold codes for a Gold code generator with *m* stages. For a generator with *m* stages, the number of balanced Gold codes available is equal to $2^{m-1} + 1$.

Consider for example two sequences a and b which are two maximal length sequences generated by preferred pairs of degree 3.

a = 1 1 1 0 1 0 0 b = 0 0 1 0 1 1 1

If a and b are added together mod 2, the resulting sequence c is a balanced Gold code.

a = 1 1 1 0 1 0 0
+b = 0 0 1 0 1 1 1
c = 1 1 0 0 0 1 1

If sequence b is rotated to the left by one position, the sequence b' is formed and when added to a mod 2, the resulting sequence is another balanced Gold code.

a = 1 1 1 0 1 0 0
+ b' = 0 1 0 1 1 1 0
c = 1 0 1 1 0 1 0

If sequence b' is rotated to the left by one position, the sequence b" is formed and when added to a mod 2, the resulting sequence is an unbalanced Gold code.

a = 1 1 1 0 1 0 0
+b" = 1 0 1 1 1 0 0
c = 0 1 0 1 0 0 0

In the first two cases the initial symbol of the Gold code is a 1 which resulted in a sequence which is balanced. In the third case, however, the initial symbol of the Gold code was a 0 which resulted in an unbalanced Gold code. If the sequence b was shifted such that the initial symbol of the resulting Gold code is 0, then the code will be

unbalanced. Therefore, it is concluded that to generate *balanced* Gold codes, the initial symbol resulting from the mod 2 addition must be 1.

Initial Conditions

The initial conditions of the SRG's used in the Gold code generator have a restriction that at least one of the two must be in its characteristic phase. Every SRG has a characteristic phase. When a sequence is generated and sampled at every other symbol from a SRG in its characteristic phase, the same sequence results. Consider the following example. The following sequence was generated from a register in its characteristic phase.

100101110.....

Starting at the first symbol and sampling at every other symbol thereafter results in

10010.....

which is the same as the original sequence.

To determine the characteristic phase of an SRG, Holmes[2] states a procedure developed by Gold[9]. If f(X) is the characteristic polynomial of an m-stage SRG, then the characteristic phase of that SRG is the first m coefficients of the generating function G(X) where

$$G(X) = \frac{g(X)}{f(X)}$$

and the numerator of the generating function is given by

$$g(X) = \begin{cases} \frac{d}{dX}[X \cdot f(X)] & m \text{ odd} \\ f(X) + \frac{d}{dX}[X \cdot f(X)] & m \text{ even} \end{cases}$$

As an example, the characteristic phase for the register in figure 4 will then be determined. The characteristic polynomial for the register is

$$f(X) = 1 + X + X^3$$

Since m is of odd degree, the numerator of the generating function is given by

$$g(X) = d/dX[X + X^2 + X^4]$$

$$= 1$$

So, the generating function is given by

$$G(X) = \frac{1}{1 + X + X^3}$$

Performing long division,

$$\begin{array}{r} 1 + X + X^2 \ldots \\ 1 + X + X^3 \overline{)\,1} \\ \underline{1 + X + X^3} \\ X + X^3 \\ \underline{X + X^2 + X^4} \\ X^2 + X^3 + X^4 \\ \vdots \end{array}$$

Therefore, the characteristic phase is { 1 1 1 }. Loading { 1 1 1 } into the register and generating two periods of the output sequence results in the following.

11101001110110

Sampling the first symbol and every other symbol thereafter results in

1110100

which is one period of the original sequence, verifying that { 1 1 1 } is the characteristic phase of the SRG described by $f(X) = 1 + X + X^3$.

VI. Gold Code Generators for a CDMA System

This section outlines a procedure for generating Gold codes for a Code Division Multiple Access (CDMA) communication system with a specified number of users. An example of the procedure will be carried out concurrently with the explanation.

1) Determine the jamming margin necessary to accommodate the maximum number of users

It has been shown by [8] that the jamming margin needed to sustain a finite number of users (U) in a CDMA system is related by the following equation.

$$\mathbf{JM = 10 \cdot log(U - 1) \ \ dB}$$

For example, suppose it is desired that a CDMA system support a maximum number of users equal to 20. Then the jamming margin necessary to sustain the specified capacity is

$$JM = 10 \cdot \log(19) = 12.788 \ \ dB = JM_u$$

where J_u denotes jamming margin due to users.

2) Estimate the jamming margin required for the rejection of any additional interference in the frequency band. Find the total jamming margin.

[8] equation does not take into account any other signals being present at the carrier. This step is necessary because many of the frequencies used in personal communications are unlicensed and can therefore contain a substantial amount of interference.

Continuing the example from before, suppose the system is being designed for use in the unlicensed frequency band 902 - 928 MHz. For example, it is estimated that an

additional 4 dB of interference could be present at any given time. The additional jamming margin necessary is

$$JM_I = 4 \text{ dB}$$

where J_I denotes jamming margin due to interference. Thus, the total jamming margin necessary is the sum due to users and additional interference.

$$JM = JM_u + JM_I$$

In the example,

$$JM = 16.778 \text{ dB}$$

3) Determine the necessary signal to noise ratio needed to sustain a given probability of error.

For binary PSK, the probability of error is given by

$$P(e) = \frac{1}{2} \cdot erfc\left(\sqrt{\frac{E_b}{N_0}}\right)$$

or

$$P(e) = \frac{1}{2} \cdot \left(1 - erf\left(\sqrt{\frac{E_b}{N_0}}\right)\right)$$

where erf( ) is the error function and erfc( ) is the error function complement. Therefore,

$$erf\left(\sqrt{\frac{E_b}{N_0}}\right) = 1 - 2 \cdot P(e)$$

Solve for the value of 1 - 2P(e). Use a table of the error function to find

$$\sqrt{\frac{E_b}{N_0}}$$

Let the result be equal to some number A. Then

$$\frac{E_b}{N_0} = A^2$$

which needs to be expressed in dB. Therefore,

$$\frac{E_b}{N_0}\Big|_{dB} = 10 \cdot \log\left(A^2\right)$$

In this example, suppose it is required that the probability of error be no greater than $5 \cdot 10^{-4}$. Then

$$erf\left(\sqrt{\frac{E_b}{N_0}}\right) = 0.9990$$

It is found from the table of the error function that

$$\sqrt{\frac{E_b}{N_0}} = 2.5$$

and

$$\frac{E_b}{N_0} = 6.25$$

Therefore,

$$\frac{E_b}{N_0}\Big|_{dB} = 7.9588 \text{ dB}$$

4) Find the processing gain and determine the code length. Determine the number of stages in the generator.

The processing gain of the system is the sum of the jamming margin and the signal to noise ratio required to sustain a given P(e).

$$PG\Big|_{dB} = J\Big|_{dB} + \frac{E_b}{N_0}\Big|_{dB}$$

The processing gain is also the dB equivalent of the code length N

$$PG\big|_{dB} = 10 \cdot \log(N)$$

which can be solved to determine an expression for the code length.

$$N = 10^{\frac{PG\big|_{dB}}{10}}$$

The code length is therefore related to the number of stages m by

$$N = 2^m - 1$$

which when rearranged can be used to determine the number of stages.

$$m = \log_2(N+1)$$

Continuing the example, the processing gain of the system is

$$PGl_{db} = 16.778 \text{ dB} + 7.9588 \text{ dB} = 24.737 \text{ dB}$$

The code length is

$$N = 10^{2.4737} = 297.64$$

Since N is an integer, round up.

$$N = 298$$

Therefore, the number of stages in each SRG comprising the gold code generator is

$$m = \log_2(299) = 8.22$$

which also has to be an integer so round up.

$$m = 9$$

The actual code length is

$$N = 2^9 - 1 = 511$$

and the actual processing gain is

$$PGl_{dB} = 10 \cdot \log(N) = 27.084 \text{ dB}$$

5) Calculate the number of balanced Gold codes available and compare with the number of users.

This step is necessary to insure that the number of users does not exceed the number of codes given by

$$\text{number of users} = 2^{m-1}$$

In this example,

$$2^{m-1} = 2^8 = 256 > 20$$

6) Determine the preferred pairs of characteristic polynomials for the Gold sequence generator.

It is necessary to have Appendix C of [5] on hand for this step which will be explained entirely by example. Since m = 9, the degree of each characteristic polynomial will be 9. Look up the section labeled degree 9 in Table C.2, Appendix C of [5]. Select any polynomial which ends with the letters E,F,G, or H. All Numbers are in octal. For this example, the polynomial 1021F will be selected. 1021 octal corresponds to 1000010001 binary. These are the coefficients of the characteristic polynomial. The characteristic polynomial is therefore,

$$f_1(X) = X^9 + X^4 + 1$$

There is a number to the left of 1021F in the table. That is the root of $f_1(X)$. Reading directly from the table, the root of $f_1(X)$ is $\alpha_1 = 1$. Since m is odd, the root of the second characteristic polynomial comprising the preferred pair is $\alpha_2 = 2^{(m-1)/2} + 1 = 17$. Looking up the root 17 under degree 9 of Table C.2, the second characteristic polynomial is 1333F. The binary equivalent 1333 is 1011011011 and the corresponding polynomial is

$$f_2(X) = X^9 + X^7 + X^6 + X^4 + X^3 + X + 1$$

$f_1(X)$ and $f_2(X)$ are the preferred pairs of characteristic polynomials used to comprise the Gold code generator in this example.

7) Determine the characteristic phase for one register.

This will also be explained by example. Since the degree of the characteristic polynomial is odd, the numerator of the generating function is given by

$$g(X) = \frac{d}{dx}[X \cdot f(X)]$$

There is no benefit of choosing one polynomial versus the other. The one not chosen will be phased for the development of channels. In this example, $f_2(X)$ will be used. The numerator of the generating function is

$$g(X) = X^6 + X^4 + 1$$

By performing long division (not shown here), the generating function G(X) is found to be

$$G(X) = 1 + X + X^2 + X^4 + X^5 + X^7 + X^8 + \cdots\cdots$$

The characteristic phase of the register is the coefficients of the generating function.

$$\{\ 1\ 1\ 0\ 1\ 1\ 0\ 1\ 1\ 1\ \}$$

This is the characteristic phase of register 2.

8) Determine the necessary contents of the second register to produce a balanced Gold code.

Recall that to produce a balanced Gold code, the initial symbol of the Gold code has to be a 1. Therefore, since register 2 is in its characteristic phase, the initial symbol of the m^{th} stage of register 1 must be chosen such that when added to the contents of the m^{th} stage of register 2 results in a 1. Since the m^{th} stage of register 2 is a 1, the m^{th} stage of register 1 must be a 0. Therefore, the contents of register 2 is

{ x x x x x x x x 0 }

where x denotes a "don't care" symbol and may contain either a 0 or 1.

9) Phase the "don't care" symbols of register 1 to create the necessary number of channels.

The easiest way to do this is to make a channel table using the contents of register 1. Since the m^{th} stage always contains the symbol 0, it is not necessary to include the m^{th} stage in the table. The table will be comprised of stages 1 through m-1. Complete the table until the required number of channels is achieved. The channel table for the first 8 stages of register 1 in the example is shown below.

Stage / Channel	1	2	3	4	5	6	7	8
1	0	0	0	0	0	0	0	0
2	0	0	0	0	0	0	0	1
3	0	0	0	0	0	0	1	0
4	0	0	0	0	0	0	1	1
5	0	0	0	0	0	1	0	0
6	0	0	0	0	0	1	0	1
7	0	0	0	0	0	1	1	0
8	0	0	0	0	0	1	1	1
9	0	0	0	0	1	0	0	0
10	0	0	0	0	1	0	0	1
11	0	0	0	0	1	0	1	0
12	0	0	0	0	1	0	1	1
13	0	0	0	0	1	1	0	0
14	0	0	0	0	1	1	0	1
15	0	0	0	0	1	1	1	0
16	0	0	0	0	1	1	1	1
17	0	0	0	1	0	0	0	0
18	0	0	0	1	0	0	0	1
19	0	0	0	1	0	0	1	0
20	0	0	0	1	0	0	1	1

This completes the design. The Gold code generator for channel 1 is shown in figure 14.

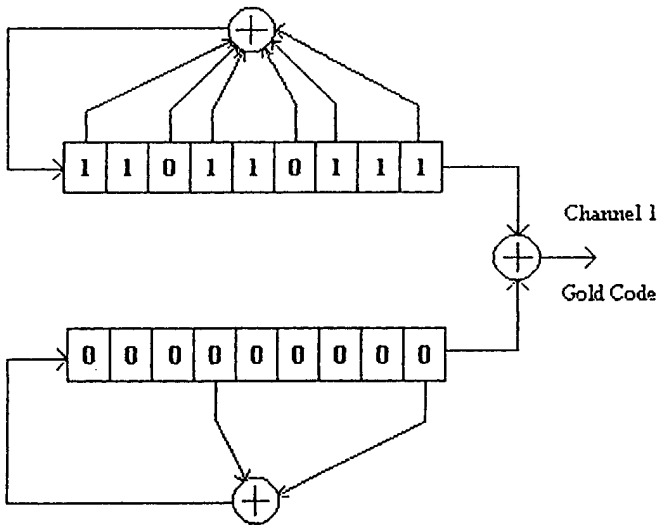

Figure 14: Sequence Generator for Channel 1

The implementation of gold sequence generators can be done with relative ease and flexibility using a programmable logic device which supports hardware description language design entry. The next section illustrates the design of a gold sequence generator/modulator using the VHDL hardware description language.

VII. Gold Sequence Generator/Modulator Implementation

Figure 15 shows a block diagram of a PN sequence generator/modulator implemented on an Altera EPM5032 erasable programmable logic device (EPLD).

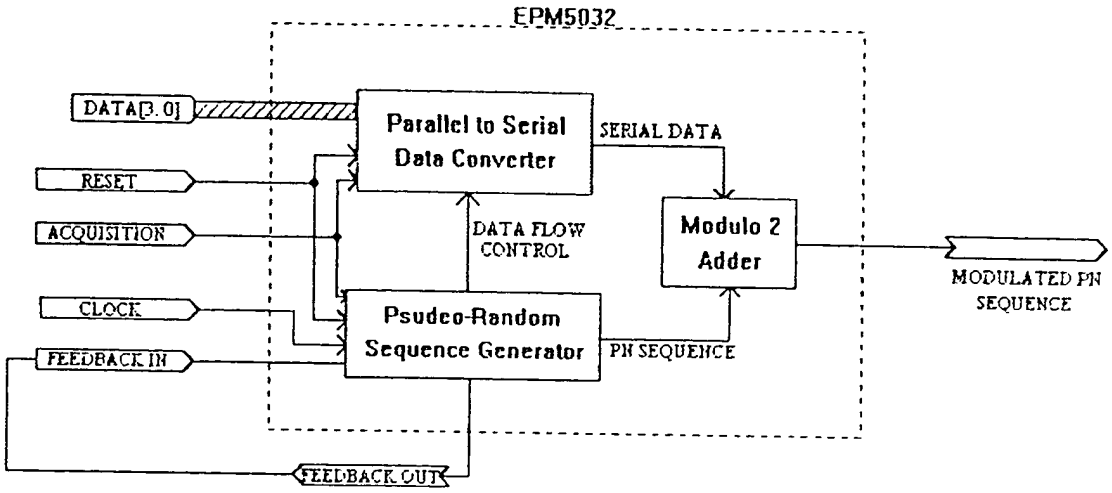

Figure 15: PN sequence generator/modulator

The device reads in and stores 4 data bits in parallel format. The data is then converted from parallel to serial data format. Each data bit then modulates a pseudo-random sequence through a modulo 2 adder. The output of the device is a pseudo-random sequence formatted to represent a value of one or zero as shown in figure 16.

Figure 16: Pseudo-random sequences formatted to represent data bit values

It is determined from figure y that the design of the pseudo-random sequence generator/modulator can be divided into subcomponents of the parallel to serial converter,

the sequence generator and the modulo-2 adder. Identifying the subcomponents of the design is necessary to show the effectiveness of VHDL as a design entry tool.

VHDL may be used to describe a design at three levels of abstraction[9]. They are the behavior, dataflow, and structural levels. It is necessary to examine the behavioral and structural levels since the design of the pseudo-random sequence generator/modulator requires the utilization of both. The following define the behavior and structural levels of abstraction as stated by Navabi:

> *The **behavior level** is the most abstract. It describes the function of the design in a software-like procedural form, and provides no detail of how the design is to be implemented.*[9]

> *A **structural description** is the lowest and most detailed level of description considered and is the simplest to synthesize into hardware. The corresponding function of the hardware is not evident from such descriptions unless the components used are known.*[9]

When a component is described in VHDL at the behavior level, the information in the design file describes the *operation* of the module. In contrast, a structural level design file would contain information about what *components* are being used and their *interconnections*.

VHDL was developed as a tool for simulation of systems at all levels of abstraction.[9] A design would normally be simulated first at the behavior level to verify the functionality of the design. After verifying the functionality, the design would be divided into smaller components and connected using a structural level design file. The design would then be resimulated to ensure functionality was preserved. This process was repeated until the design was completely structural consisting of primitive logic gates.

This is known as top-down design[9] in which the design process moves from general to specific. The same process can be applied using VHDL as a design entry tool.

As a design entry tool, manufacturers of programmable logic devices (PLD's) incorporate VHDL into their logic design software specific to their product. The design software has an internal logic synthesizer which will take a design file at either the behavioral or the structural level and design the necessary logic for implementation on a PLD. Since the manufacturer provides the synthesis tool, it would seem unnecessary to design at any other level of abstraction other than the behavior level letting the synthesizer design the low level logic. This technique is discouraged for the following reasons:

1. To implement a design file at the behavior level, the logic synthesizer will execute an algorithm to translate the behavioral description into the necessary logic equations for implementation on a specific PLD. However, the algorithm may terminate with no solution. The result is a behavioral design file which is not able to be realized in hardware. It is important that any behavior design be *synthisizable* and the more complex the behavioral description, the lower the probability of synthesis.

2. By creating a design using behavior level components, customization and modification may be realized by editing specific components rather than an entire design.

To obtain the highest probability of synthesis, the following design procedure may be utilized:

1. Determine the block description of the function to be performed. Identify all inputs and outputs.

2. Divide the function into sub-functions which support the operation of the main design.

3. Repeat step 2 until all subfunctions can be expressed in the form of primitive behavioral components. Examples of primitive behavior components would be:

a. State Machines
b. adders
c. multipliers
d. shift registers
e. counters

4. Write behavior design files to represent the derived primitive components. Use the synthesizer to design the logic equations. Simulate the components to demonstrate correct functionality.

5. Write structural design files to describe the interconnections between subcomponents.

This PLD design procedure deviates from top down design only in that the primitive behavior models are left to be designed by the synthesizer.

Parallel to Serial Data Converter

Figure 17 displays the source code for the implementation of a zero - delay parallel to serial data converter. The number which appears at the end of each line of code is not part of the program, but serves for a reference to line number.

```
entity partoser is                                                          1
        port(                                                               2
                xin             :       in      bit_vector(3 downto 0);     3
                clock           :       in      bit;                        4
                reset           :       in      bit;                        5
                acq             :       in      bit;                        6
                serout          :       out     bit);                       7
end partoser;                                                               8

architecture behv of partoser is                                            9

        signal  temp1           :       bit_vector(3 downto 0);             10
        signal  temp2           :       bit_vector(3 downto 0);             11
        signal  hold            :       bit;                                12
        signal  clk             :       bit;                                13
        signal  rst1            :       bit;                                14
        signal  rst2            :       bit;                                15

begin                                                                       16

clk <= clock and (not acq);                                                 17
rst1 <= reset and acq;                                                      18
rst2 <= reset and (not acq);                                                19

        process(clk,rst1,rst2)                                              20
                variable  count1    :       integer range 0 to 3;           21
                variable  count2    :       integer range 0 to 3;           22
                variable  flag      :       integer range 0 to 1;           23
        begin                                                               24
                if rst1 = '1' then                                          25
                        temp1 <= xin;                                       26
                        hold <= '1';                                        27
                        count1 := 3;                                        28
                        flag := 0;                                          29
                elsif rst2 = '1' then                                       30
                        temp2 <= xin(2 downto 0) & '0';                     31
                        hold <= xin(3);                                     32
                        count2 := 2;                                        33
                        flag := 1;                                          34
                elsif clk'event and clk = '1' then                          35
                        if flag = 0 then                                    36
                                if count1 = 0 then                          37
                                        hold <= temp1(3);                   38
                                        temp1 <= xin;                       39
                                        count1 := 3;                        40
                                elsif count1 /= 0 then                      41
                                        hold <= temp1(3);                   42
                                        temp1 <= temp1(2 downto 0) & '0';   43
                                        count1 := count1 - 1;               44
                                end if;                                     45
                        elsif flag = 1 then                                 46
                                if count2 = 0 then                          47
                                        hold <= temp2(3);                   48
                                        temp2 <= xin;                       49
                                        count2 := 3;                        50
                                elsif count2 /= 0 then                      51
                                        hold <= temp2(3);                   52
                                        temp2 <= temp2(2 downto 0) & '0';   53
                                        count2 := count2 - 1;               54
                                end if;                                     55
                        end if;                                             56
                end if;                                                     57
        end process;                                                        58
        serout <= hold or acq;                                              59
end behv;                                                                   60
```

Figure 17: VHDL description of a zero - delay parallel to serial converter

The first 8 lines of the program is the ENTITY[9] which provides the component name and specifies the input and output ports of the component. The visual description of the entity is shown in figure 18.

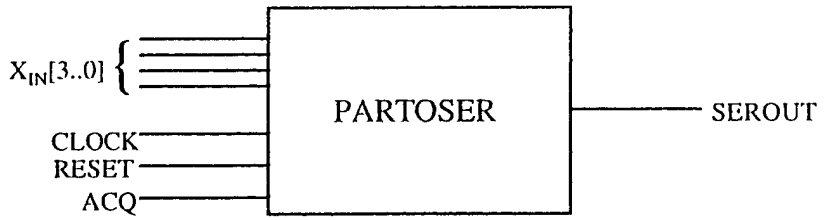

Figure 18: Visual representation of the ENTITY of figure 17

Lines 9 through 60 describe the ARCHITECTURE[9] of the program. This is the portion of the program which describes the operation of the box shown in figure 17. While the ACQ input has a voltage applied representing a logic level '1', the parallel to serial converter exhibits the behavior corresponding to when the radio is in its acquisition mode. In the acquisition mode, the local PN code generator at the receiver is trying to synchronize with the transmitted code. The SEROUT output will remain at a constant value of 1 until the ACQ signal transfers from high to low upon which the converter will begin its operation. This is shown in figure 19.

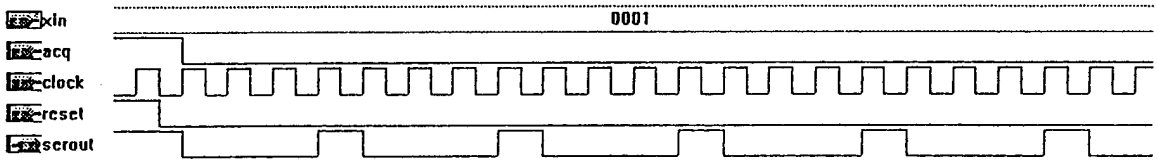

Figure 19: Simulation results of the zero - delay parallel to serial converter

Once the ACQ signal has transferred from high to low the converter begins to shift the data out in serial format. This begins immediately after the ACQ signal has transferred

from high to low with no clock period delay for the first bit to be shifted out. Therefore, it can be assumed that for bit synchronization, that immediately after the ACQ signal returns to a low state the next output bit will be valid data with zero delay.

The attractive feature of using VHDL for implementation of digital designs is its flexibility. For example, once a module such as the parallel to serial converter has been developed for 4 bit parallel data, it can be easily modified to accommodate 8, 16, or 32 bit data by the constants of the program which dictate the size of the data.

Gold Code Generator

The VHDL code for a PN sequence generator of sequence length 7 is shown in figure 20.

```
entity pn3 is                                                                    1
        port(                                                                    2
                clock                   :       in              bit;             3
                reset                   :       in              bit;             4
                fin                     :       in              bit;             5
                acq                     :       in              bit;             6
                fout                    :       out             bit;             7
                shift                   :       out             bit;             8
                pn                      :       out             bit);            9
end pn3;                                                                         10

architecture behv of pn3 is                                                      11
        signal  temp    :               bit_vector(2 downto 0);                  12
        signal  trig    :               bit;                                     13
begin                                                                            14
pn <= temp(2);                                                                   15
fout <= temp(2) xor temp(0);                                                     16
shift <= '1' when (trig = '1' and acq = '0') else '0';                           17
        process(clock,reset)                                                     18
                variable  count     :       integer range 0 to 6;                19
        begin                                                                    20
                if reset = '1' then                                              21
                        temp <= "101";                                           22
                        count := 0;                                              23
                        trig <= '1';                                             24
                elsif clock = '1' and clock'event then                           25
                        if count = 6 then                                        26
                                trig <= '1';                                     27
                                temp <= temp(1 downto 0) & fin;                  28
                                count := 0;                                      29
                        elsif count /= 6 then                                    30
                                trig <= '0';                                     31
                                temp <= temp(1 downto 0) & fin;                  32
                                count := count + 1;                              33
                        end if;                                                  34
                end if;                                                          35
        end process;                                                             36
end behv;                                                                        37
```

Figure 20: VHDL implementation of a PN Sequence Generator with shift control

The source code of figure 20 generates a PN sequence of length 7 and also has an internal counter which tracks the position of the sequence. When the counter has determined that the sequence has generated its N-1th symbol (N being the sequence length), a pulse is generated on a control signal which is sent to the clock input of the parallel/serial converter. This pulse shifts the next data bit into position for modulation. During acquisition, this shift control signal is disabled. This is illustrated in figure 21.

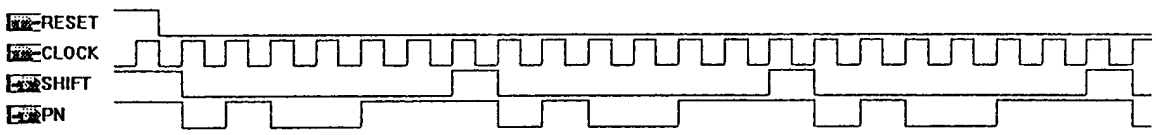

Figure 21: Simulation results of the PN sequence generator with shift control

To generate a gold code, it is necessary to take the modulo 2 addition of the output of 2 PN sequence generators, with the appropriate initial conditions. The first sequence generator was designed with the appropriate control logic for the modulation process. This allows the second sequence generator to be designed without the control logic to minimize the hardware resources needed for implementation. This is shown in figure 22.

```
entity pn3d is
        port(
                        clock       :       in      bit;
                        reset       :       in      bit;
                        fin         :       in      bit;
                        fout        :       out     bit;
                        pn          :       out     bit);
end pn3d;

architecture behv of pn3d is

        signal    temp    :       bit_vector(2 downto 0);

begin

pn <= temp(2);
fout <= temp(2) xor temp(1);

        process(clock,reset)
        begin
                if reset = '1' then
                        temp <= "011";
                elsif clock = '1' and clock'event then
                        temp <= temp(1 downto 0) & fin;
                end if;
        end process;
end behv;
```

Figure 22: Second PN Sequence Generator Having No Control Logic

The output of the sequence generators become the input signals to a modulo 2 adder whose output is a Gold code of length 7. This is implemented at the structural level of abstraction where each sequence generator is a component and only the connectivity information is supplied. This is shown in figure 23.

```
entity pn3gold is
        port(
                clock           :       in      bit;
                reset           :       in      bit;
                fin1            :       in      bit;
                fin2            :       in      bit;
                acq             :       in      bit;
                fout1           :       out     bit;
                fout2           :       out     bit;
                shift           :       out     bit;
                gold3           :       out     bit);
end pn3gold;

architecture struct of pn3gold is

        component  pn3  port(clock,reset,fin,acq : in bit; fout,shift,pn : out bit);
        end component;
        component  pn3d port(clock,reset,fin : in bit; fout, pn : out bit);
        end component;

        for all : pn3 use entity work.pn3(behv);
        for all : pn3d use entity work.pn3d(behv);

        signal x1  :        bit;
        signal x2  :        bit;

begin

        c0: pn3 port map (clock,reset,fin1,acq,fout1,shift,x1);
        c1: pn3d port map (clock,reset,fin2,fout2,x2);

        gold3 <= x1 xor x2;

end struct;
```

Figure 23: Structural Level representation of the Mod 2 addition of two PN sequences

The simulation results of figure 23 are shown in figure 24. The gold sequence generated by the source code of figure 23 should yield a minimum cross correlation with the sequence produced by figure 20.

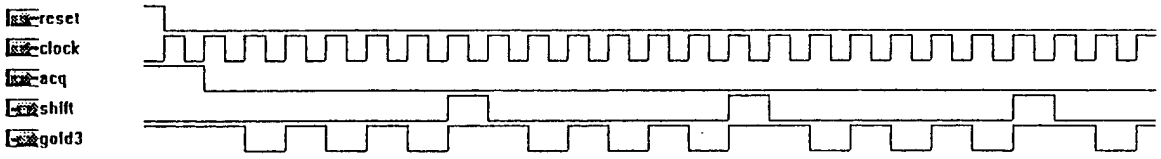

Figure 24: Gold Sequence Produced by figure y8

It is at this point where the flexibility of using a hardware description language for Gold sequence generation can be illustrated. To implement a sequence of different length,

only specific lines of the existing source code need be modified. Figure 25 shows the source code of figure 20 modified to produce a PN sequence of length 31. The modifications are in italics.

```
entity pn5 is
        port(
                clock           :       in      bit;
                reset           :       in      bit;
                fin             :       in      bit;
                acq             :       in      bit;
                fout            :       out     bit;
                shift           :       out     bit;
                pn              :       out     bit);
end pn5;

architecture behv of pn5 is

        signal  temp    :       bit_vector(4 downto 0);
        signal  trig    :       bit;

begin

pn <= temp(4);
fout <= temp(4) xor temp(1);
shift <= '1' when (trig = '1' and acq = '0') else '0';

        process(clock,reset)
                variable  count     :       integer range 0 to 30;

        begin
                if reset = '1' then
                        temp <= "10000";
                        count := 0;
                        trig <= '1';
                elsif clock = '1' and clock'event then
                        if count = 30 then
                                trig <= '1';
                                temp <= temp(3 downto 0) & fin;
                                count := 0;
                        elsif count /= 30 then
                                trig <= '0';
                                temp <= temp(3 downto 0) & fin;
                                count := count + 1;
                        end if;
                end if;
        end process;
end behv;
```

Figure 25: Modified VHDL source code of figure 20 producing a sequence of length 31

PN Sequence Generator/Modulator

With all the necessary subcomponents defined, the structural design file to implement the PN sequence generator/modulator may be described. This is shown in figure 26.

```
entity seqmod is
        port(
                        xin             :       in      bit_vector(3 downto 0);
                        clock           :       in      bit;
                        reset           :       in      bit;
                        fin1            :       in      bit;
                        fin2            :       in      bit;
                        acq             :       in      bit;
                        fout1           :       out     bit;
                        fout2           :       out     bit;
                        modpnseq        :       out     bit);
end seqmod;

architecture struct of seqmod is

        component partoser port(xin : in bit_vector(3 downto 0); clock,reset,acq : in bit; serout : out bit);
        end component;

        component pn3gold port(clock,reset,fin1,fin2,acq : in bit; fout1,fout2,shift,gold3 : out bit);
        end component;

        for all : partoser use entity work.partoser(behv);

signal shift        :       bit;
signal xserout      :       bit;
signal gold         :       bit;

begin

        c0: partoser port map (xin,shift,reset,acq,xserout);
        c1: pn3gold port map (clock,reset,fin1,fin2,acq,fout1,fout2,shift,gold);

modpnseq <= not(xserout xor gold);

end struct;
```

Figure 26: VHDL Source Code Describing the PN Sequence Generator/Modulator

The structure of the source code of figure 26 is similar to that of figure 23. In figure 23 subcomponents were declared and connected to form the gold code generator. In figure 26 the PN generator/modulator is conceived using the same process where the components are the gold code generator and the parallel to serial converter. The modulo 2 adder is implemented using the exclusive or command.

Figure 27a shows the simulation results during acquisition. The resulting output will be the unmodulated output of the gold code generator.

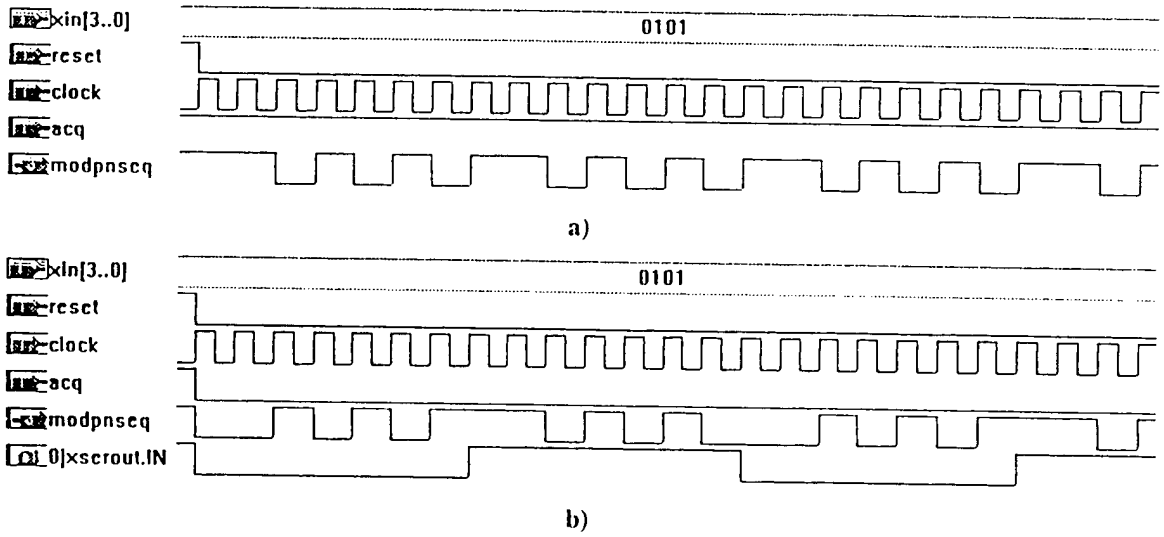

Figure 27: PN Modulator Simulation Results a) Acquisition b) Modulation

Figure 27b shows the PN modulator operating during the modulation mode. When the ACQ input transfers from high to low, the PN sequence is modulated by the current data bit at the output of the parallel to serial converter. If the current data bit is a '1', the gold code will be as if it was unmodulated during acquisition. If the data bit is a '0', then the PN sequence occurs with each symbol in the sequence inverted from its normal value.

This completes the design of the gold sequence generator/modulator. However, the output waveform has the following voltage levels representing their corresponding logic levels:

Level	Voltage (Volts)
Logic '0'	0
Logic '1'	5

The output waveform will have to be converted such that the voltage levels representing the logic states are equal in magnitude and opposite in sign. This conversion provides the ability to measure the correlation properties of the sequence. Therefore, additional support circuitry will be needed.

Support Circuitry

The dc level shifting circuit in figure 28 converts the NRZ on-off[10] output waveform of the PN generator/modulator to an NRZ polar waveform.[10]

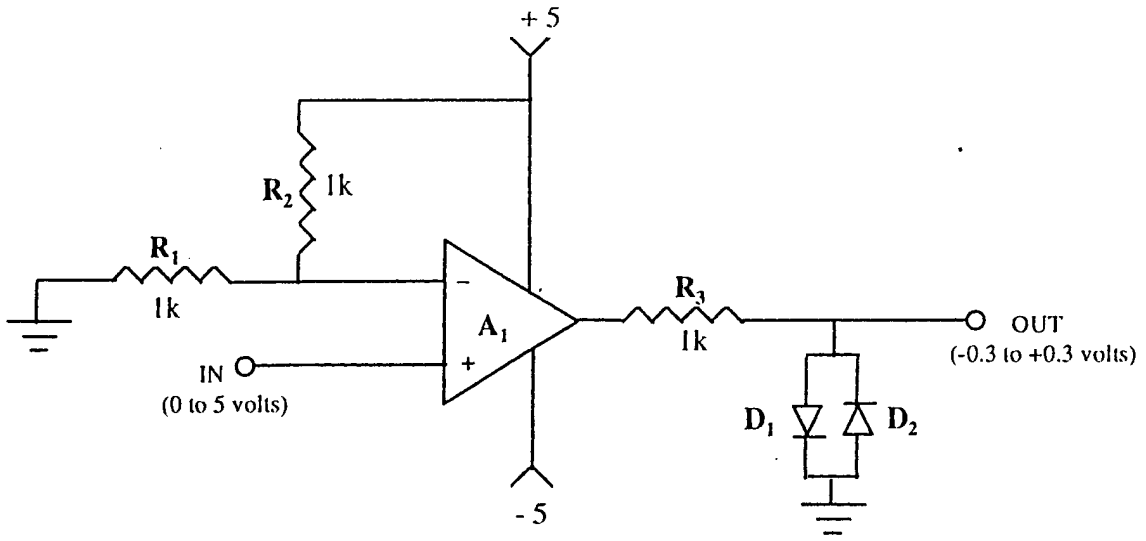

Figure 28: NRZ on-off to NRZ polar waveform converter

Resistors R_1 and R_2 provide a reference voltage of 2.5 volts to the inverting input of operational amplifier A_1. The amplifier is functioning as a voltage comparator in this configuration. The output waveform of the PN generator/modulator is applied to the non-inverting input. If the voltage at the non-inverting input rises above 2.5 volts, the output voltage of A_1 will be forced to the positive supply voltage (+5 volts). Similarly, if the voltage at the non-inverting input falls below 2.5 volts, the output voltage of the amplifier will be forced to the negative supply voltage (-5 volts). Diodes D_1 and D_2 are Shottkey

diodes (part number HP2835508) having a threshold voltage of approximately 0.3 volts. The diodes were inserted at the output of the amplifier to limit the voltage swing of amplifier A_1 to ± 0.3 volts. Resistor R_3 serves to limit the current supplied by the operational amplifier.

The most critical element in this circuit is the operational amplifier, since the integrity of the output waveform is determined by the step response, or the slew rate. The amplifier used to obtain the experimental data was the Motorola MC34083 having a slew rate specification of 40 $\frac{V}{\mu S}$. This allowed for a maximum clocking rate of 1 MHz before distortion of the output waveform occurs. Higher clocking rates can be achieved by using an operational amplifier with a larger slew rate, however, this results in a significant increase in cost.

VIII. Experimental Results

The experimental results of a three stage gold code generator is shown in figure 29. Figure 29a and 29b are gold sequences of length 7 generated using two distinct phases of a three stage gold code generator. Theoretically, the normalized cross correlation should have a maximum which is less than or equal to 0.7143. Figure 29d shows the plot of the normalized experimental cross correlation results of the sequences shown in figure 29a and 29b whose maximum is within the specified theoretical requirements. It should be noted that by examining the normalized autocorrelation function of figure 29c, a three stage generator does not provide a high enough $\mathbf{ID}_{\mathbf{auto}}$ or $\mathbf{ID}_{\mathbf{cross}}$ to be an effective tool for spectrum spreading. To increase the respective indices of discrimination, sequences of greater length will have to be utilized. This is illustrated by figure 30.

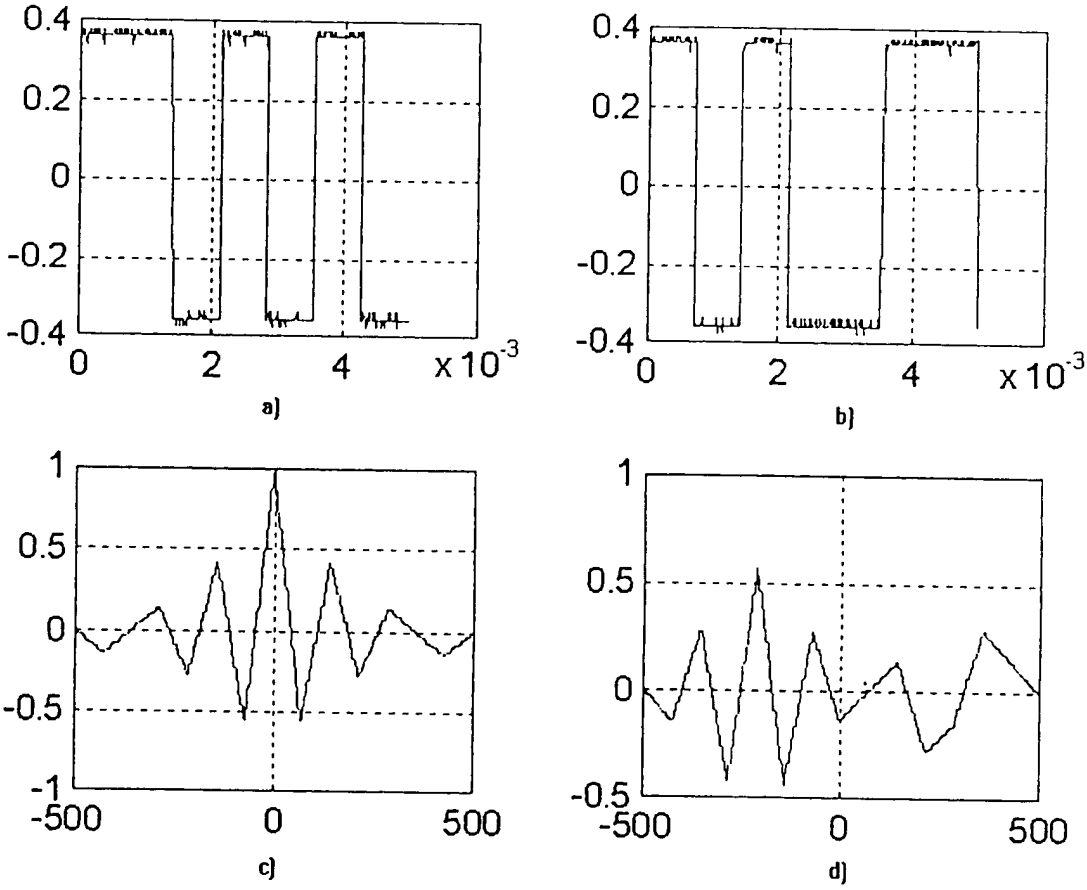

Figure 29: a) Gold Sequence of length 7. b) Gold Sequence from the same family. c) Autocorrelation function of the sequence in a. d) Cross Correlation function of sequence a and sequence b.

Increasing the length of the sequence to 31, shown in 30a and 30b, results in a significant increase in both $\mathbf{ID_{auto}}$ and $\mathbf{ID_{cross}}$ which can be seen by examining figures 30c and 30d. The maximum of the normalized cross correlation function of the sequences in figure 30 is 0.2647 which is less than the theoretical maximum of 0.2903. This shows agreement between the theoretical performance expectations of the sequences and the experimental waveforms. Further increase in performance can be achieved by using sequences of greater length as shown in figure 31.

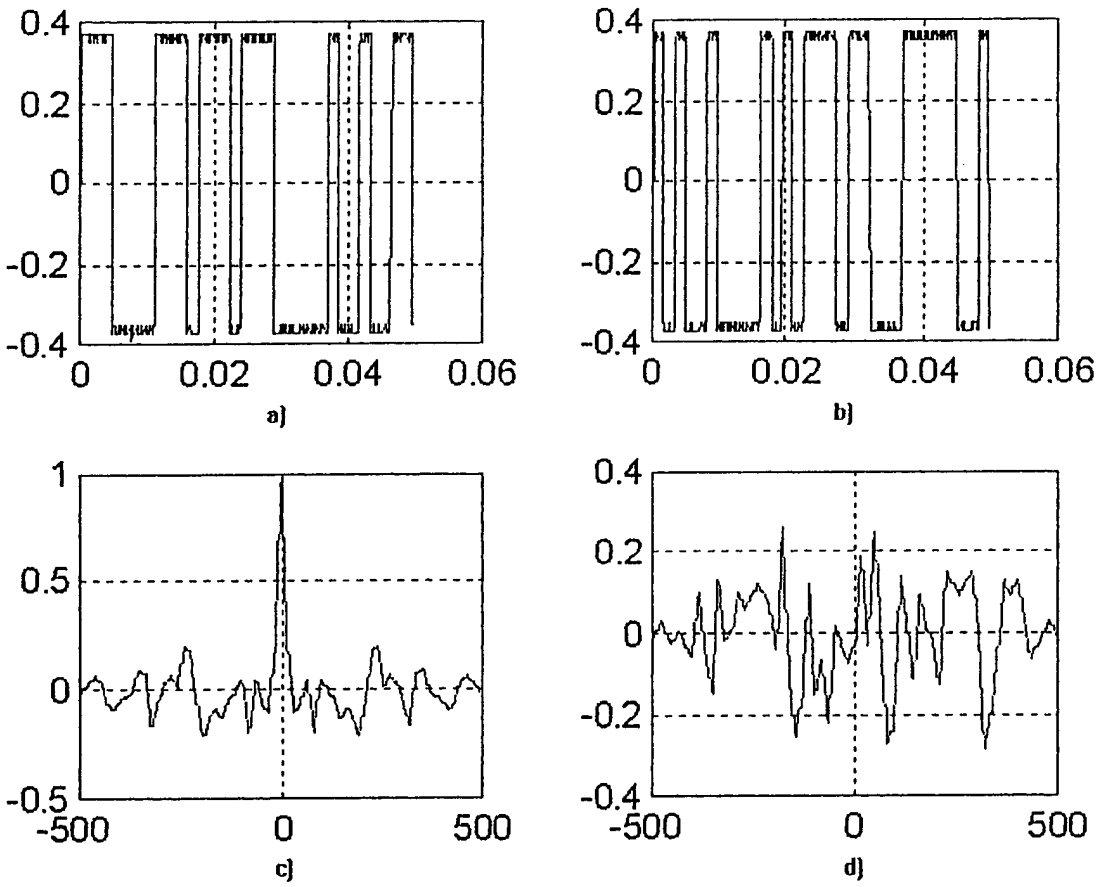

Figure 30: a) Gold Sequence of length 31. b) Gold Sequence from the same family. c) Autocorrelation function of the sequence in a. d) Cross Correlation function of sequence a and sequence b.

A summary of the theoretical expectations and the performance measurments is illustrated by the graph of figure 32.

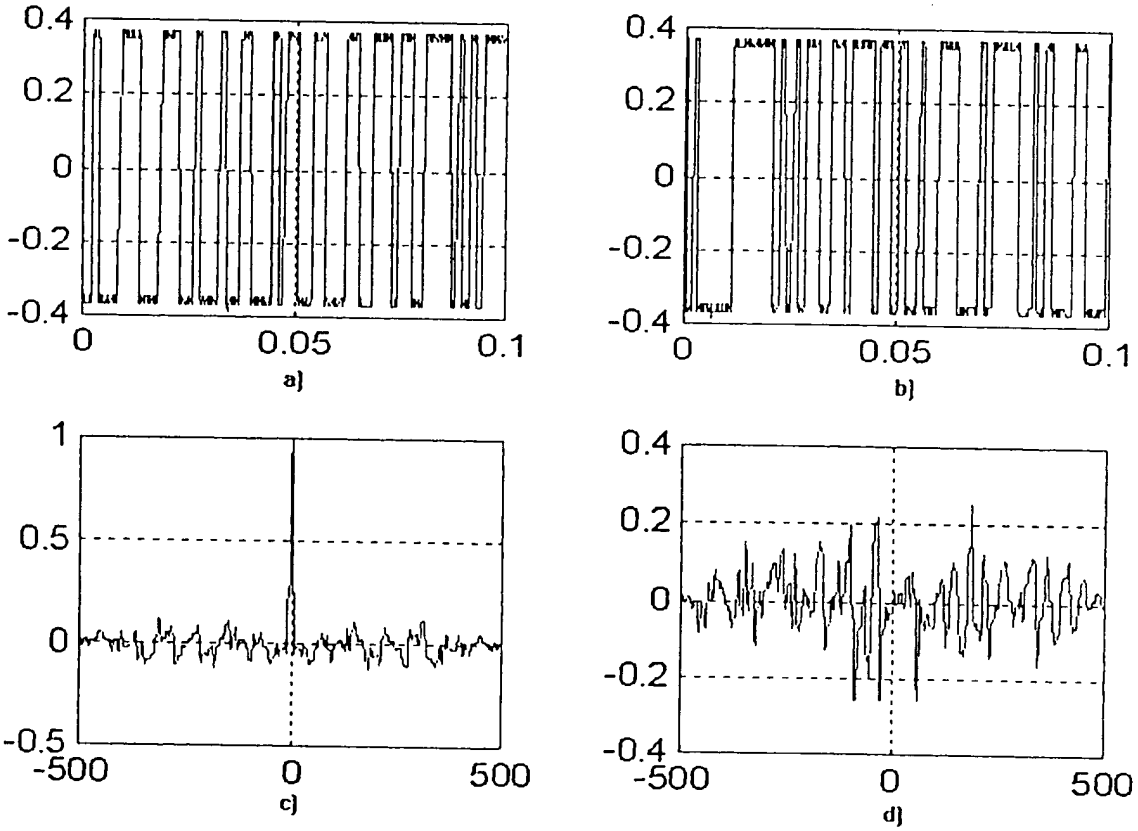

Figure 31: a) Gold Sequence of length 63. b) Gold Sequence from the same family. c) Autocorrelation function of the sequence in a. d) Cross Correlation function of sequence a and sequence b.

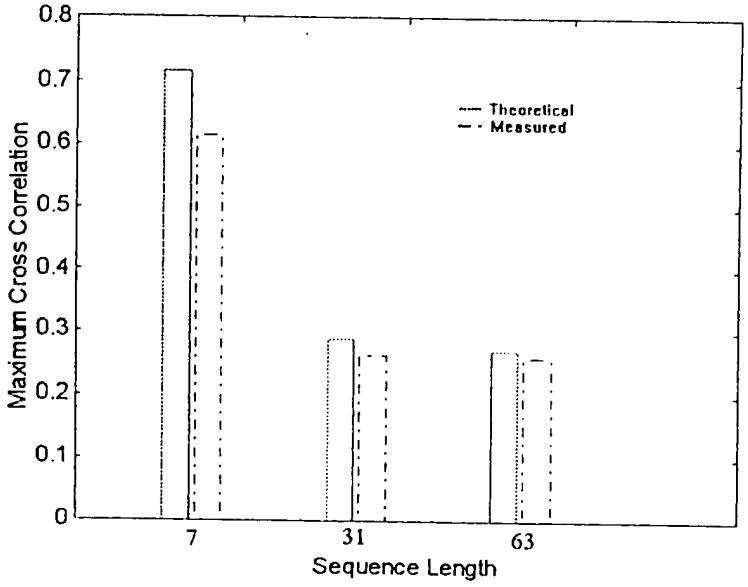

Figure 32: Summary of Cross Correlation Experimental Data

IX. Conclusion

A design method for generating families of orthogonal PN sequences has been presented. This procedure uses both the specifications for the number of users and the antijam performance to determine the necessary code length of the PN sequence. Using the theory of shift register sequence generators, a PN sequence generator was implemented using the VHDL hardware description language and a programable logic device (PLD). Implementation of shift register generators using a hardware description language proved to provide additional design flexibility for prototyping by allowing for data modulation to occur concurrently during the generation process.

The cross correlation performance of the experimental waveforms generated by the designed PLD proved to meet the expected performance criteria. Three different sequence lengths were used to provide the experimental data for the comparison. Two sequences from each set were arbitrarily chosen to provide the experimental correlation data for that set. The maximum of the cross correlation experimental measurements for each sequence length were below the specified theoretical maximum.

X. References

[1] G. Hoffmann de Visme. Binary Sequences. London: The English University Press Ltd: 1971.

[2] J. Holmes. Coherent Spread Spectrum Systems. New York: John Wiley & Sons: 1982.

[3] R. Dixon. Spread Spectrum Systems. New York: John Wiley & Sons: 1982.

[4] K. Feher. Wireless Digital Communications. New Jersey: Prentice-Hall Inc.: 1995.

[5] W. Peterson. Error Correcting Codes. New York: John Wiley & Sons: 1961.

[6] S. Gupta, J. Painter. "Correlation Analyses of Linearly Processed Pseudo-Random Sequences" IEEE Transactions on Communication Technology. December 1966.

[7] H. Hartmann. "Analysis of a Dithering Loop for PN Code Tracking" IEEE Transactions on Aerospace and Electronic Systems. January 1974.

[8] A. Salmasi, K. Gilhousen: "On the system design aspects of code division multiple access (CDMA) applied to digital cellular and personal communications networks" IEEE-VTC-91. St. Louis, MO.

[9] Z. Navabi. VHDL: Analysis and Modeling of Digital Systems. New York: McGraw-Hill Inc.: 1993.

[10] M. Schwartz. Information Transmission, Modulation, and Noise. New York: McGraw-Hill Inc.: 1990.

APPENDIX C

Investigation of an Indoor Digital Wireless System at 900 MHz

Overview of System Design Concerns

by

Christopher J. Karpinsky

TABLE OF CONTENTS

INTRODUCTION 1
Overview 1
Terminology 1
System Specifications 2
Operating Environment 2
Operating Frequency 2
Modulation Technique 2
Information Transmission Rate 2
Transmission Duty Cycle 2
INDOOR PATH LOSS ESTIMATION 3
Overview 3
Large-Scale Path Loss 3
Small-Scale Fading 5
Implications 6
SPREAD SPECTRUM COMMUNICATIONS 7
Introduction 7
Types of Spread Spectrum Systems 7
Frequency Hopping Spread Spectrum 7
Direct Sequence Spread Spectrum 7
Benefits of Spread Spectrum 8
Code Division Multiple Access 8
Benefits for Proposed System 9
FCC PART 15 REGULATIONS 10
Overview 10
Part 15 Highlights 10
Part 15 Specifics 10
Spread Spectrum Allocations 10
Transmit Power Limits 10
Antenna Requirements 10
Field Strength Limits 11
Frequency Hopping Spread Spectrum 11
Direct Sequence Spread Spectrum 11
Conclusion 11
SYSTEM CAPACITY PREDICTION 12
Overview 12
Typical Scenario for Cellular Architecture 12
System Capacity 12
Capacity Estimation 12
Performance of QPSK With Spread Spectrum Techniques 13
Special Considerations for Proposed System 13
Circular Cellular Geometry Investigation 14
NETWORK TOPOLOGY 19
Overview 19

Determination of Cell Size 19
Location of Cell Receivers 19
Interconnection of Cell Receivers 19
Central Monitoring System 20
CONCLUSIONS 21
Topics Covered 21
Future Investigation 21
BIBLIOGRAPHY 23

INTRODUCTION

Overview

This investigation describes some of the design considerations of an indoor wireless telemetry system. The design discussion is focused around the use of spread spectrum and code division multiple access techniques in the unlicensed 902-928 MHz spectrum.

The system imagined is that which is responsible for gathering the statistics of a building. What is meant by statistics is any measurable quantity within the building such as temperature, occupancy, air quality, etc. that the building engineers would care to monitor. The intent is to design a system that allows transducers to be scattered about the building which transmit data back to a centrally located computer responsible for monitoring the building.

This paper describes some of the issues associated with the design and implementation of such a system. The remainder of this section defines some common terminology that is used throughout this report and states some specifications of the system. The topic of path loss estimation is treated next followed by a discussion of spread spectrum modulation and its benefits.

A description of the FCC Part 15 regulations is included since these rules define unlicensed operation in the targeted band of operation. Following that discussion, an estimation of the capacity (number of users) of the system is developed. Finally, a discussion on the interconnection of the whole system is presented including the requirements of the central monitoring computer.

Terminology

In order to distinguish the various parts of this system, we must identify some common terms that will be used throughout our discussion. First off, the concept of the *cell* must be introduced. A cell is an organization of one receiver and multiple transmitters that are physically close to each other and operating in a common bandwidth in a coordinated fashion. In this application, a cell might consist of all the transmitters found in a single room, or those occupying small adjacent rooms.

The transmitters scattered about the building will be identified as the *users* of the system while the fixed receivers of each cell will be identified as the *base stations*. In a typical cellular system, the link between the base station and the users is generally full duplex. The link from the base station to the user is known as the *forward link* while the link from the user back to the

base station is known as the *reverse link*. In this system, however, a full duplex link is not required and therefore the forward link does not exist.

System *capacity* is the number of users a particular cell can accommodate under specific reliability requirements. It will be seen that the capacity of a code division multiple access system is dependent mostly on the available bandwidth and the number of users that must share this bandwidth.

System Specifications

Operating Environment

It is expected that the system will be operating in a typical office building setting. The receivers, as stated above, will be placed in fixed locations while the transmitters will be placed where needed, not necessarily on a fixed surface. Typical office events occur in the building including the movement of doors and elevators which constantly change the propagation characteristics of the environment.

Operating Frequency

The system will operate in the 902-928 MHz allocation designated for unlicensed operation by FCC Part 15 regulations.

Modulation Technique

QPSK data modulation will be used. The resulting baseband signal will then be modulated using direct sequence spread spectrum using code division multiple access techniques for channel access.

Information Transmission Rate

At this time the information rate is unspecified. It is imagined, however, that the rate will be fairly low due to the nature of the building parameters to be monitored. Estimated transmission rates would be in the order of 1200 to 9600 bps.

Transmission Duty Cycle

Separate from the information transmission rate is the actual duty cycle of the telemetry transmission. This is a measure of the percentage of time that any single telemetry transmitter will be active. It will be seen shortly that this parameter will be important in determining system capacity.

INDOOR PATH LOSS ESTIMATION

Overview

A major obstacle in the system design is the characterization of the communication path. For most applications, both the transmitters and receivers will be installed in an indoor environment. Obviously, the transmitter-receiver distances are shorter than the typical outdoor path geometry, but the indoor path experiences greater losses due to the variability of a building's interior and number of floors. Additional loss is produced by shadowing as the building's occupants perform their activities. Finally, multipath is an issue as various parts of a building move, such as large metal doors and elevators.

The distinction made here is between large-scale and small-scale fading statistics. Large-scale fading, or flat fading, is a function of distance and is useful in determining coverage area. On the other hand, small-scale fading, or fast fading, is a function of time and is used to predict bit-error rates and outage probabilities. By assuming that large-scale path loss (distance) and small-scale fading (time) can be separated, the channel statistics can be described by a probability density function which is the product of the density functions of each fading mechanism.

Large-Scale Path Loss

The large-scale path loss experienced in an indoor environment is dictated by the materials used in constructing partitions and floors. Empirical results from the reduction of measured data has provided a few models to predict mean path loss[4]. These models are adjusted by selecting the appropriate coefficients for the particular building environment being investigated. The major models used to predict indoor mean path loss include the log-distance path loss model, the Ericsson multiple breakpoint model, and the attenuation factor model.

The attenuation factor model is investigated here since it has been shown to reduce the standard deviation between predicted and measured path loss to around 4 dB as opposed to the log-distance path loss model's result of 13 dB. The attenuation factor model, giving mean path loss in dB at a distance d, is given as

$$L_{PL}(d) = L_o + 10n_{sf}\log\left(\frac{d}{d_o}\right) + FAF + X_\sigma$$

where L_o is the free space path loss in dB at a distance d_o and n_{sf} represents the path loss exponent value for the "same floor" measurement. The floor attenuation factor FAF accounts for the additional attenuation experienced between multiple floors. Finally, X_σ is a zero-mean log-normally distributed random variable with standard deviation σ in dB.

The key factor in assessing the usefulness of attenuation factor model is the ability to accurately determine the coefficients n_{sf} and FAF. Much experimental work has been done to determine these coefficients for various building environments. Table 1.1 gives typical values for n_{sf}. Typical values for FAF are given in Table 1.2 for two buildings investigated. Notice that the additional amount of attenuation experienced by the addition of each floor increases at a decreasing rate.

Building	Frequency (MHz)	n	σ (dB)
Retail Stores	914	2.2	8.7
Grocery Store	914	1.8	5.2
Office, hard partition	1500	3.0	7.0
Office, soft partition	900	2.4	9.6
Office, soft partition	1900	2.6	14.1
Factory LOS			
Textile/Chemical	1300	2.0	3.0
Textile/Chemical	4000	2.1	7.0
Paper/Cereals	1300	1.6	5.8
Metalworking	1300	1.6	5.8
Suburban Home			
Indoor Street	900	3.0	7.0
Factory OBS			
Textile/Chemical	4000	2.1	9.7
Metalworking	1300	3.3	6.8

Table 1.1: Measured values of path loss exponent and standard deviation[4].

Building	FAF (dB)	σ (dB)	Number of Locations
Office Building 1:			
One Floor	12.9	7.0	52
Two Floors	18.7	2.8	9
Three Floors	24.4	1.7	9
Four Floors	27.0	1.5	9
Office Building 2:			
One Floor	16.2	2.9	21
Two Floors	27.5	5.4	21
Three Floors	31.6	7.2	21

Table 1.2: Average values of floor attenuation factor for two sites[4].

Small-Scale Fading

As mentioned above, the small-scale fading component of the overall channel fading describes the temporal changes of the channel due to a multipath environment. The following are a few of the common parameters that are used in describing the small-scale fading statistics of a channel:

Fast Fading Channel - A channel in which the impulse response changes rapidly within the symbol duration, that is the coherence time of the channel is less than the symbol duration. This change in channel impulse causes frequency dispersion (also called time selective fading) due to Doppler spreading.

Slow Fading Channel - A channel in which the impulse response stays relatively constant over a time much larger than the symbol duration. In the frequency domain, the Doppler spread of the channel is much less than the bandwidth of the baseband signal.

Delay Spread - The delay spread measures the excess delay in the multipath environment. It is the time between the first received signal to the last received multipath component above a specified threshold.

Coherence Bandwidth - The coherence bandwidth B_C is a measure derived from the RMS delay spread of a channel. The coherence bandwidth is a statistical measure of the range of frequencies over which the channel can be considered to have a flat magnitude spectrum and linear phase spectrum.

Doppler Spread - Doppler spread is a measure of the spectral broadening caused by the time rate of change of the channel. It is defined as the range of frequencies over which the received Doppler spectrum is essentially non-zero. Doppler spread B_D exists when there is either a change in relative position of

the transmitter and/or receiver or a change in the position of surfaces creating multipath.

Coherence Time - The coherence time T_c of a channel is inversely proportional to Doppler spread and is a measure of the time duration over which the channel impulse response can be treated as invariant.

Flat Fading - A fading channel that induces a time-vary attenuation of a signal but maintains its spectral shape is known as a flat fading channel. This is a common fading model and assumes the amplitude to be Rayleigh distributed.

Frequency Selective Fading - Frequency selective fading occurs when the coherence bandwidth of the channel is smaller than the bandwidth of the transmitted signal. Frequency selective fading occurs when the excess delay spread is greater than the symbol duration.

Implications

The above parameters generally apply to narrowband transmission and are more or less severe depending on the environment both ends of the communication link exist within. In an indoor environment, the moving objects would consist mostly of doors, people, elevators, etc., thus the Doppler spread would be minimal due to their relatively small velocity. The excess delay, for most cases, would be fairly small due to the small additional distance multipath components would have to travel before recombining at the receiver.

A majority of the small-scale fading effects can be avoided, however, by using spread spectrum techniques. The next section explains this form of modulation and why it is advantageous in multipath environments.

SPREAD SPECTRUM COMMUNICATIONS

Introduction

The idea behind spread spectrum communications is to move away from the idea of achieving impressive bps/Hz ratios and use the entire available bandwidth for signaling. This is accomplished by spreading the signal throughout the given bandwidth with a pseudorandom noise (PN) signal. In this scenario, the relatively narrowband data signal is modulated by a relatively wideband noiselike spreading signal. This product is then transmitted across the wireless channel.

At the receiver, the same noiselike signal is mixed with the downconverted received signal with a resulting despreading of the original waveform. It is important to note here that the desired received signal is wideband, whereas most interfering signals are narrowband. Received narrowband signals are actually spread by the receiver's noiselike signal such that their energies are distributed over a wide bandwidth with the effect of slightly increasing the receiver's noise floor.

Types of Spread Spectrum Systems

The two major techniques for spreading a narrowband signal into a larger bandwidth are frequency hopping and direct sequence spread spectrum modulation.

Frequency Hopping Spread Spectrum

Frequency Hopping (FH) spread spectrum systems preserve the narrowband quality of the original signal, but only on an instantaneous basis. One can visualize a FH system as a traditional narrow band transmitter, but with a constantly varying carrier frequency. It is the carrier frequency that is being chosen pseudorandomly on a short, regular basis. With the carrier frequency changing over a large range and the transmit duration on any one channel brief, the modulation technique is effectively wideband.

Direct Sequence Spread Spectrum

The Direct Sequence (DS) spread spectrum system utilizes the entire wideband spectrum simultaneously. Once the baseband signal is modulated to the carrier frequency, the resultant is then modulated again, but by the pseudorandom bit sequence. DS systems offer an advantage over FH techniques due to their ability to implement a RAKE receiver (described below) for improved decoding in multipath environments.

Benefits of Spread Spectrum

The benefits of using spread spectrum techniques are grouped into four main categories:

Interference suppression - As mentioned above, the bandwidth spreading of the desired signal that occurs does not apply to the noise received at the receiver. Here, while the desired wideband signal is despread, the received narrowband noise signal is actually spread. This spreading of the noise at the receiver effectively distributes the energy of the noise throughout a wide bandwidth.

Removes time and frequency dimension constraints - Spread spectrum systems inherently do not require coordination of transmission timing or frequency planning between users. Each user can transmit continuously, not needing to relinquish the channel for another user. Each user also uses the entire bandwidth available, without the worry that another user is using a specific channel assignment. The actual timing of the system comes from the correlation operation performed at the receiver, matching the received spread signal with its internal representation of the noiselike spreading signal.

Energy density reduction - Because the same amount of power used for a traditional narrowband signal is being spread across a much larger bandwidth, the energy density (W/Hz) of the signal is decreased. This leads to many other qualities of spread spectrum systems including their low probability of detection/interception and their ability to share the same spectrum assignment with narrowband users and other coordinated wideband users.

Reduction of multipath interference - One of the most exciting areas of investigation is that of using the timing information contained within the spreading signal to resolve multiple instances of the original transmission at the receiver. Because the spreading signal is chosen to have excellent autocorrelation properties, the receiver can detect the various components of the received signal which are shifted in time and recombined them to enhance the detection process. The receiver used for this purpose is known as the RAKE receiver. Whereas most communication systems struggle to remove the interfering multipath components, the RAKE receiver actually uses this so-called interference to increase decision confidence. Incidentally, it is this same principle that is used by the Global Positioning System to determine a user's location from propagation delay.

Code Division Multiple Access

The idea behind code division multiple access, referred to as CDMA, is to assign each user of a system a unique noiselike spreading signal, known as a

code since it is usually of the form of a PN sequence. The spreading code is chosen such that it has a high peak autocorrelation, but the cross correlation with codes of other users is extremely small.

With this arrangement, a receiver can keep track of the users in a given cell by constantly correlating the composite received signal with each user's spreading code. When the correlation process produces data, the receiver knows which user is transmitting. With multiple correlators, the receiver can actually receive data from multiple users simultaneously, keeping the individual data streams separate with the low cross correlation property of the spreading codes.

Received energy from users of other cells has low correlation with the receiver's code set and appears as interference at the receiver. This factor is what distinguishes a CDMA system as a interference constrained system as opposed to a noise constrained system. The interference from users of the cell and of other cells is more of a limiting factor for the CDMA system than the energy from thermal, atmospheric, or man-made noise sources.

Benefits for Proposed System

The advantages of using CDMA with the building telemetry system make it worth while to investigate its use and implementation. The biggest benefit is that of uncoordinated access of the channel. Each transmitter can begin sending data whenever it is necessary, without having to listen to the channel first for activity. The second benefit of using CDMA techniques is that we will avoid the need of setting a single frequency of operation for each transmitter. The difficulty that is overcome is the case of interference on one specific frequency that would render the transmitter assigned to that frequency ineffective. With CDMA, the only coordination necessary would be the initial assignment of a unique PN sequence to each user which, ideally, would allow all transmitters to access the channel in an equally effective manner.

FCC PART 15 REGULATIONS

Overview

This section describes the FCC regulations that will have the be met with the design of an indoor wireless system operating in the unlicensed allocation of 902-928 MHz.

Part 15 Highlights

The FCC Part 15 regulations clearly state the imposed constraints and requirements of devices designed to produce emissions without the need of a license. These devices typically take the form of handheld or small fixed-location transmitters that are battery operated. Some spectrum allocations allow continuous information transmission while others limit the duration of which a particular transmitter may be active.

Of interest to our investigation is that of the regulations for operation in the 902-928 MHz spectrum allocation. This allocation is part of what is known as the Industrial, Scientific, and Medical bands, or ISM bands. Other spectrum allocations included in the ISM bands are the 2435-2465 MHz, 5785-5815 MHz, 10500-10550 MHz, and 24075-24175 MHz frequency allocations.

Part 15 Specifics

Spread Spectrum Allocations

The Part 15 regulations permit spread spectrum operation in the allocations of 902-928 MHz, 2400-2483.5 MHz, and 5725-5850 MHz. Both frequency hopping and direct sequence spread spectrum systems are allowed to operate in this region. It is important to note that spread spectrum systems are sharing this spectrum on a noninterference basis with other Government systems and ISM equipment.

Transmit Power Limits

The maximum peak output power of the transmitter shall not exceed 1 watt[15.247(b)]. Restrictions apply dependent on directive gain of antenna.

Antenna Requirements

The antenna for a system operating in these unlicensed bands must be either permanently attached to the transmitter, or attached via a nonstandard connection. The intent here is to prevent the end user from modifying the system for operation at an increased range thus producing increased interference[15.203].

If a directional antenna is used with directional gain greater then 6 dBi the transmit power must be reduced by the amount in dB that the directional gain of the antenna exceeds 6 dBi[15.247(b)].

Field Strength Limits

The field strength of intentional emissions within the 902-928 MHz must be less than 50 mV/m measured at a distance of 3 m. The field strength of spurious emissions within this band must be less than 500 uV/m measured at a distance of 3 m[15.249].

Emission outside of the 902-928 MHz allocation must not exceed 200 uV/m at a distance of 3 m[15.209(a)]. Further restrictions include that in any 100 kHz bandwidth outside the 902-928 MHz band, the RF power that is produced by the modulation products, the information sequence, and the carrier frequency must be at least 20 dB below that in any 100 kHz bandwidth within the 902-928 MHz band[15.247(c)].

Frequency Hopping Spread Spectrum

Specific requirements are necessary for systems employing frequency hopping in the 902-928 MHz region. FH systems shall have hopping channel carrier frequencies separated by a minimum of 25 kHz or the 20 dB bandwidth of the hopping channel, whichever is greater. At least 50 hopping frequencies must be used with each frequency occupied equally on the average. The maximum allowed 20 dB bandwidth of the hopping channel is 500 kHz. Finally, the average time of occupancy (known as dwell time) on any frequency shall not be greater than 0.4 seconds within a 20 second period[15.247(a)(1)].

Direct Sequence Spread Spectrum

The requirements for direct sequence systems in the 902-928 MHz region are as follows: A DS system must possess a processing gain of at least 10 dB. The processing gain is determined from the ratio in dB of the SNR with the system spreading code turned off to the SNR with the spreading code turned on, as measured at the demodulated output of the receiver[15.247(e)].

For any DS transmitted spectrum, the minimum 6 dB bandwidth must be at least 500 kHz to ensure a low power density[15.247(a)(2)]. In fact, the transmitted power density averaged over any 1 second interval must not be greater then 8 dBm in any 3 kHz bandwidth[15.247(d)].

Conclusion

The above summarizes the FCC requirements for unlicensed operation in the 902-928 MHz spectrum. Generally, less strict regulations exists as one moves the frequency of operation into the higher spread spectrum allocations.

SYSTEM CAPACITY PREDICTION

Overview

The goal of this section is to develop an estimation of the capacity of the spread spectrum channel.

Typical Scenario for Cellular Architecture

The common configuration of a CDMA system, as alluded to previously, is to have one base station in each cell that controls and coordinates the individual users in the cell. The base station uses the forward link to send data and control information to each user. When a particular users wishes to transmit information to the base station, it uses the reverse link.

The most important process that occurs between the base station and each user, second to the actual information transmission, is that of power control. Since the base station can measure the received power from each user on the reverse link on an instantaneous basis, the base station can instruct the user, on the forward link, to increase or decrease power. It is expected that the received power from a user will change quite rapidly with the various propagation conditions in different environments. In this way, the base station can instruct a particular user to adjust its transmit power to that which is sufficient for the desired bit error rate.

This power control mechanism helps to decrease the user's power consumption, which is typically supplied by a battery, by controlling its transmit power. But more importantly, power control decreases the level of interference both to the local cell and to other surrounding cells, thus playing an important role in determining the achievable system capacity.

System Capacity

Capacity Estimation

We now proceed to develop an idea of the capacity of a system implementing spread spectrum techniques[5].

The first step in this development is to realize the major issue in a multi-user environment is not thermal or man-made noise but rather the interference from other users of the system. Assume k_u users, each transmitting a wideband signal, are using a common frequency allocation of bandwidth W Hz. Assume the transmitters are power controlled such that the received power from each user is P_S watts. Then the interference I seen at the receiver is

$$I = (k_u - 1)P_S$$

if we assume that each user's signal is Gaussian noise due to the spreading signal used. The analog to the traditional E_b/N_0 metric becomes bit-energy-to-noise-density

$$\frac{E_b}{I_0} = \frac{P_S/R}{I/W}$$

for a spread spectrum system operating at R bps. Finally, by combining the above equations, we can estimate the number of simultaneous users as

$$k_u = \frac{W/R}{E_b/I_0} + 1.$$

We see common trends with the above expression, namely that as available bandwidth is increased, system capacity is increased. A decrease in data rate also increases system capacity. Finally, system capacity is increased as we are able to operate at lower E_b/N_0 values with the help of channel coding.

Performance of QPSK With Spread Spectrum Techniques

If we continue to use the assumption that interference dominates the noise process in the system, the traditional expression for the bit error rate of QPSK still holds:

$$P_b = \frac{1}{2}\operatorname{erfc}\left(\sqrt{\frac{E_b}{I_0}}\right)$$

Special Considerations for Proposed System

The difficulty with the above capacity estimation is that it assumes both the forward and reverse links are present and available for user transmitter power control. Controlling the power of each user in the cell maintains reliable communications with the cell's base station while also minimizing the interference to other users of the cell. The assumption of equal received signal strength from all users is not valid for the system proposed in this report where only the reverse link exists.

In this system, the transmit power from each user will be fixed. The received power from each user as seen by the cell base station will depend solely on the propagation characteristics of the indoor path from each user to the base station. The base station will have no way of directing a user to increase

transmit power if its signal is too weak or instruct the user to decrease power to reduce interference. The implication of this is that the interference received at the base station is not uniformly distributed as is the case when implementing power control.

The attenuation factor model investigated in the first section is adopted for the following capacity estimation. Recall this model predicts the mean path attenuation for various indoor environments over variations in distance between the transmitter and the receiver.

A second uniqueness of this system is that there is no requirement for all users to be transmitting simultaneously. Because the system is interference limited by its own users, decreasing the duty cycle of transmission of each user has the net effect of increasing the capacity of the system. Therefore we can take advantage of this discontinuous transmission mode in our capacity calculations.

Circular Cellular Geometry Investigation

An interesting analysis technique is that of assuming a circular arrangement of cells in a system[1]. The arrangement is to have the cell under investigation as a circular cell while all other interfering cells are arranged in circular layers around the center cell. The area occupied by each cell is assumed to be constant therefore the surrounding cells are formed as sectors of area equal to that of the circular center cell.

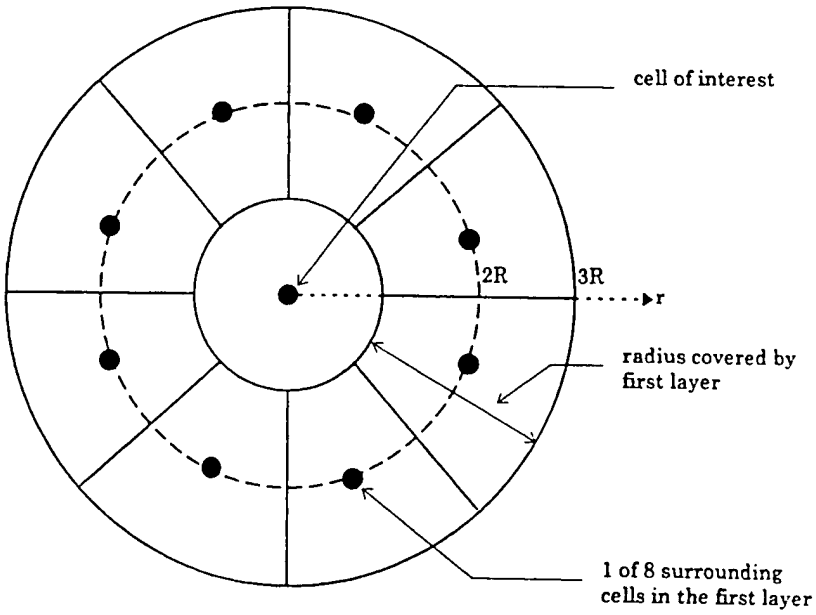

The center cell is of radius R and exists for $d_0 < r < R$ while the first layer of surrounding cells exists for $R < r < 3R$. The small radius d_0 about the origin is necessary when using the attenuation factor model. With this arrangement, to have equal area in all cells, the number of cells in the first layer, M_1, is 8. In fact, the number of cells in the i^{th} layer is

$$M_i = 8i.$$

Analysis with this technique can be varied in magnitude by choosing the total number of surrounding layers of interfering cells N.

We can use the circular cellular geometry technique to investigate our system by assuming that there is only one user per cell transmitting P_0 watts from the center of each cell. If the size of each cell is decreased, the net effect is that of modeling a single cell. Thus the arrangement of the multiple surrounding layers in this model actually becomes the composition of the single cell.

Let us define the duty cycle, or the percentage of time a particular user is expected to be transmitting, as the parameter α. We are interested in determining the received E_b/I_0 for the outermost user of the cell in the N^{th} layer. The received energy per bit from this desired user at a distance of

$$d = 2NR$$

is given by

$$E_b = \frac{P_0}{R_b}\left(\frac{d_0}{2NR}\right)^n.$$

Likewise, the distance from the center cell to an interfering user in the i^{th} layer becomes

$$d_i = 2iR$$

with received power at the center cell from this user of

$$P = \left(\frac{d_0}{d_i}\right)^n \alpha P_0 \text{ watts}$$

where d_0 and n describe the path loss as described previously. Then the total received power at the center cell for all the users in the i^{th} layer becomes

$$P = M_i\left(\frac{d_0}{2iR}\right)^n \alpha P_0 \text{ watts.}$$

The total interference power I received at the center cell is the summation of all received power from all the users in the N layers under investigation and is given by

$$I = \sum_{i=1}^{N} 8i\left(\frac{d_0}{2iR}\right)^n \alpha P_0 \text{ watts.}$$

We are now at a point to determine an expression for the E_b/I_0 metric observed at the center cell using our new expressions for bit energy E_b and interference power I.

$$\frac{E_b}{I_0} = \frac{\frac{P_0}{R_b}\left(\frac{d_0}{2NR}\right)^n}{\frac{I}{W}}$$

$$= \frac{P_0 W\left(\frac{d_0}{2NR}\right)^n}{R_b \sum_{i=1}^{N} 8i\left(\frac{d_0}{2iR}\right)^n \alpha P_0}$$

$$= \frac{W\left(\frac{d_0}{2NR}\right)^n}{8\alpha R_b \sum_{i=1}^{N} i\left(\frac{d_0}{2iR}\right)^n}$$

$$= \frac{W\left(\frac{d_0}{2R}\right)^n\left(\frac{1}{N}\right)^n}{8\alpha R_b\left(\frac{d_0}{2R}\right)^n \sum_{i=1}^{N} i^{1-n}}$$

$$\frac{E_b}{I_0} = \frac{W}{8\alpha R_b N^n \sum_{i=1}^{N} i^{1-n}}$$

We see from this result that we are able to determine the received E_b/I_0 from the outermost user, the user in the N^{th} layer, as a function of bandwidth W, bit rate R_b and path loss exponent n. This expression does not lend itself to finding a closed form solution as the previous development. We can inspect

the behavior of this expression, however, while varying the three main parameters.

The first parameter to be varied is bandwidth. As one would expect, larger bandwidths allow greater capacity. The following graph shows the performance of the system operating at 9600 bps with a path loss exponent of 2 as bandwidth is varied.

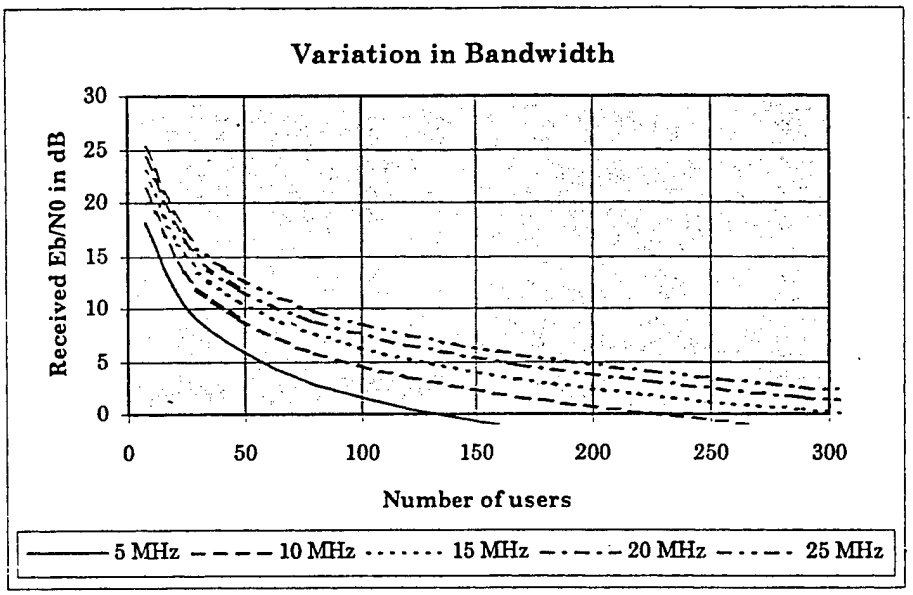

For a spread bandwidth of 15 MHz we can see that we can expect to accommodate approximately 50 users at a bit error rate P_b of 10^{-6}. The maximum bandwidth available in this allocation is 26 MHz and would support approximately 75 users at this same bit error rate.

Next we vary the path loss exponent n that is used with the attenuation factor model. With higher path loss exponents there is higher attenuation from the users at further distances from the central receiver. In this case the interference sources close to the receiver dominant as system capacity decreases. The following graph shows this relationship for a system operating at 9600 bps in a 15 MHz bandwidth.

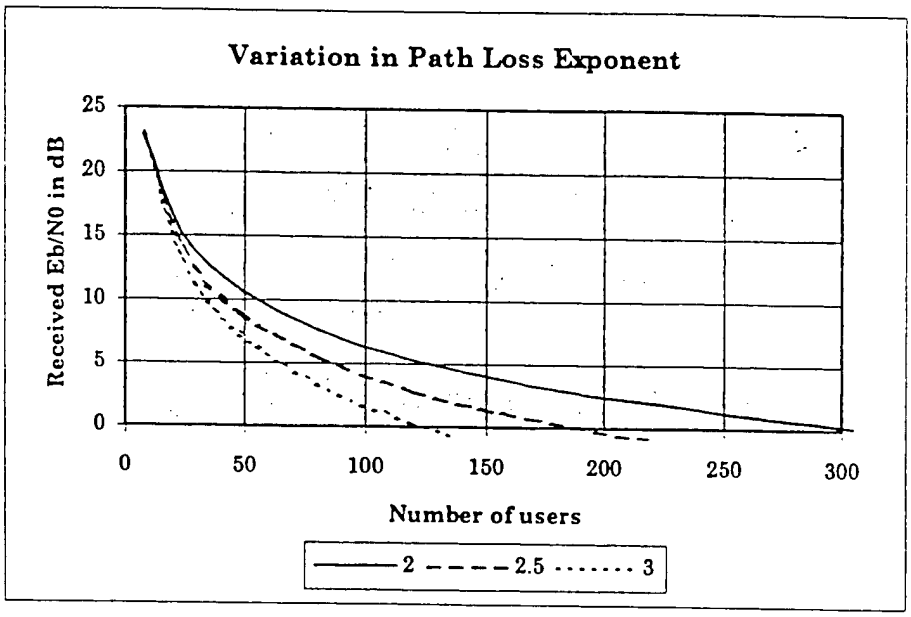

The last parameter to be varied is transmission bit rate. The following graph shows the change in system capacity for a system operating in a 15 MHz bandwidth with path loss exponent of 2 while transmission rate is varied.

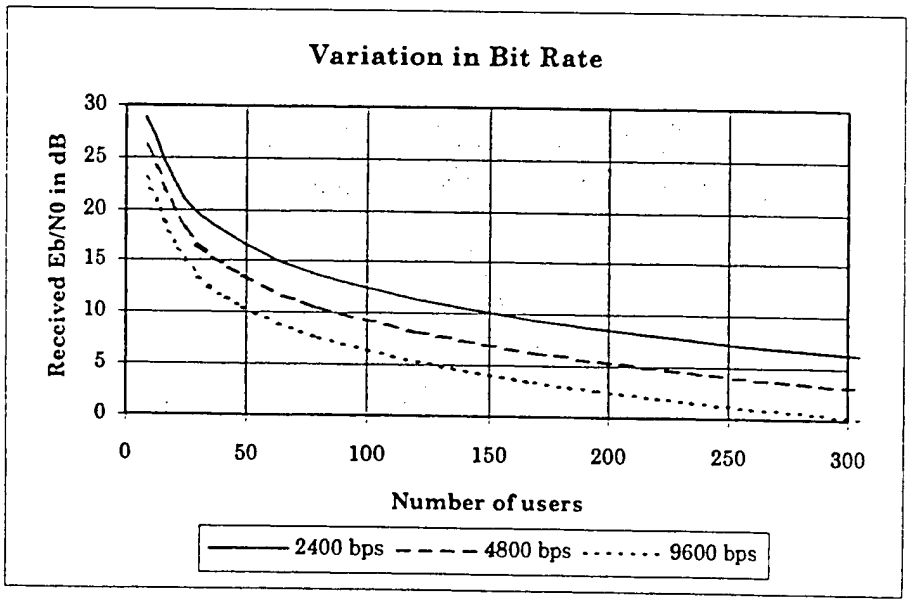

This parameter seems to have the most pronounced impact on the capacity of the system. If we are able to operate at lower bit rates, we can dramatically increase the capacity of the system. Operating at 2400 bps allows the system capacity to increase to approximately 150 users for a bit error rate P_b of 10^{-6}.

Overview

This section deals with the issues involved with the interconnection of the various cells of the telemetry monitoring system. Once the individual cells have been laid out it is necessary to develop a structure to interconnect the various cells to a network server that can accumulate the telemetry from each transmitter, archive it, and process it.

Determination of Cell Size

Probably one of the most difficult implementation problems would be that of determining the correct size for each cell. The major factor influencing this decision is that of the physical layout of the space to be monitored and the number of expected users in a certain area.

It is the location of walls, floors, and other large reflecting surfaces that will determine which propagation parameters will be used with the attenuation factor model and hence determine the propagation loss from each user to the cell's base station.

The number of users for a given cell must be below the capacity estimations developed previously. This is mostly dependent on the transmit power of each telemetry transmitter, transmitter density, and the required E_b/I_0 to support the desired bit error rate.

If it is possible to use directional antennas directed towards the cell user's alone, the capacity of the cell will increase because the base station receiver will be able to block out interference from other cells.

Location of Cell Receivers

The location of the cell receivers should be such that they are centered within the location of the cell's users and furthest from the users of neighboring cells. In this way, the cell receivers will receive the largest possible signal from its users while at the same time trying to achieve isolation from the interference from surrounding cells.

Interconnection of Cell Receivers

Since the cell receivers will be placed in fixed locations it would most likely be easiest to interconnect them with a wired network such as an Ethernet. Since most buildings already are wired with an Ethernet, the receivers could connect to the existing network structure of the building. Or if security and/or reliability is an issue, the receivers can be placed on an Ethernet dedicated to the telemetry monitoring system.

Central Monitoring System

From the individual cell receivers, the data from the telemetry transmitters would be routed to a central computer that would be able to record the telemetry, perform any necessary data reduction, and be able to act on any specific event detected in the telemetry data. More importantly this computer, known as the central server, would be able to interact with client software running on the computers of the system administrators. The administrators would be able to review the received telemetry as well as perform system maintenance.

The actual hardware that would be required for the central server could consist of a modern desktop PC running an operating system such as Microsoft Windows NT or a UNIX operating system such as Linux. An operating system of this nature is designed for network servers and would be much more robust than other operating systems meant for a desktop PC. The rate at which the telemetry would be arriving would dictate the necessary processing power, however a 90 MHz 586-based system would most likely be adequate for a few hundred users.

The main issue would be that of data logging capacity of the central server. The incoming telemetry would be spooled to disk for analysis and reduction. But this storage resource would quickly be consumed with enough data. Therefore it will be necessary to archive the data periodically either on magnetic tape or an optical storage device. The idea here is to preserve as much of the raw data as possible so that it may be analyzed in various ways later on.

CONCLUSIONS

Topics Covered

This report is meant as an introduction to the issues involved with the design of a wireless spread spectrum system. The following list summarizes each topic covered.

Path Loss - The path loss to be experienced within the indoor environment was uncertain. With this report we have investigated a few of the more popular models and have "adopted" the attenuation factor model for the analysis. General parameters of multipath channels have been introduced.

Spread Spectrum Techniques - A general introduction to spread spectrum systems is offered. Much further investigation into this interesting subject is necessary for advanced system analysis.

FCC Part 15 Regulations - These regulations have been researched and summarized in this report. The restrictions do not seem too severe and appear to allow a lot of flexibility in the design. A thorough reading of the Part 15 regulations is suggested.

System Capacity - A general technique of capacity estimation is presented. Due to the specific requirements/capabilities of the system under investigation, a method for predicting the system capacity is developed.

Network Topology - An overview of the actual interconnection of the system is presented. With further specifications, the computing resources required to manage the system can be better forecasted. In any case, the effort required to write the software to archive and process the telemetry would be much greater than that required to configure the hardware.

Future Investigation

As with everything in life, the further we look into something, the more questions we generate. Below is a list of items that can be investigated:

Actual path loss measurements - It would be interesting to see how well the attenuation factor model represents reality. This would require multiple measurements in different types of building environments.

Channel coding - An investigation into how well channel coding would improve the system capacity by decreasing the required E_b/I_0 value.

Cell size determination - Cell size is limited by the number of users a specific cell can accommodate. But what other limitations are there? How do specific types of building construction techniques limit the cell size? How about the impact of using directive antennas at the base station receivers?

Codes - How does the specific PN sequence create the system bandwidth? How can the correlation properties of the sequence influence the capacity of the system?

Capacity - The circular cellular geometry is primarily a two dimensional representation of the user distribution. Would it be possible to develop a spherical cellular geometry to model cells that span across multiple floors?

BIBLIOGRAPHY

[1] Rappaport, Theodore S., *Wireless Communications: Principles and Practice*, Prentice Hall, Inc., 1996.

[2] Sklar, Bernard, *Digital Communications: Fundamentals and Applications*, Prentice Hall, Inc., 1988.

[3] Rappaport, Theodore S., *Indoor Radio Communications for Factories of the Future*, IEEE Communications Magazine, pp. 15-24, May, 1989.

[4] Seidel, Scott Y., and Theodore S. Rappaport, *914 MHz Path Loss Prediction Models for Indoor Wireless Communications in Multifloored Buildings*, IEEE Transactions on Antennas and Propagation, pp. 207-217, Vol. 40, No. 2, Feb, 1992.

[5] Viterbi, Andrew J., *CDMA: Principles of Spread Spectrum Communications*, Addison-Wesley, 1995, ISBN 0-201-63374-4.

[6] Drake, Alvin W., *Fundamentals of Applied Probability Theory*, McGraw-Hill, 1967

[7] Viterbi, Andrew J., *Spread Spectrum Communications: Myths and Realities*, IEEE Communication Magizine, vol. 17, no. 3, pp. 11-18, May 1979.

[8] Newman, David B. Jr., *FCC Authorizes Spread Spectrum*, IEEE Communications Magazine, vol. 24, no 7, pp46-47, July 1986.

DISTRIBUTION LIST

DTRA-TR-98-47

DEPARTMENT OF DEFENSE

ASSISTANT TO THE SECRETARY OF DEFENSE
NUCLEAR CHEMICAL AND
DEFENSE PROGRAMS
THE PENTAGON, ROOM 3C125
WASHINGTON, DC 20301
ATTN: DEPUTY FOR NUCLEAR MATTERS

DEFENSE TECHNICAL INFORMATION CENTER
8725 JOHN J KINGMAN ROAD, SUITE 0944
FORT BELVOIR, VA 22060 6218
2 CYS ATTN: DTIC/OCP

DEFENSE THREAT REDUCTION AGENCY
8725 JOHN J KINGMAN RD., STOP 6201
FORT BELVOIR, VA 22060 - 6201
ATTN: CSA
ATTN: CSOS, W. WITTER
ATTN: TDANP

JOINT CHIEFS OF STAFF
DIRECTOR FOR OPERATIONS (J-3)
3000 DEFENSE PENTAGON
WASHINGTON, DC 20318 3000
ATTN: J-34, RM 2E230

OFFICE OF SPECIAL TECHNOLOGY
TECHNICAL SUPPORT WORKING GROUP
1111 JEFFERSON DAVIS HIGHWAY
CRYSTAL GATEWAY NORTH, SUITE #116
ARLINGTON, VA 22212
ATTN: J. DAVID

OFFICE OF THE ASSISTANT
SECRETARY OF DEFENSE
COMMAND, CONTROL, COMMUNICATIONS
AND INTELLIGENCE
THE PENTAGON, ROOM 1E760
WASHINGTON, DC 20301 3000
ATTN: COL G MCCURDY

OUSD ACQUISITION
DIRECTOR OF DEFENSE ACQUISITION
THE PENTAGON
WASHINGTON, DC 20301 2600
ATTN: S&TS/ LW, CHAIRMAN PSEAG, RM
3B1060

U.S. NUCLEAR COMMAND & CONTROL
SYSTEMS SUPPORT STAFF (NSS)
SKYLINE 3
5201 LEESBURG PIKE, SUITE 500
FALLS CHURCH, VA 22041 3202
ATTN: SECURITY PROGRAM MANAGER

DEPARTMENT OF THE AIR FORCE

HEADQUARTERS
ELECTRONICS SYSTEMS COMMAND
5 EGLIN STREET
HANSCOM AFB, MA 10731 2100
ATTN: ESC/FD

HQ EUCOM/J4
UNIT 30400 BOX 1000
APO AE 09128
ATTN: ECJ4- LW

U.S. AIR FORCE SPECIAL FORCES COMMAND
1720 PATRICK STREET
LACKLAND AFB, TX 76236 5228
ATTN: AFSFC/SFOR

COMMANDER IN CHIEF
US AIR FORCES IN EUROPE
APO AE 09094 5001
ATTN: USAFE/ SPO
ATTN: USAFE/ SPX

DEPARTMENT OF THE ARMY

HEADQUARTERS
DEPARTMENT OF THE ARMY
400 ARMY PENTAGON
WASHINGTON, DC 20310 2118
ATTN: DAMO - ODL

ENGINEER RESEARCH AND
DEVELOPMENT CENTER
WATERWAYS EXPERIMENT STATION
3909 HALLS FERRY ROAD
VICKSBURG, MS 39180 6199
ATTN: CEERD - GS- M, M. KEOWN

PRODUCT MANAGER
PHYSICAL SECURITY EQUIPMENT
COMMUNICATIONS ELECTRONICS COMMAND
5900 PUTMAN ROAD, SUITE 1
FORT BELVOIR, VA 22060 5420
ATTN: AMSEL - DSA - PSE

DISTRIBUTION LIST

COMMANDER
US ARMY NUCLEAR & CHEMICAL AGENCY
7150 HELLER LOOP, SUITE 101
SPRINGFIELD, VA 22150 3198
ATTN: MONA - SU

DEPARTMENT OF THE NAVY

NAVAL FACILITIES ENGINEERING
SERVICE CENTER
1100 23RD AVENUE
PORT HUENEME, CA 93043 4370
ATTN: CODE ESC 66

OFFICE OF THE CHIEF OF
NAVAL OPERATIONS (N34)
NAVY YARD
716 SICARD STREET, SE BUILDING 111
WASHINGTON, DC 20388
ATTN: L. TARGOSZ

SPACE AND NAVAL WARFARE
SYSTEMS CENTER
53560 HULL STREET
SAN DIEGO, CA 92152 5000
ATTN: E. BAXTER

U.S. MARINE CORPS
2 NAVY ANNEX
WASHINGTON, DC 20380 1775
ATTN: CODE POS-10

DEPARTMENT OF ENERGY

DEPARTMENT OF ENERGY
GTN
WASHINGTON, DC 20545
ATTN: NN - 513.4

OTHER GOVERNMENT

NATIONAL ARCHIVES AND
RECORDS ADMINISTRATION
8601 ADELPHI ROAD, ROOM 3360
COLLEGE PARK, MD 20740 6001
2 CYS ATTN: USER SERVICE BRANCH

DEPARTMENT OF DEFENSE CONTRACTORS

ANRO ENGINEERING INC
ELECTRONICS DIVISION
63 GREAT ROAD
MAYNARD, MA 01754
ATTN: G.F. ROSS
ATTN: L.R. CRAIN
ATTN: S.M. CICCARELLI

COMPUTER SCIENCE CORPORATION
7405 ALBAN STATION COURT, SUITE B-200
SPRINGFIELD, VA 22150
ATTN: B. BRLETICH

ITT INDUSTRIES
ITT SYSTEMS CORPORATION
1680 TEXAS STREET SE
KIRTLAND AFB, NM 87117 5669
2 CYS ATTN: DTRIAC

JAYCOR
1410 SPRING HILL ROAD, SUITE 300
MCLEAN, VA 22102
ATTN: DR. C.P. KNOWLES